

EFFECT OF BUBBLE HYDRODYNAMIC AND LIQUID PHASE ON MASS TRANSFER
MECHANISM IN BUBBLE COLUMN.

Miss Chomthisa Chuenchaem



จุฬาลงกรณ์มหาวิทยาลัย

CHULALONGKORN UNIVERSITY

A Thesis Submitted in Partial Fulfillment of the Requirements
for the Degree of Master of Science Program in Environmental Management
(Interdisciplinary Program)
Graduate School
Chulalongkorn University
Academic Year 2013

Copyright of Chulalongkorn University

บทคัดย่อและแฟ้มข้อมูลฉบับเต็มของวิทยานิพนธ์ตั้งแต่ปีการศึกษา 2554 ที่ให้บริการในคลังปัญญาจุฬาฯ (CUIR)

เป็นแฟ้มข้อมูลของนิสิตเจ้าของวิทยานิพนธ์ ที่ส่งผ่านทางบัณฑิตวิทยาลัย

The abstract and full text of theses from the academic year 2011 in Chulalongkorn University Intellectual Repository (CUIR)
are the thesis authors' files submitted through the University Graduate School.

ผลกระทบของอุทกพลศาสตร์ของฟองอากาศและเฟสของเหลวต่อกลไกการถ่ายเทมวลสารใน
ถังปฏิกรณ์แบบฟองอากาศ



นางสาวชมทิตา ชื่นเข้ม

จุฬาลงกรณ์มหาวิทยาลัย

CHULALONGKORN UNIVERSITY

วิทยานิพนธ์นี้เป็นส่วนหนึ่งของการศึกษาตามหลักสูตรปริญญาวิทยาศาสตรมหาบัณฑิต

สาขาวิชาการจัดการสิ่งแวดล้อม (สหสาขาวิชา)

บัณฑิตวิทยาลัย จุฬาลงกรณ์มหาวิทยาลัย

ปีการศึกษา 2556

ลิขสิทธิ์ของจุฬาลงกรณ์มหาวิทยาลัย

Thesis Title	EFFECT OF BUBBLE HYDRODYNAMIC AND LIQUID PHASE ON MASS TRANSFER MECHANISM IN BUBBLE COLUMN.
By	Miss Chomthisa Chuenchaem
Field of Study	Environmental Management
Thesis Advisor	Associate Professor Pisut Painmanakul, Ph.d.

Accepted by the Graduate School, Chulalongkorn University in Partial
Fulfillment of the Requirements for the Master's Degree

.....Dean of the Graduate School
(Associate Professor Amorn Petsom, Ph.d.)

THESIS COMMITTEE

.....Chairman
(Assistant Professor Chantra Tongcumpou, Ph.d.)

.....Thesis Advisor
(Associate Professor Pisut Painmanakul, Ph.d.)

.....Examiner
(Associate Professor Jin Anothai, Ph.D.)

.....Examiner
(Assistant Professor Patiparn Punyapalakul, Ph.D.)

.....External Examiner
(Marupatch Jamnongwong, Ph.D.)

ชมทิตา ขึ้นแฉ่ม : ผลกระทบของอุทกพลศาสตร์ของฟองอากาศและเฟสของเหลว ต่อกลไกการถ่ายเทมวลสารในถังปฏิกรณ์แบบฟองอากาศ. (EFFECT OF BUBBLE HYDRODYNAMIC AND LIQUID PHASE ON MASS TRANSFER MECHANISM IN BUBBLE COLUMN.) อ.ที่ปรึกษาวิทยานิพนธ์หลัก: รศ. ดร. พิสุทธิ์ เพียรมนกุล, 128 หน้า.

งานวิจัยนี้ศึกษากระบวนการดูดซึมของอากาศและสารอินทรีย์ระเหยง่ายชนิดไม่ชอบน้ำ (ชนิดเบนซีน) ที่เกิดขึ้นในถังปฏิกรณ์อากาศ โดยอุปกรณ์ที่ใช้เติมอากาศ (Diffuser) มี 2 ชนิดคือ หัวกระจายอากาศชนิดแข็ง (Rigid Diffuser) และหัวกระจายอากาศชนิดยืดหยุ่น (Flexible Diffuser) สารดูดซึมที่ใช้ในงานวิจัยนี้มี น้ำประปา และน้ำปนเปื้อนด้วยสารลดแรงตึงผิว (Surfactant) ชนิดประจุลบ ประจุบวก และไม่มีประจุ ที่ความเข้มข้นของสารลดแรงตึงผิวชนิดต่าง ๆ เท่ากับ 0.01 และ 0.1 ซีเอ็มซี ในการทดลองใช้กับอากาศ และ 0.1, 1 และ 3 ซีเอ็มซี ในการทดลองใช้กับเบนซีน โดยประยุกต์ใช้ร่วมกับค่าความเร็วอากาศต่างๆ ในการนี้ค่าตัวแปรทางอุทกพลศาสตร์ของฟองอากาศ สามารถหาได้จากกล้องถ่ายภาพความเร็วสูง (340 ภาพ/วินาที) และโปรแกรมวิเคราะห์ภาพถ่าย

จากผลการวิจัยพบว่า หัวกระจายอากาศชนิดแข็งให้ค่าสัมประสิทธิ์การถ่ายเทมวลสารรวมสูงสุด สืบเนื่องมาจากการการสร้างฟองที่มีขนาดเล็กเป็นผลให้เกิดการเพิ่มขึ้นของพื้นที่ผิวสัมผัสจำเพาะ (a) ระหว่างเฟส โดยพื้นที่ผิวสัมผัสจำเพาะของฟองอากาศ และการถ่ายเทมวลสารรวม (kLa) เพิ่มขึ้นตามความเร็วของกระแสอากาศ เมื่อพิจารณาค่าสัมประสิทธิ์การถ่ายเทมวลสารย่อย (kL) พบว่า ค่า kL ของสารลดแรงตึงผิวแต่ละชนิด มีค่าต่ำกว่าค่า kL ของน้ำ ผลเหล่านี้ขัดแย้งด้วยการเพิ่มขึ้นของค่าพื้นที่ผิวสัมผัสจำเพาะ นอกจากนี้ได้พิจารณาตัวแปรที่มีอิทธิพลต่อค่า kL เช่น ชนิด น้ำหนัก ความเข้มข้น และค่าแรงตึงผิว เพื่อแก้ไขตัวแปรของการถ่ายเทมวลสาร และตัวแปรทางด้านอุทกพลศาสตร์ให้เกิดความเหมาะสมกับงานนี้ เนื่องจากงานวิจัยนี้มีวัตถุประสงค์เพื่อให้เกิดการประยุกต์ใช้และการพัฒนากระบวนการดูดซึมของเบนซีนในถังปฏิกรณ์อากาศ ด้วยเหตุนี้จึงเลือกใช้ถ่านกัมมันต์ชนิดเกล็ดเติมลงในถังปฏิกรณ์อากาศ เพื่อช่วยดูดซับเบนซีนร่วมกับสารดูดซึม จากผลการทดลองพบว่าการใช้ถ่านกัมมันต์ชนิดเกล็ดร่วมกับน้ำประปาให้ประสิทธิภาพในการบำบัดสูงถึง ร้อยละ 74.45 ซึ่งนับว่ามีค่าร้อยละของการบำบัดสูงกว่ากรณีที่ใช้เพียงสารลดแรงตึงผิวชนิดไม่มีประจุ นอกจากนี้ยังพบว่าการใช้สารลดแรงตึงผิวร่วมกับการใช้ถ่านกัมมันต์นั้นส่งผลกระทบต่อประสิทธิภาพการดูดซับของเบนซีน เนื่องจากลดกลไกการเกาะติดที่พื้นผิว โดยสรุป การเลือกใช้หัวกระจายอากาศชนิดแข็งที่ความเร็วของกระแสอากาศเท่ากับ 0.0032 เมตรต่อวินาที ร่วมกับการใช้ถ่านกัมมันต์ชนิดเกล็ดร่วมกับน้ำประปามีความเหมาะสมสูงสุดต่อกระบวนการดูดซึมเบนซีนในถังปฏิกรณ์อากาศของงานวิจัยนี้

สาขาวิชา การจัดการสิ่งแวดล้อม

ลายมือชื่อนิสิต

ปีการศึกษา 2556

ลายมือชื่อ อ.ที่ปรึกษาวิทยานิพนธ์หลัก

5587529020 : MAJOR ENVIRONMENTAL MANAGEMENT

KEYWORDS: BUBBLE COLUMN BUBBLE HYDRODYNAMIC PARAMETERS HYDROPHOBIC
VOLATILE ORGANIC COMPOUNDS MASS TRANSFER PARAMETERS GRANULAR ACTIVATED
CARBON ABSORPTION BENZENE

CHOMTHISA CHUENCHAEM: EFFECT OF BUBBLE HYDRODYNAMIC AND LIQUID
PHASE ON MASS TRANSFER MECHANISM IN BUBBLE COLUMN.. ADVISOR:
ASSOC. PROF. PISUT PAINMANAKUL, PH.D., 128 pp.

The absorption mechanism of aeration and hydrophobic Volatile Organic Compounds (benzene) was investigated in a bubble column. The diffusers used in this study were rigid and flexible orifices. Tap water, and aqueous solution of commercial surfactants: cationic (DTAB), anionic (SES) and non-ionic (Dehydol LS 5 TH and Tween 80) were used as absorbents in this experiment. Moreover, the range of surfactant concentrations for aeration and benzene are 0.01, 0.1 CMC, and 0.1, 1, 3 CMC, respectively. Those were analyzed with the superficial gas velocity applied. The bubble hydrodynamic parameters were determined by using a high speed camera (340 frames/sec) and an image analysis program.

The results showed the rigid orifice provides the highest mass transfer rate due to the small bubble size generated and thus the increase of interfacial area (a). The values of interfacial area and volumetric mass transfer coefficients (kLa) increased roughly linearly with the superficial gas velocity. Moreover, the kL coefficients obtained with surfactant solutions were less than those obtained with tap water: these results compensates with the increase of interfacial area. Furthermore, the parameters such as the type of surfactants, molecular weight, CMC, and surface tension were proven for significantly altering mass transfer and bubble hydrodynamic parameters in this research. Due to the application and improvement of benzene absorption in bubble column, the granular activated carbon (GAC) was filled into a bubble column reactor. It can be noted that the addition of (GAC) into the reactor with tap water can provide the highest benzene removal efficiency (up to 74.45%) compared with the non-ionic surfactant as absorbent. Moreover, the presence of non-ionic surfactant molecules can cause the negative effect onto the GAC adsorption capacity due to their attachment mechanism. Finally, it has been suggested that rigid diffuser applied with the superficial gas velocity at 0.0032 m.s⁻¹, and water combined with granular activated carbon are the optimal design and operation for hydrophobic VOCs absorption in the bubble column used in this study.

Field of Study: Environmental Management Student's Signature

Academic Year: 2013

Advisor's Signature

ACKNOWLEDGEMENTS

I wish to express my profound gratitude and sincerest appreciation to my advisor Dr. Pisut Painmanakul for his precious guidance, shape advice, helpful suggestions, and continuous encouragement throughout this research. He gave me the useful knowledge and systematic thinking for the environmental application and management. He has always taught several important points to gain the completion to work without his creative ideas and devotion, this study would not been successful. I also would to extend my profound gratitude to Dr. Chanta Tongcumpou, Chairman of the committee, Dr.Patiparn Punyapalakul, Dr. Jin Anothai, and Dr. Marupatch Jamnongwong, my committee members, for their useful and valuable comments.

This research was financially supported by the National Center of Excellence for Environmental and Hazardous Waste Management (NCE-EHWM), Graduate School Chulalongkorn University. Without this scholarships, this research would not been achieved.

My cordial thanks should be given to all the NCE-EHWM staffs and laboratory staffs for their kind cooperation and help. Moreover, I would like to thank Department of Environmental Engineering, Chulalongkorn University for laboratory facilities.

Finally, deepest and most sincere appreciation is extended to my parents for their support, love and encouragement.

CONTENTS

	Page
THAI ABSTRACT	iv
ENGLISH ABSTRACT	v
ACKNOWLEDGEMENTS	vi
CONTENTS	vii
LIST OF FIGURE.....	ix
LIST OF TABLE	xi
CHAPTER I.....	1
INTRODUCTION.....	1
1.1 Statement of problem.....	1
1.2 Objectives.....	3
1.3 Hypotheses	3
1.4 Scope of study	4
CHAPTER II.....	6
BACKGROUND AND LITERATURE REVIEW.....	6
2.1 VOCs: Benzene	6
2.2 Control of gaseous and volatile organic compounds.....	7
2.3 Absorption.....	9
2.4 Bubble column	10
2.5 Mass transfer parameters.....	12
2.6 Bubble hydrodynamic parameters.....	24
2.7 Diffuser	27
2.8 Surfactant	28
2.9 Micelles.....	29
2.10 Adsorption.....	31
2.11 Literature Review.....	32
2.12 Research focuses	35
CHAPTER III.....	36

	Page
METHODOLOGY.....	36
3.1 Research overview.....	36
3.2 Experimental setup.....	37
3.3 Benzene gas generator.....	38
3.4 Gas Chromatography Detector FID, Agilent Technologies 6890N.....	38
3.5 UV-Visible spectrophotometer.....	39
3.8 Analytical methods.....	42
3.9 Experimental Procedures.....	45
CHAPTER IV.....	52
RESULTS AND DISCUSSION.....	52
4.1 The effect of different gas diffusers (rigid and flexible) in bubble column.....	52
4.2 Study the effect of absorbents at difference concentrations.....	54
4.3 The effect of absorbents and concentrations on hydrophobic VOCs absorption process.....	63
4.4 Liquid-side mass transfer coefficient (k_L) for aeration and hydrophobic VOCs...	75
4.5 VOCs Removal efficiency.....	84
CHAPTER V.....	91
CONCLUSIONS AND RECOMMENDATIONS.....	91
5.1 Conclusions.....	91
5.2 Recommendations for future work.....	93
REFERENCES.....	94
APPENDIX.....	96
VITA.....	128

LIST OF FIGURE

	Page
Figure 2. 1 Equipments for absorption process.....	10
Figure 2. 2 Bubble column (Seeger, 2001)	11
Figure 2. 3 Concept of two-resistance theory	18
Figure 2. 4 Interfacial compositions as predicted by the two-resistance theory.	19
Figure 2. 5 Concentration driving forces for two-resistance theory.	21
Figure 2. 6 The relationship between bubble rising velocity and bubble diameter	25
Figure 2. 7 Generalized surfactant structures	28
Figure 2. 8 Schematic representation of a micelle in aqueous solution	30
Figure 3. 1 Experiment framework of this research.....	36
Figure 3. 2 Schematic diagram of the experimental setup.....	37
Figure 3. 3 Benzene generator.....	38
Figure 3. 4 Basler camera.....	30
Figure 3. 5 Software with License Dongle	39
Figure 3. 6 Rigid and flexible diffuse.....	40
Figure 3. 7 Flow diagram for selection of optimal diffuser in bubble column.....	45
Figure 3. 8 Flow diagram for study the effect of absorbents at different concentrations.....	46
Figure 3. 9 Flow diagram for the effect of absorbents and concentrations on hydrophobic VOCs absorption process.....	48
Figure 3. 10 Flow diagram for liquid-side mass transfer coefficient (k_L) for aeration and hydrophobic VOCs.....	49
Figure 3. 11 Flow diagram for the effect of hydrophobic VOCs on hybrid processes (absorption and adsorption).....	50
Figure 4. 1 Volumetric mass transfer coefficient versus gas flow rate in tap water.....	53

Figure 4. 2 The oxygen concentration in liquid phase at different experimental times	54
Figure 4. 3 Volumetric mass transfer coefficient versus gas flow rate for different liquid phases (tap water and surfactant solutions).....	55
Figure 4. 4 Site distribution for aeration in water.....	57
Figure 4. 5 Site distribution for aeration in anionic solution.....	57
Figure 4. 6 Bubble diameter versus superficial gas velocity.....	58
Figure 4. 7 Specific interfacial area versus superficial gas velocity	60
Figure 4. 8 Liquid-side mass transfer coefficient versus superficial gas velocity.....	61
Figure 4. 9 The volumetric mass transfer coefficient ($k_L a$) for the different liquid phases.....	64
Figure 4. 10 Volumetric mass transfer coefficient versus gas flow rate for different liquid phases (tap water and surfactant solutions).....	65
Figure 4. 11 Site distribution for hydrophobic VOCs in water	68
Figure 4. 12 Site distribution for hydrophobic VOCs in non-ionic surfactant solution .	68
Figure 4. 13 Bubble diameters versus superficial gas velocity for different liquid phases (tap water and surfactant solutions).....	69
Figure 4. 15 Interfacial area versus superficial gas velocity for different liquid phases	71
Figure 4. 16 Liquid-side mass transfer coefficient versus gas flow rate for different liquid phases (tap water and surfactant solutions).....	73
Figure 4. 17 Attachment of each surfactant molecule on air bubbles surface.....	77
Figure 4. 18 Experimental liquid-side mass transfer coefficient versus bubble for aeration part	78
Figure 4. 19 Experimental liquid-side mass transfer coefficient versus bubble for hydrophobic VOCs part	80
Figure 4. 20 Liquid-side mass transfer coefficient predicted by the models proposed versus the bubble diameters for the different liquid phases	82

Figure 4. 21 VOCs removal efficiency	84
Figure 4. 22 Absorbance versus time for non-ionic surfactant.....	86
Figure 4. 23 Absorbance versus time for water.....	86
Figure 4. 24 Effect of surfactant (non-ionic) on GAC adsorption	88
Figure 4. 25 Mechanism for benzene absorption and adsorption	88
Figure 4. 26 The VOCs removal efficiency.....	89



LIST OF TABLE

	Page
Table 2. 1 Technology for removal volatile organic compounds (VOCs).....	8
Table 3. 1 The condition of GC parameters	39
Table 3. 2 Physical characteristic of diffuser and operating conditions.....	40
Table 3. 3 Characteristics of surfactant and water	41
Table 3. 4 Variable of study benzene absorption in water	46
Table 3. 5 Variable of study benzene absorption in water	46
Table 3. 6 Variable of study benzene absorption in liquid phases	48
Table 3. 7 Variable of VOCs removal efficiency.....	50
Table 4. 2 The saturation concentration of benzene in liquid phase.....	64
Table 4. 3 The saturation concentration of benzene in liquid phase.....	67
Table 4. 5 Comparing the CMC value and molecular weight of each surfactant.....	75
Table 4. 6 The surface tension and molecular weight of each surfactant.....	76
Table 4. 7 The characteristic of each absorbent	81
Table 4. 6 The volumetric mass transfer coefficient in different phase.....	88

CHAPTER I

INTRODUCTION

1.1 Statement of problem

Over the last decade, there has been increased air pollution problem owing to emission from a variety of industries contains volatile organic compounds (VOCs), especially benzene into the atmosphere. Many research proved that benzene is human carcinogen, which are harmful to human health directly (EPA, 1998; Ross, 1996). Therefore, the removal of benzene from waste water or exhaust air is of great interest.

A number of methods have been developed to remove VOCs in the gas phase. Among them, the absorption process, which allows the transfer of a pollutant from the gas phase to a liquid phase, with or without any chemical reaction, is one of the well-known methods. In gas-liquid reactors, the most important goal of the process is mass transfer from the gas phase to liquid phase. In order to increase the absorption efficiency, the VOCs gas is released in form of small bubble to yield a large surface area and also an efficient mass transfer between gas and liquid phases in bubble column. Bubble columns are gas-liquid contactors encountered in a wide range of applications. This is because of their simple construction, low operating cost and high efficiency. Due to its many advantages, this process is applied into a purification process for VOCs, and abatement, particularly for benzene (Heymes, Demoustier, Charbit, Fanlo, & Moulin, 2007). In this process, the gas-liquid mass transfer is one of the key determinant reactor performances which relate to hydrodynamics and physical properties.

When hydrophobic VOCs such as benzene are to be removed from industrial exhaust gases, an absorption reactor filled with pure water is not efficient because of the low solubility of hydrophobic VOCs in water. Therefore, other kinds of absorbents are required. Surfactants composed of a hydrophilic head group and a hydrophobic tail can be well solubilized in water forming a micelle. The hydrophilic groups are headed to water while the hydrophobic tails aggregates in the middle of the micelle. As hydrophobic VOCs are captured in the hydrophobic tails due to the hydrophobic interaction, their solubility in the surfactant solution is much larger than solubility in pure water. Hence, an absorption reactor filled with the surfactant solution is more efficient than one with pure water.

However, no single method can be used in all cases: most of methods are specific in nature. Thus this research work aims to study a combination between two processes: absorption and adsorption, to enhance the removal efficiency of benzene with low cost and installation. For adsorption process, various types of adsorbent in large scale use include activated carbon, zeolite, silica gel, etc. Up to now, activated carbon (AC) has been used to adsorb air pollution to remove all the volatile as a gas or vapor. The previous studies have shown AC removal efficiency for benzene of greater than 99% at an influent concentration of 0.4 mg/L (U.S., 2001). Consequently, it is expected that a combination between absorption and adsorption can be used to lower benzene concentration.

Nevertheless, there is a very limited number of qualitative data related to the effect of bubble hydrodynamic and mass transfer parameter on the benzene absorption efficiency. In practice, the overall mass transfer coefficients ($k_L a$) are often worldwide and

thus insufficient to understand the gas-liquid mass transfer mechanism, which is directly to the associate efficiency.

To fill this gap, this research was mainly focused on the effect of different gas diffusers and liquid phase on mass transfer and bubble hydrodynamic parameters in bubble column. Then, a hybrid process between absorption and adsorption was designed and the effects of operational parameters on its performance for the treatment of benzene as a model compound were investigated.

1.2 Objectives

The three main objectives of this research are:

1. To study the effect of different gas diffusers.
2. To study the effect of liquid phase (surfactant) and addition of adsorbent.
3. To apply into a purification for benzene absorption process.

1.3 Hypotheses

The hypotheses for this study are:

1. Diffuser and liquid phase have directly effect on bubble hydrodynamic and mass transfer mechanism.
2. Hybrid processes (absorption and adsorption) improve purification for benzene absorption process.

1.4 Scope of study

This experiment is carried out in laboratory scale with a bubble column of 10 cm in diameter and 100 cm in height, and at condition. The scope of this work is as followed:

Part 1: Effect of different gas diffusers (rigid and flexible) in Bubble column

The rigid orifice and flexible membrane are compared by considering the overall mass transfer coefficient ($k_L a$). The diffuser that has the highest $k_L a$ value will be applied in the next step.

Part 2: Study the effect of surfactant at different concentrations

The liquid phases used in this study are tap water, and aqueous solutions of surfactants (anionic, cationic, and non-ionic). The ranges of surfactant concentrations and gas flow rates applied are 0.1 and 1 CMC, and 0.2, 0.5, 1, 1.5, 2.0 mL/s, respectively. Then, bubble hydrodynamic and mass transfer parameters will be measured and the results will be discussed.

Part 3: The effect of surfactant and concentrations on hydrophobic VOCs absorption process

In this work, benzene is chosen as hydrophobic VOCs gas emission. The overall mass transfer coefficients ($k_L a$) are determined by using the experimental data based on the variation of VOCs concentration in gas phase with time. Note that the VOCs concentrations obtained in this study are measured by UV-Visible spectrophotometer. The calculation of interfacial area (a) is based on the experimental results of the bubble diameter (d_B) and the bubble rising velocity (U_B) determined by using the high speed camera (100 images/second) and image analysis program.

Part 4: Liquid-side mass transfer coefficient (k_L) for aeration and hydrophobic VOCs

The type and concentration of absorbent that affect to the k_L values of aeration and hydrophobic VOCs system were study. Moreover, modeling of the liquid-side mass transfer coefficient was analyzed.

Past 5: VOCs removal efficiency

The VOCs removal efficiency (%Eff) indicated the performance of the absorption process and also the combination between absorption and adsorption processes that occurred in the small bubble column. Note that granular activated carbon is chosen as adsorbent.

CHAPTER II

BACKGROUND AND LITERATURE REVIEW

2.1 VOCs: Benzene

VOCs are a large class of chemicals which are found in atmosphere. VOCs are used in many household products and industrial processes. Most VOCs commonly found in indoor air are extremely toxic, having been linked to cancer and other negative health effects. An example of hazardous VOCs linked to cancer is benzene.

Benzene, also known as benzol, is a colorless liquid, petroleum-based chemical that has a sweet smell, highly flammable, and can dissolve slightly in water. Due to benzene evaporate into the air easily at the normal temperature and pressure, this thing always has an impact on environment and human health.

Short term exposure to high concentration of benzene may be harmful to central nervous system (CNS) disturbances consistent with solvent exposure, such as; drowsiness, dizziness, headache, tremor, delirium, ataxia, loss of consciousness, respiratory arrest and death. Long term exposure may effect to blood production, bone marrow, and damage to immune system Moreover, benzene can causes leukemia, which is the cancer of blood forming organs.

In this work, benzene was chosen as a model of a VOC with low solubility in water. If VOCs are insoluble, it may be leak and emitted to the atmosphere. Therefore, the water cannot be used as an absorbent. Other kinds of absorbent are required. Hence, an

absorption reactor filled with surfactant solution is more efficient than one with pure water.

2.2 Control of gaseous and volatile organic compounds

The reduction of concentrations of VOCs for acceptable levels can be carried out by a numbers of methods, including incineration, absorption, adsorption, etc. A brief of description of each follows:

- **Incineration**

Incineration is the process of oxidizing combustible gases or vapors by raising the temperature of the gases or vapors above its auto-ignition point in the presence of oxygen, and maintaining it at high temperature for sufficient time to complete combustion. This technique is a proven method for destroying VOCs, which efficiencies possible up to 99%. However, thermal incinerator is too expensive in terms of equipment cost, installation cost, supplemental fuel costs, and cannot recover VOCs for reuse in the process.

- **Absorption**

Absorption technique is used to remove one or more gaseous components from a gas flow using a solvent that rely on the gaseous component to be removed. Due to its high efficiency to remove VOCs up to 98% as shown in Table 2.1, it is frequently used to remove unwanted contaminant and odorous from an exhaust gas flow.

- **Adsorption**

The principle of this technique is used to remove individual components from a gas or liquid mixture. The component to be removed is physically or chemically bonded

to a solid surface. The component that is removed from a gas or liquid mixture by adsorption can either be a product that is wanted or an impurity. Normally, this technique is used to clean exhaust gases.

Table 2. 1 Technology for removal volatile organic compounds (VOCs)

Technique	Inlet Conc. PPMV	Efficiency	Advantages	Disadvantages
Absorption	250 1,000 5,000	90% 95% 98%	Especially good for inorganic acid gasses	Limited applicability
Adsorption	200 1,000 5,000	50% 90-95% 98%	Low capital investment good for solvent recovery	Selective applicability moisture and temperature constraints
Thermal incineration	20 100	95% 99%	High destruction efficiency Wide applicability can recover heat energy	No organics can be recovered Capital intensive
Catalytic incineration	50	90%	High destruction efficiency	No organics can be recovered
Flares	100	>95% >98%	Can be less expensive than thermal High destruction efficiency	Technical limitations that can poison No organics can be recovered Large emissions only

Due to incineration technique is costly and cannot recover gas for reuse, absorption and adsorption technique will be chosen in this study in order to provide a better understanding of these processes mechanism and optimize operating conditions. For more understanding, the deep detail of absorption and adsorption processes are described in the next section.

2.3 Absorption

Absorption technique is used to remove one or more gaseous components from a gas flow using a solvent that rely on the gaseous component to be removed. Due to its high efficiency to remove VOCs up to 98%, it is frequently used to remove unwanted contaminant and odorous from an exhaust gas flow. Absorption basically involved the transfer of one or more species from the gas phase to the liquid phase. It is defined as the operation in which a gas mixture is contacted with a liquid for the purpose of preferentially dissolving one or more components of the gas mixture and to provide a solution of them in the liquid. The gaseous component that transfers to the liquid phase is said to be adsorbent, and the transferred component is known as the solute.

However, there are many equipment that were used in an absorption process such as trayed tower (plate column), packed columns, spray tower, bubble column, and centrifugal contactor, as shown in schematically in Figure 2.1.

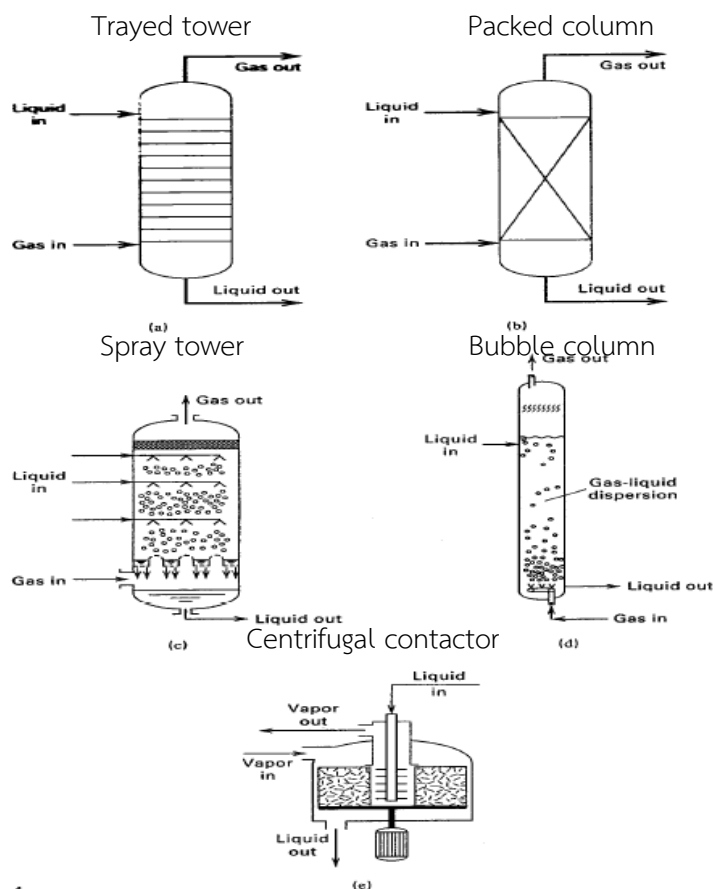


Figure 2. 1 Equipments for absorption process

In this study, bubble column is chosen as equipment for removal of gaseous contaminants from an exhaust air stream. Principle of this equipment is described below.

2.4 Bubble column

Bubble column reactors belong to the general class of multiphase reactors which consist of three main categories namely, the trickle bed reactor (fixed or packed bed), fluidized bed reactor, and the bubble column reactor. Bubble columns are the devices in which gas, in the form of bubbles, come in contact with the liquid. The purpose is to mix the two phases or substances transferred from one phase to another i.e. when the gaseous reactants are dissolved in liquid or when liquid reactant products are stripped. The bubble

column in which the gas is fed into the column at the bottom and rises in the liquid escaping from it at the upper surface; the gas is consumed to a greater or lesser extent depending on the intensity of mass transfer and chemical reaction as shown in figure 2.2 (Kantarci, Borak, & Ulgen, 2005).

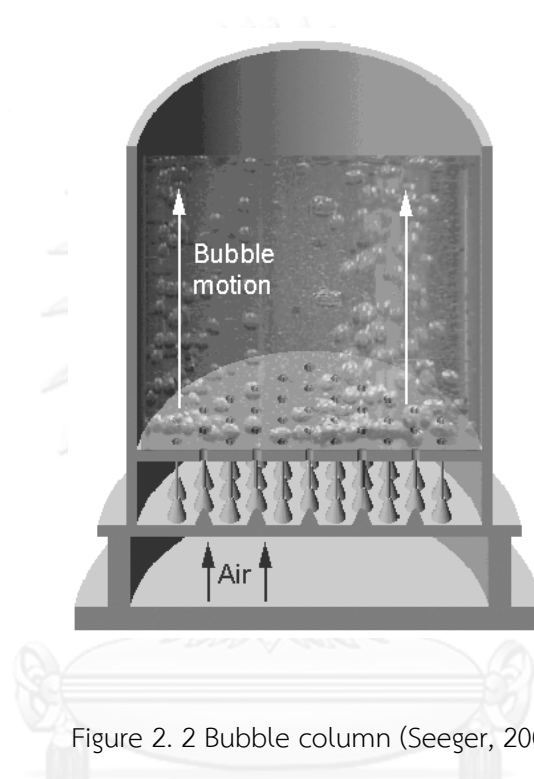


Figure 2. 2 Bubble column (Seeger, 2001)

Bubble column reactors have a number of advantages. First of all, they have excellent heat and mass transfer characteristics, meaning high heat and mass transfer coefficients. Little maintenance and low operating costs are required due to lack of moving parts and compactness. Due to its many advantages, bubble column were applied into the treatment process such as biochemical and chemical industries.

In order to apply the technique in this work, there are two parameters that have to be focused on:

1. Mass transfer parameters (i.e. the specific interfacial area and the individual mass transfer coefficient)

2. Hydrodynamic parameters (i.e. bubble size, gas distributor design, Bubble formation frequency, Bubble rising velocity)

2.5 Mass transfer parameters

Mass transfer is the movement of component molecules in a mixture from one place to another under the influence of a concentration difference in the system. However, the focus here is not on mass transported by this bulk fluid motion, but rather on the transport of one chemical species (or component) within a mixture of chemical species that occurs as a direct result of a concentration gradient and is independent of a pressure gradient. This type of mass transfer is called diffusion. In general, there are two types of mass transfer:

1. Molecular diffusion

Mass transfer is transferred by the random motion of molecules across a concentration gradient in a gas, liquid, or solid as a result of thermal motion.

2. Eddy diffusion

Mass transfer is occurred in turbulent flow, by the rapid process of mixing of the swirling eddies of fluid.

Normally, eddy diffusion often occur than in case of molecular diffusion because eddy diffusion is transferred by the rapid process of mixing, whereas molecular diffusion is transferred by the random motion of molecules. However, these two types of mass transfer can be occurred in the same time. Mass transfer of VOCs such as methanol in the solution, which is absorbed in the absorbate, is the mass transfer between phase and convective phase mass transfer. Mass transfer that is occurred between fluid and area depends on the characteristics of movement and the dynamics of fluid. The equation of convective mass transfer is given by Newton's law:

$$N_A = k_C \Delta C_A \quad (2.1)$$

Where: N_A = Molar flux of specie A with respect to coordinates that are fixed in space.

ΔC_A = the different of concentration of specie A between the area and average of fluid.

k_C = convective mass transfer coefficient.

The mass transfer was found in a low concentration of liquid phase. The equation 2.1 shows the relation between flux diffusion of substance and concentration gradient. Due to fluid through the area have a layer that occur near the surface of laminar flow the particles near the area of solid are fix in space. The mechanism of mass transfer between area and fluid are involved the diffusion of molecules in a layer of fluid fix flow or laminar flow, which is controlled by fluid film. Thus k_C value is defined as film coefficient that depends upon the system, fluid properties, and flow.

2.5.1 Fick's law of Diffusion

Fick's laws of diffusion describe about the diffusion and used to analyzed for the diffusion coefficient, D . They were derived by Adolf Fick in the year 1855.

Fick's first law relates the diffusive flux to the concentration field, by postulating that the flux goes from regions of high concentration to regions of low concentration, with a magnitude that is proportional to the concentration gradient (spatial derivative).

The Fick's first law defines the diffusion of A component in Z direction at constant temperature and pressure.

$$J = -D_{AB} \left(\frac{\partial C_A}{\partial z} \right) \quad (2.2)$$

where: J = the flux in Z direction

D_{AB} = the diffusion constant of A component that is diffusing in the specific solvent (B)

$\frac{\partial C_A}{\partial z}$ = the concentration gradient in Z direction.

The diffusion constant of a material is also referred to as diffusion coefficient or simply diffusivity. It is expressed in units of length²/time. The negative sign of the right side of the equation indicates that the impurities are flowing in the direction of lower concentration.

For de Groot's mathematic, the relation of flux does not specific at constant temperature and pressure thus; it means that the mass transfer flux was found by multiple of concentrations, the diffusion constant, and concentration gradient. This mathematic can be written as:

$$J = -cD_{AB} \left(\frac{\partial x_A}{\partial z} \right) \quad (2.3)$$

where: c = total molar concentration or molar density ($c = 1/U = \rho / M$)

x_A = mole fraction of species A

The equation (2.3) can also be written in the following equivalent mass form, where J_A is the mass flux of A by ordinary molecular diffusion relative to the mass-average velocity of the mixture in the positive z-direction, ρ is the mass density, and W_A is the mass fraction of A.

$$J = -\rho D_{AB} \left(\frac{\partial W_A}{\partial z} \right) \quad (2.4)$$

2.5.2 Diffusion coefficient

Diffusion coefficient is the proportionality factor D in *Fick's law* that implied the mass of the substance diffuses through a unit surface in a unit time at a concentration gradient of unity.

Owing to absorption process relate to solubility of gaseous molecule in liquid phase, one of the earliest equations for determining the diffusion coefficient in dilute solutions was the Stokes-Einstein equation, based on the model of motion of a spherical particle of diffusing substance A in a viscous liquid continuum B.

$$D_{AB} = \frac{kT}{b\pi r_0 \eta_B} \quad (2.5)$$

Where: D_{AB} = the diffusion coefficients of the component A in the solvent B

k = the Boltzmann's constant

T = temperature

r_0 = the particle (molecule) radius

η_B = the liquid viscosity

The constant b depends on the size of diffusing molecules: $b = 6$ for molecules larger than those of the base substance; $b = 4$ for identical molecules; and b can be less than 4 for smaller molecules.

2.5.3 Interphase mass transfer mechanism

The transport of mass within a single phase depends directly on the concentration gradient of the transporting species in that phase. Mass may also transport from one phase to another, and this process is called interphase mass transfer. Many physical situations occur in nature where two phases are in contact, and the phases are separated by an interface. Like single-phase transport, the concentration gradient of the transporting species (in this case in both phases) influences the overall rate of mass transport. More precisely, transport between two phases requires a departure from equilibrium, and the equilibrium of the transporting species at the interface is of principal concern. When a multiphase system is at equilibrium, no mass transfer will occur. When a system is not at equilibrium, mass transfer will occur in such a manner as to move the system toward equilibrium.

2.5.4 Two-resistance theory

(Whitman, 1924) proposed a two-resistance theory, which has been shown to be appropriate for many interphase mass transfer problems. Interphase mass transfer involves three steps include:

1. The transfer of oxygen from the bulk air to the surface of the water.
2. The transfer of oxygen across the interface.
3. The transfer of oxygen from the surface of the air to the bulk water.

The general theory has two principal assumptions, which for the case of oxygen transporting from air to water are:

1. The rate of mass transfer between two phases is controlled by the rate of diffusion through the phases on each side of the interface.
2. No resistance is offered to the transfer of the diffusing component across the interface.

The transfer of component A from the gas phase to the liquid phase may be graphically illustrated as in Figure 2.3, with a partial pressure gradient from the bulk gas composition, $p_{A,G}$, to the interfacial gas composition, $p_{A,i}$, and a concentration gradient in the liquid from, $c_{A,i}$, at the interface to the bulk liquid concentration, $c_{A,L}$. If no resistance to mass transfer exists at the interfacial surface, $p_{A,i}$ and $c_{A,i}$ are equilibrium concentrations; these are the concentration values which would be obtained if the two phases had been in contact for an infinite period of time. The concentrations $p_{A,i}$ and $c_{A,i}$ are related by thermodynamic relations. The interfacial partial pressure, $p_{A,i}$, can be less than, equal to, or greater than $c_{A,i}$ according to the equilibrium conditions at the temperature and pressure of the system. When the transfer is from the liquid phase to the gas phase, $c_{A,L}$ will be greater than $c_{A,i}$ and $p_{A,i}$ will be greater than $p_{A,G}$.

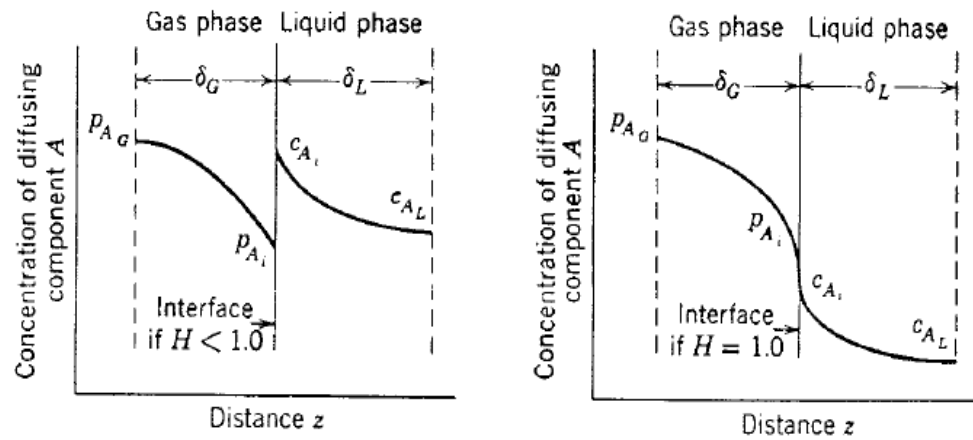


Figure 2. 3 Concept of two-resistance theory

2.5.5 Individual mass transfer coefficients

Restricting our discussion to the steady-state transfer of component A , we can describe the rates of diffusion in the z direction on each side of the interface by the equations

$$N_{A,Z} = k_G(p_{A,G} - p_{A,i}) \quad (2.6)$$

and

$$N_{A,Z} = k_L(c_{A,i} - p_{A,G}) \quad (2.7)$$

where k_G is the convective mass-transfer coefficient in the gas phase, in [moles of A transferred/(time) (interfacial area) (Δp_A units of concentration)]; and k_L is the convective mass-transfer coefficient in the liquid phase, in [moles of A transferred/(time) (interfacial area) (Δc_A units of concentration)]. The partial pressure difference, $p_{A,G} - p_{A,i}$, is the driving force necessary to transfer component A from the bulk gas conditions to the interface separating the two phases. The concentration difference, $c_{A,G} - c_{A,i}$, is the driving force

necessary to continue transfer of A into the liquid phase. Under steady-state conditions, the flux of mass in one phase must equal the flux of mass in the second phase. Combining equations (2.6) and (2.7), we obtain

$$N_{A,Z} = k_G(p_{A,G} - p_{A,i}) = k_L(c_{A,i} - p_{A,G}) \quad (2.8)$$

The ratio of the two convective mass-transfer coefficients may be obtained from equation (2.8) by rearrangement, giving

$$-\frac{k_L}{k_G} = \frac{p_{A,G} - p_{A,i}}{c_{A,L} - c_{A,i}} \quad (2.9)$$

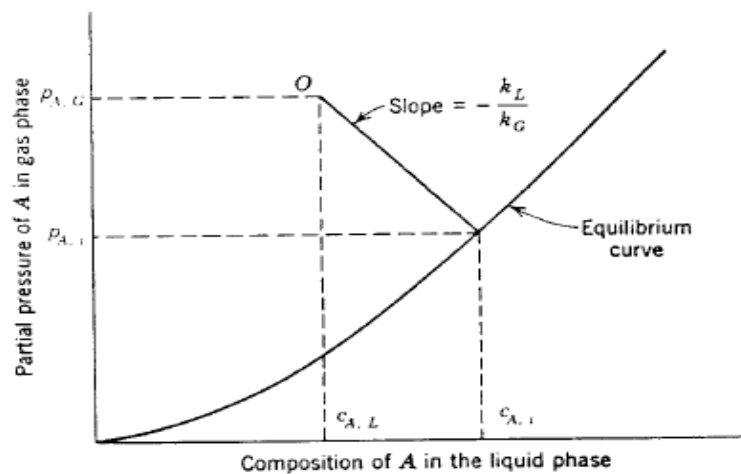


Figure 2. 4 Interfacial compositions as predicted by the two-resistance theory.

2.5.6 Overall mass transfer coefficients

It is quite difficult to measure physically the partial pressure and concentration at the interface. It is therefore convenient to employ overall coefficients based on an overall driving force between the bulk compositions, $p_{A,G}$ and $c_{A,L}$. An overall mass transfer coefficient may be defined in terms of a partial pressure driving force. This coefficient, K_G , must account for entire diffusional resistance in both phases; it is defined by

$$N_A = K_G(p_{A,G} - p_A^*) \quad (2.10)$$

where $p_{A,G}$ is the bulk composition in the gas phase; p_A^* is the partial pressure of A in equilibrium with the bulk composition in the liquid phase, $c_{A,L}$, and K_G is the overall mass-transfer coefficient based on a partial pressure driving force, in moles of A transferred/(time) (interfacial area) (pressure). Since the equilibrium distribution of solute A between the gas and liquid phases is unique at the pressure and temperature of the system, then p_A^* , in equilibrium with $c_{A,L}$, is as good a measure of $c_{A,L}$ as $c_{A,L}$ itself, and it is on the same basis as $p_{A,G}$. An overall mass transfer coefficient, K_L , including the resistance to diffusion in both phases in terms of liquid phase concentration driving force, is defined by

$$N_A = K_L(c_A^* - c_{A,L}) \quad (2.11)$$

where c_A^* is the concentration of A in equilibrium with $p_{A,G}$ and is accordingly, a good measure of $p_{A,G}$; K_L is the overall mass-transfer coefficient based on a liquid concentration driving force, in [moles of A transferred/(time) (interfacial area) (moles/volume)]. Figure 2.5 illustrates the driving forces associated with each phase and the overall driving forces. The ratio of the resistance in an individual phase to the total resistance may be determined by:

$$\frac{\text{resistance in gas phase}}{\text{total resistance in both phases}} = \frac{\Delta p_{A,gasfilm}}{\Delta p_{A,total}} = \frac{1/k_G}{1/K_G} \quad (2.12)$$

$$\frac{\text{resistance in liquid phase}}{\text{total resistance in both phases}} = \frac{\Delta p_{A,liquidfilm}}{\Delta p_{A,total}} = \frac{1/k_L}{1/K_L} \quad (2.13)$$

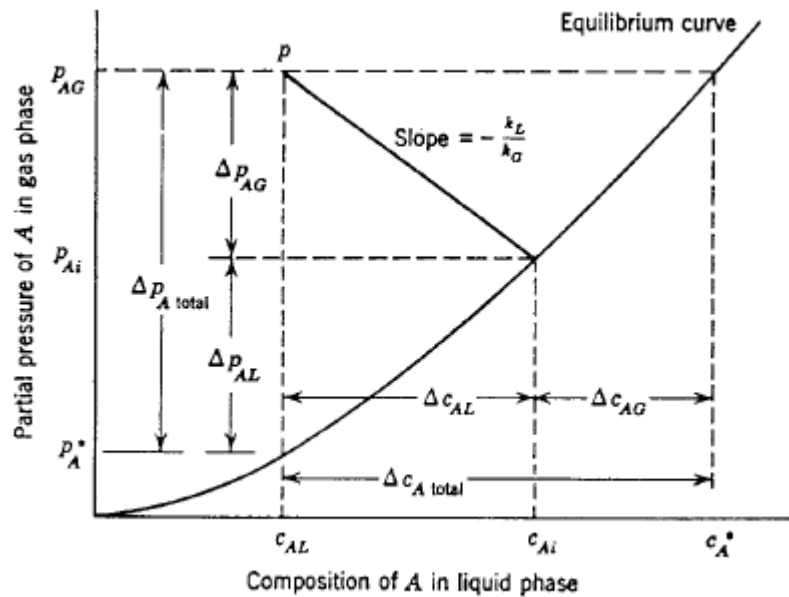


Figure 2. 5 Concentration driving forces for two-resistance theory.

A relation between these overall coefficients and the individual phase coefficients can be obtained when the equilibrium relation is linear as expressed by

$$p_{A,i} = mc_{A,i} \quad (2.14)$$

This condition is always encountered at low concentrations, where Henry's law is obeyed; the proportionality constant is then the Henry's law constant, H . Utilizing equation (2.14), we may relate the gas- and liquid-phase concentrations by:

$$p_{A,G} = mc^*$$

$$p_A^* = mc_{A,L}$$

$$p_{A,G} = mx_A^*$$

Rearranging equation (2.10),

$$\frac{1}{K_G} = \frac{p_{A,G} - p_A^*}{N_{A,Z}} = \frac{p_{A,G} - p_{A,i}}{N_{A,Z}} + \frac{p_{A,i} - p_A^*}{N_{A,Z}} \quad (2.15)$$

or, in terms of m ,

$$\frac{1}{K_G} = \frac{p_{A,G} - p_{A,i}}{N_{A,Z}} + \frac{m(c_{A,i} - c_{A,L})}{N_{A,Z}} \quad (2.16)$$

The substituting of equation (2.6) in (2.7) into the above relation relates K_G to the individual phase coefficients by

$$\frac{1}{K_G} = \frac{1}{k_g} + \frac{m}{k_L} \quad (2.17)$$

A similar expression for k_L may be derived as follows:

$$\frac{1}{K_G} = \frac{c_A^* - c_{A,L}}{N_{A,Z}} = \frac{p_{A,G} - p_{A,i}}{mN_{A,Z}} + \frac{c_{A,i} - c_{A,L}}{N_{A,Z}}$$

or

$$\frac{1}{K_G} = \frac{1}{mk_g} + \frac{1}{k_L} \quad (2.18)$$

Equation (2.17) and (2.18) stipulate that the relative magnitudes of the individual phase resistances depend on the solubility of the gas, as indicated by the magnitude of the proportionality constant.

For a system involving a soluble gas, such as ammonia in water, m is very small. From equation (2.17), we may conclude that the gas-phase resistance is essentially equal to the overall resistance in such a system. When this is true, the major resistance to mass transfer lies in the gas phase, and such a system is said to be *gas phase controlled*.

Systems involving gases of low solubility, such as carbon dioxide in water, have such a large value of m that equation (2.18) stipulates that the gas-phase resistance may be neglected, and the overall coefficient, k_L , is essentially equal to the individual liquid phase coefficient, k_L . This type of system is designated *liquid phase controlled*. In many systems, both phase resistances are important and must be considered when evaluating the total resistance.

2.5.7 Overall mass transfer coefficient in liquid phase ($k_L a$)

In the case of benzene absorption in water, it can be noted that this process is the liquid phase controlled. Thus the $k_L a$ value is used to analyze the absorption process. The mathematic used to determine $k_L a$ value can be described as follows.

The gas concentrations at different times can be determined from measurements with a semi-batch reactor to calculate mass balance between gas and liquid phases. The mass balance equation can be applied:

$$Q_g C_{g,in} = Q_g C_{g,out}(t) + V_L \frac{\partial C_L(t)}{\partial t} \quad (2.19)$$

where: Q_g = the flow rate

V_L = the absorbent volume

$C_{g,in}$ = the inlet concentration of hydrophobic benzene in the gas phase

$C_{g,out}$ = the outlet concentration of hydrophobic benzene in the gas phase.

Therefore, the concentration of benzene in the liquid phase $C_L(t)$ can be determined by using the equation below.

$$C_L(t) = \frac{Q_g}{V_L} (C_{g,in} t - \int C_{g,out}(t) dt) \quad (2.20)$$

From equation 2.20, the concentrations of benzene in the liquid phase at different times and also the saturated benzene concentration can be obtained.

According to the non-stationary or dynamic method (Deckwer, 1992), the overall mass transfer coefficient in liquid phase ($k_L a$) can be written as the following equation;

$$\frac{\partial C_L}{\partial t} = k_L a (C_L^S - C_L) \quad (2.21)$$

or

$$\ln[C_L^S - C_L] = \ln C_L^S - k_L a \cdot t \quad (2.22)$$

where: C_L = the hydrophobic benzene concentration

C_L^S = the saturation benzene concentration in the liquid phase.

The $k_L a$ coefficient can be deduced from the slope of the curve relating the variation of $\ln(\Delta C/C_L^S)$ with time.

2.5.8 Liquid-side mass transfer coefficient (k_L)

The volumetric mass transfer coefficient ($k_L a$) is the product of the liquid-side mass transfer coefficient and the interfacial area. Normally, the local liquid-side mass transfer coefficient is determined by:

$$k_L = \frac{k_L a}{a} \quad (2.23)$$

Where: k_L = liquid-film mass transfer coefficient (m/s)

$k_L a$ = the overall mass transfer coefficient in liquid phase (s^{-1})

a = specific interfacial area (m^{-1})

2.6 Bubble hydrodynamic parameters

Due to the bubble hydrodynamic parameters is a significant factor that effect to removal efficiency of benzene by using absorption process, this section will talk about bubble hydrodynamic parameters that are used to determine interfacial area of bubbles in this process.

2.6.1 Bubble diameter (d_b)

In practice, the measurement of bubble diameter at any flow rate (Q_g) can be determined by image treatment technique. This technique has been captured and analyzed 100-200 bubbles at any flow rate to be a good statistical representative. In this study, the average diameter (d_{avg}) and Sauter diameter (d_{32}) can be calculated by using the equations below.

$$d_{avg} = \frac{\sum_{i=1}^N d_i}{N} \quad (2.24)$$

$$d_{32} = \frac{\sum_{i=1}^N d_i^3}{n \sum_{i=1}^N d_i^2} \quad (2.25)$$

2.6.2 Bubble rising velocity (U_B)

Fig. 2.6 shows, for the different liquid phases, the relation existing between the terminal rising bubble velocity and the bubble diameter generated. This also presented the experimental U_B values obtained by (Grace & Wairegi, 1986).

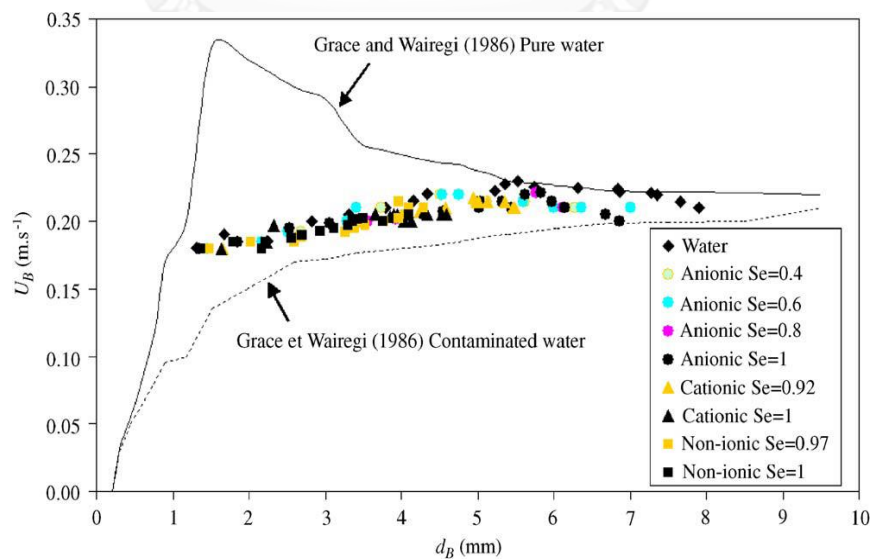


Figure 2. 6 The relationship between bubble rising velocity and bubble diameter

2.6.3 Bubble formation frequency (f_B)

The frequency of bubble formation is the amount of bubbles that is sparged within one second. It can be calculated from the number of orifices multiply with gas flow rate of each orifices, and divided by volume of bubble as following the equation (2.26) (Painmanakul et al., 2005).

$$f_B = \frac{N_{OR} \times q}{V_B} \quad (2.26)$$

where: f_B = bubble formation frequency, s^{-1}

N_{OR} = number of orifices

q = gas flow rate through the orifice, m^3/s

V_B = bubble volume, m^3

2.6.4 Specific interfacial area (a)

Specific interfacial area is defined as the ratio between interfacial area of bubble and capacity of reactor at a certain time. Because there are some limitations about data analysis such as chemical method, analysis of reactor, type of bubble generator, and conditions, the interfacial area is commonly included with mass transfer coefficient for considering the ability of mass transfer between gas and liquid phases.

For more understand the mechanism of mass transfer of bubble reactor, this research will be essential to the interfacial area (a) and mass transfer coefficient (k_L). In general, the interfacial can be calculated by using the equations below.

$$N_B = f_B \times \frac{H_L}{U_B} \quad (2.27)$$

$$a = N_B \times \frac{S_B}{V_{total}} = f_B \times \frac{H_L}{U_B} \times \frac{\pi D_B^2}{4H_L + N_B V_B} \quad (2.28)$$

where: a = interfacial area, m^{-1}

N_B = number of bubbles generated

S_B = total bubble surface, m^2

V_{total} = total volume in reactor, m^3

f_B = bubble formation frequency, s^{-1}

H_L = liquid height, m

U_B = bubble rising velocity (cm/s)

D_B = bubble diameter, m

A = cross-sectional area of reactor, m^2

V_B = bubble volume, m^3

2.7 Diffuser

Air Diffuser also known as bubble diffuser is a device that was used to generate air bubbles into water or wastewater in order to increase the dissolved oxygen content to supply micro-organisms with oxygen. Bubble diffusers typically consist of tubes, plates, or discs perforated with a large number of regularly spaced holes. Air is pumped through the diffuser heads, thereby generating the bubbles which facilitate the process. Bubble size plays an important role in the efficiency of a bubble diffuser. In the past, fairly coarse diffuser holes were used; it was believed that a larger bubble size ensured quicker rise rates and better distribution of oxygen. Current trends have tended to use smaller holes because research has shown that a finer bubble mass is more efficient at oxygenation in most applications (EPA, 1989). Diffused aeration systems can be classified into three categories:

- Porous (fine bubble) diffusers: Fine pore diffusers are mounted or screwed into the diffuser header pipe (air manifold) that may run along the length or width of the tank or on a short manifold mounted on a movable pipe (lift pipe). These diffusers come in various shapes and sizes, such as discs, tubes, domes, and plates.

- Nonporous (coarse bubble) diffusers: The common types of nonporous diffusers are fixed orifices (perforated piping, spargers, and slotted tubes); valve orifices; and static tubes. The bubble size of these diffusers is larger than the porous diffusers, thus lowering the oxygen transfer efficiency.

- Other diffusion devices: These include jet aerators (which discharge a mixture of air and liquid through a nozzle near the tank bottom); aspirators (mounted at the basin surface to supply a mixture of air and water); and U tubes (where compressed air is discharged into the down leg of a deep vertical shaft).

2.8 Surfactant

A surfactant is defined as a material that can greatly reduce the surface tension of water though low concentrations are used. This molecule is made up of a water soluble (hydrophilic) and a water insoluble (hydrophobic) component as shown in Figure 2.7.

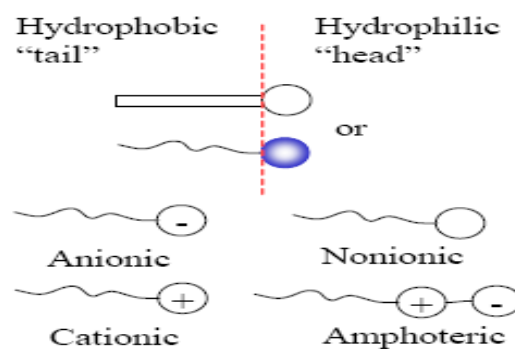


Figure 2. 7 Generalized surfactant structures

Surfactants can be grouped by the charge characteristic of their polar (hydrophilic) head groups (Figure 2.7). The four groups include:

1. Anionic surfactants are those that have a negative charge on their polar head group. They include groups like carboxylic acids, sulfates, sulfonic acids, and phosphoric acid derivatives.

2. Cationic surfactants contain cationic functional groups at their head such as, amines, alkylimidazolines, alkoxylated amines, and quaternized ammonium compounds.

3. Amphoteric surfactants have both cationic and anionic centers attached to the same molecule. This characteristic is termed “zwitterionic”.

4. Non-ionic surfactants contain no specific charge. These are termed non-ionic surfactants and are used most often as emulsifiers and conditioning ingredients.

2.9 Micelles

In aqueous solution, molecules having both polar or charged groups and non-polar regions form aggregates called micelles. In a micelle, polar or ionic heads form an outer shell in contact with water, while non-polar tails are sequestered in the interior. Hence, the core of a micelle, being formed of long non polar tails, resembles an oil or gasoline drop. The length of the non-polar tail, the nature and size of the polar or ionic head, the acidity of the solution, the temperature, and the presence of added salts are the most important factors determining the kind of the obtained aggregate. If those parameters are changed, it is possible to change shape and size of the micelles. The micelle in aqueous solution is shown in Figure 2.8.

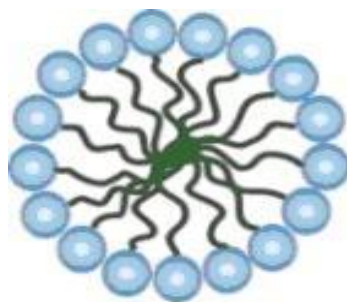


Figure 2. 8 Schematic representation of a micelle in aqueous solution

Micelles are widely used in industrial and biological fields for their ability to dissolve and move non polar substances (VOCs) through an aqueous medium, or to carry drugs which are, often, scarcely soluble in water. The carrying ability of micelles can be altered if parameters determining their size and shape are changed.

Micelle aggregates form only when the concentration of the amphiphilic molecule reaches a given concentration called critical micelle concentration (cmc). The condition is monitored by the sudden change in the chemical and physical properties of the solution. On the contrary, below cmc micelles are completely absent.

From the ability of the surfactant that can absorb VOCs, this research will applied it as an absorbent (solvent) for comparison with tap water in order to study the effect of mass transfer mechanism in bubble column reactor.

Due to objective of this study is to develop a technique to lower concentration of benzene, adsorption technique is the one technique that was chosen for working with absorption technique to enhance removal efficiency of benzene. The deep detail of adsorption process is described below.

2.10 Adsorption

The principle of this technique is used to remove individual components from a gas or liquid mixture. The component to be removed is physically or chemically bonded to a solid surface. The component that is removed from a gas or liquid mixture by adsorption can either be a product that is wanted or an impurity. Various types of adsorbent in large scale have been used activated carbon, zeolite, silica gel etc. For this work, activated carbon was chosen as an adsorbent in order to enhance benzene removal efficiency.

Activated carbon is an adsorbent that is widely used in adsorption processes. It consists of a network of interconnected pores of varying sizes which are classified by their diameter; micropores < 2.0 nm, mesopores 2-50 nm, and macropores > 50.0 nm. The pores provide a large internal surface area typically ranging from 800 to 1,200 m²/g, which enables activated carbon to adsorb contaminants from water. Activated carbon has been successfully employed as adsorbent catalyst support because of their well-developed porous structures, and surface functional groups. These porous materials can be used for the adsorption of a wide range of species from either gas or liquid phases. An important aspect in the treatment of aqueous systems using activated carbon is that it can be used to remove both organic and inorganic species.

2.11 Literature Review

2.11.1 Absorption technique

Bouaifi (2001) have studied the comparison of the gas hold-up, bubble size, interfacial area and mass transfer coefficients in stirred gas-liquid reactors and bubble columns. The results indicated that there are no important difference between bubble diameters provided by the two reactors. For the same total power consumption, the interfacial area created by the bubble columns is about 30% higher than that created by the stirred axial dual impeller systems. The volumetric transfer coefficient obtained with bubble columns are higher than those provided by the stirred gas-liquid reactor. This difference is explained by the higher values of interfacial area obtained in bubble columns.

Loubière (2003) have investigated the bubble formation generated and gas flow rates from flexible orifices (membrane) in no viscid liquid. They found that an increasing gas flow rate intensifies the phenomenon of the bubble spread on the membrane surface. The variation in the bubble diameter at detachment as a function of gas flow rate is logarithmic and its result indicates that small bubbles generated by the membrane remain stable in the face of coalescence or breaking phenomena. The industrial membranes produce bubbles of comparable sizes. Nevertheless, significant differences in the bubble frequencies between membranes are observed, involving different gas hold-up. For the bubbles generated from a flexible orifice, the real forces governing the bubble growth are the buoyancy force, the surface tension force and near detachment the inertial force.

Painmanakul (2004) have studied the performance of single orifice and four orifices that were used in waste water treatment by ONDEO-DEGREMONT Company. The two membranes were compared in terms of the interfacial area and the power consumption and the results show that the interfacial areas increase with the gas velocity through the orifice for both membranes. Also, for a given superficial gas velocity, the interfacial areas of the new membranes with a single and four orifices are smaller than those of the old ones. For a given power consumption, the interfacial areas are close in value for both membrane.

Painmanakul (2005) study the effect of surfactants (cationic and anionic) on bubble generation phenomenon, interfacial area and liquid-side mass transfer coefficient. The local liquid-side mass transfer coefficient (k_L) was obtained from the volumetric mass transfer coefficient ($k_L a$) and the interfacial area (a) was deduced from the bubble diameter (d_B), the bubble frequency (f_B) and the terminal bubble rising velocity (U_B). They report that the volumetric mass transfer coefficient increases with the gas flow rates for all liquid phases, and the $k_L a$ and k_L values for both surfactants are significantly smaller. Also the liquid-side mass transfer coefficient remains roughly constant for a given liquid phase.

2.11.2 Adsorption technique

Shepherd (2001) has studied the characteristics of activated carbon and its applicability for treatment of VOCs emission. He report that activated carbon has been shown to be applicable for treatment of a wide variety of environmental contaminants. It is a proven technology that is simple to install and easy to operate and maintain. Capital

costs are among the least expensive for most alternative treatment technologies. Operating costs are primarily related to the amount of activated carbon consumed in the adsorption process.

Pavoni, Drusian (2006) have studied the removal efficiency of five commercial activated carbons by determining their Freundlich adsorption isotherms and choosing the best among them to verify the removal efficiency of the chlorinated compounds by continuum absorption on a fixed bed of granular activated carbon. They found that the removal efficiency was always higher than 90%. Optimization of operative conditions was necessary for scaling-up to a real plant column. Based on this technology a $50 \text{ m}^3 \text{ h}^{-1}$ real plant was built to remove chlorinated organic compounds from industrial effluents in June 2004.

Asenjo (2011) have studied the performance of activated carbon in the liquid phase adsorption of benzene and/or toluene from synthetic solutions and an industrial wastewater. They indicate that a coal-tar-derived mesophasic carbon was chemically activated to produce a high surface area ($\sim 3200 \text{ m}^2/\text{g}$) carbon with a porosity made up of both micropores and mesopores. Its adsorption capacities were found to be among the highest ever reported in literature, reaching values of 860 mg/g and 1200 mg/g for the adsorption of benzene and toluene, respectively, and 1,200 mg/g for the combined adsorption of benzene and toluene from an industrial wastewater. Furthermore, they found that the adsorption capacities of the activated carbon were similar both for the synthetic mixtures and for the industrial wastewater, which confirms the suitability of this material for use under practical conditions at industrial scale.

2.12 Research focuses

From literatures of previous researches, either an absorption or an adsorption process was used to decrease concentration of benzene, which based on concentration, flow rate of the vent gas and others factors such as low cost and safety. Nevertheless, there are very few data available to found for analyzing the effect of different type of diffuser and liquid phase. Thus, this research work aims to study on the effect of bubble hydrodynamic and liquid phase on mass transfer mechanism in bubble column, Moreover, the overall mass transfer coefficient of the combination absorption and adsorption processes were also studied.

Therefore, the following points have to be considered in order to understand mechanism of these processes:

- The bubble hydrodynamic parameters (D_B , U_B , f_B , and a) and mass transfer parameters ($k_L a$ and k_L) of different diffusers, and liquid phases.
- The adsorption characteristic of granular activated carbon capacity of benzene in gas phase and liquid phase system.
- The overall mass transfer coefficient of the combination between absorption and adsorption processes was determined.

CHAPTER III

METHODOLOGY

3.1 Research overview

The experiment framework can be shown in Figure 3.1

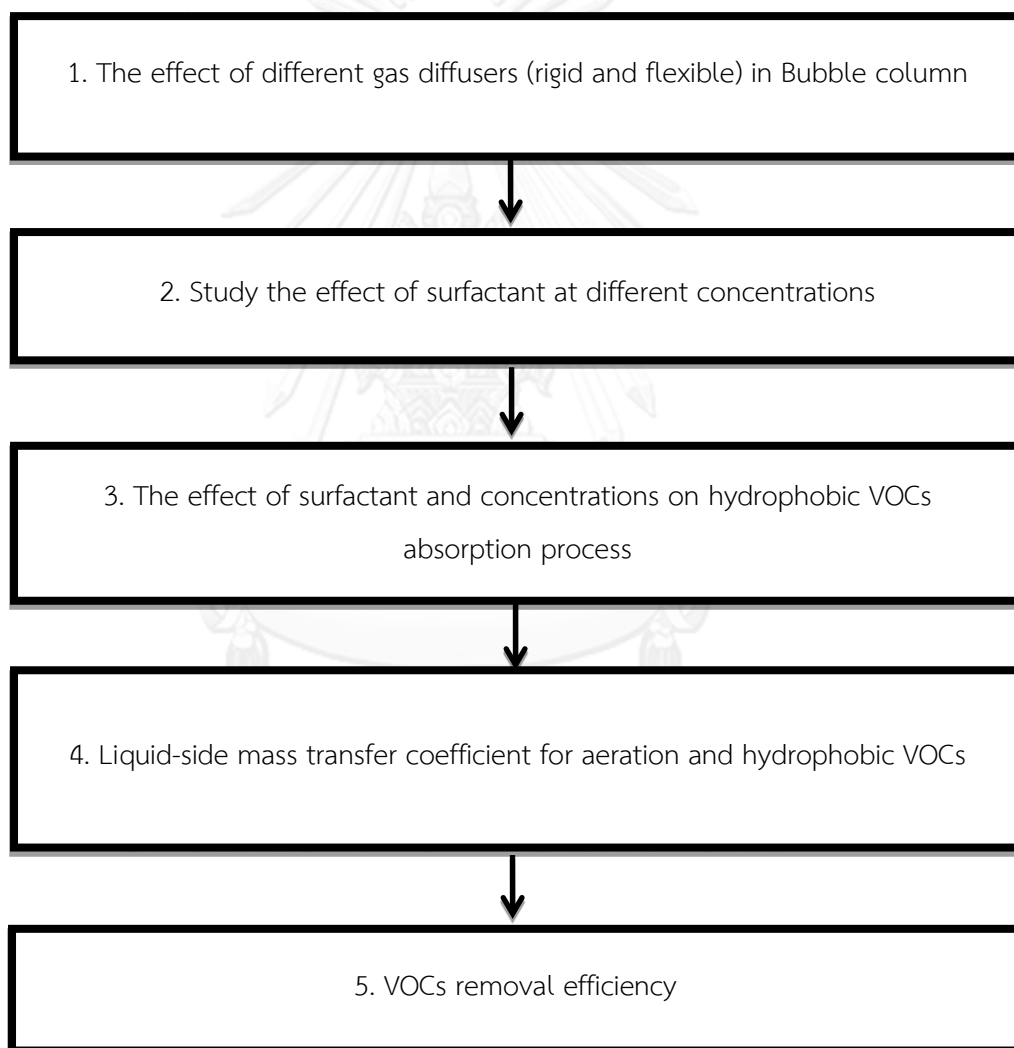


Figure 3. 1 Experiment framework of this research

3.2 Experimental setup

The experimental setup is schematically represented in Figure 3.2. The experiments are carried out in a bubble column: 10 cm in diameter (1). Air was generated by air pump (2). The flow of air is regulated by a gas flow meter (3). All chemical solutions (4) are injected at the top of the column. For analyzing the bubble hydrodynamic mechanism, the high speed camera (100 images/sec) and image analysis program (5) were used to determine the bubble hydrodynamic parameters. The operating conditions are: liquid height (H_L) = 72 cm and temperature is at room temperature.

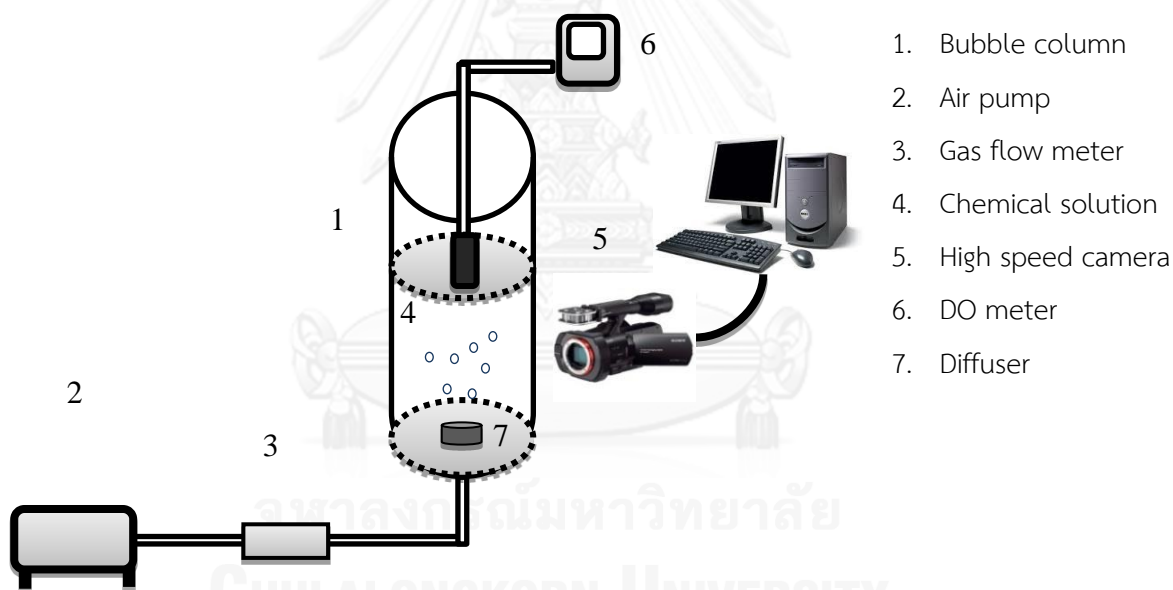


Figure 3. 2 Schematic diagram of the experimental setup

Benzene concentrations were measured by using UV-VIS spectrophotometer and gas chromatography with a Flame Ionization Detector (FID). For analyzing the bubble hydrodynamic mechanism, the high speed camera (100 images/second) and image analysis program were used to determine the bubble hydrodynamic parameters.

3.3 Benzene gas generator

In order to generate benzene gas in this study, 250 mL volumetric flask contained with pure benzene, and then the preliminary runs were carried out to verify the conditions that required for the generation of the concentration of benzene gas. After that, the air is injected at different gas flow rates to obtain the different inlet benzene gas. Finally, UV-Visible spectrophotometer and gas chromatography were used to measure the amount of benzene. System of benzene generator was shown in Figure 3.3.

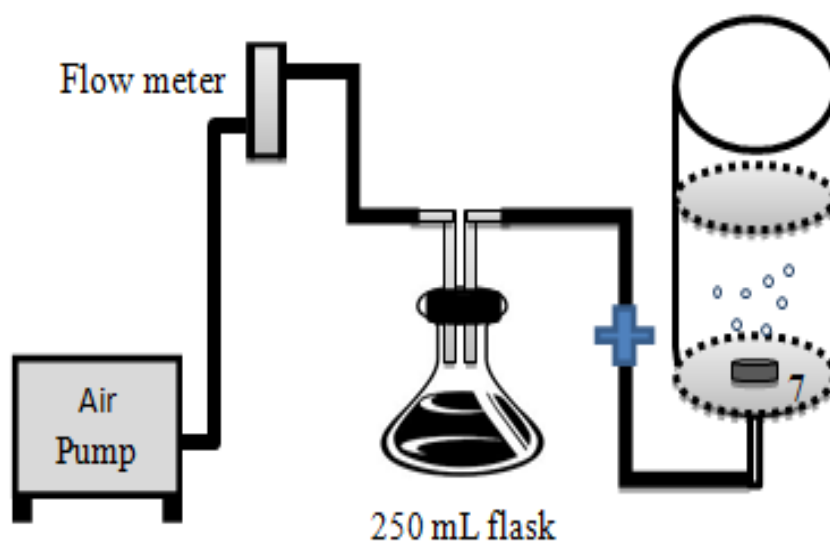


Figure 3. 3 Benzene generator

3.4 Gas Chromatography Detector FID, Agilent Technologies 6890N

In this study, the Agilent Technologies gas chromatograph 6890N with flame ionization detector (FID) and a split injector, operated in split ratio (10:1) was used for quantification of benzene. The conditions of GC parameters were shown in Table 3.1.

Table 3. 1 The conditions of GC parameters

Parameter	Condition
Temperature of injection port and detector	100 - 200 °C
Column Type	HP-1
Column Size	25 m x 0.32 mm i.d., 0.17 μ m film thickness
Detector	FID, 300 °C
Carrier gas	He

3.5 UV-Visible spectrophotometer

For this work, the concentration of benzene outlet was measured by using Genesis 10S UV-Vis spectrophotometer. The absorbance of benzene at 254 nm was recorded and the concentration of benzene was calculated using the calibration curve.

3.6 High speed camera and image analysis program

In this work, benzene bubbles were generated by rigid orifice was captured with a high speed 100 image/sec (Basler camera) as shown in Figure 3.4. Then, the images were visualized on the acquisition computer through the Pylon Viewer vision software and analyzed by the bubble measuring software as shown in Figure 3.5.



Figure 3. 4 Basler camera



Figure 3. 5 Software with License Dongle

3.7 Materials and chemicals

- Equipments

1. Flow meter
2. Air pump
3. DO meter
4. Air bag
5. Bubble column
6. UV-Visible Spectrophotometer
7. Gas chromatography, Detector FID, program Agilent Technologies
8. High speed camera and Image analysis program 6890

- Diffuser

The diffusers used were rigid orifices and flexible membrane diffusers as show in Figure 3.6. The bubbles were generated by diffuser located at the center bottom of the column. The physical characteristics of diffusers and the operating conditions were reported in Table 3.2.

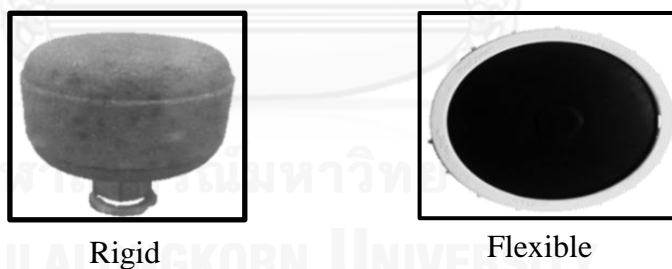


Figure 3. 6 Rigid and flexible diffuse

Table 3. 2 Physical characteristics of diffusers and operating conditions

Diffuser type	Air flow (Nm ³ /hr)	Thickness (mm)	Elongation at Failure (%)	Company
Rigid	-	-	-	-
Flexible	2.5 - 5.0	1.65	800	Envitrade Engineering Co., Ltd.

- Absorbent

To understand the effect of surfactants on the mass transfer efficiency, it is essential to well characterize the liquid phases under test: tap water and aqueous solution of commercial surfactants: cationic, anionic, and non-ionic. For this work, the liquid-phase characterizations were consisted in comparing 5 types of surfactants with the different applied gas flow rates, and studied the mass transfer and bubble hydrodynamic parameters. Characteristics of each surfactant were shown in Table 3.3.

Table 3. 3 Characteristics of surfactant and water

Absorbent	Chemical name	MW (g/mol)	CMC (mg/L)	Concentration		Surface tension (mN/m)
				CMC	mg/L	
Cationic	Dodecyl trimethyl ammonium bromide (DTAB)	308.38	4245	0.01	42.45	59.2
				0.1	425.5	41.4
Anionic	Sodium 2-ethylhexyl sulfate (SES)	232.27	2879	0.01	28.79	58
				0.1	287.9	37.4
				1.0	2879	33.2
				3.0	8637	31.7
Non-ionic	Polyoxyethylene (5) Lauryl ether (Dehydol LS 5 TH)	406.6	25.21	0.01	0.2521	57.5
				0.1	2.521	48.1
	Polyoxyethylene (20) sorbitan monooleate (Tween 80)	1310	15.7	0.1	0.000001 2	59.3
				1.0	0.00012	44.2
				3.0	0.00036	43.5
				-	-	-
Water	-	18	-	-	-	72

- **Adsorbent**

1. Granular Activated Carbon (Filtrisorb) was purchased from Calgon Carbon Corporation Company

- **Chemicals**

1. Benzene (C₆H₆, AR grade, 99%) was purchased from Roongsub Chemical Company.
2. Sodium sulfite (Na₂SO₃, AR grade, 99.99 % purity) was purchased from Ajax Finechem, Australiz Company.
3. Hydrogen (H₂, HP grade, 99.99 % purity)
4. Helium (He, HP grade, 99.99 % purity)
5. Nitrogen (N₂, HP grade, 99.99 % purity)
6. Air-zero (O₂, HP grade, 99.99 % purity)

3.8 Analytical methods

3.8.1 Determination of bubble hydrodynamic parameters

- *Bubble diameter (d_p)*

The bubble diameter at any flow rate (Q_g) can be measured by image analysis technique. The 100-150 bubbles were captured and analyzed at any flow rate to get the good statistical data. In this study, the average diameter (d_p) can be calculated by using the equation below.

$$d_{32} = \frac{\sum_{i=1}^N d_i^3}{\sum_{i=1}^N d_i^2} \quad (3.1)$$

- *Terminal rising bubble velocity (U_B)*

According to (Deckwer, 1992), in terms of the different liquid phases, the U_B values can be determined from the relation existing between the terminal rising bubble velocity and the bubble diameter generated.

- *Local interfacial area (a)*

The local interfacial area is defined as the ratio between the bubble surfaces (S_B) and the total volume in the reactor (V_{Total}):

$$a = N_B \times \frac{S_B}{V_{Total}} \quad (3.2)$$

N_B is the number of bubbles that can be deduced from the bubble rising velocities (U_B) and the bubble formation frequency (f_B). The interfacial area is expressed in Equation 3.3.

$$a = N_B \times \frac{S_B}{V_{total}} = f_B \times \frac{H_L}{U_B} \times \frac{\pi D_B^2}{A H_L + N_B V_B} \quad (3.3)$$

A and H_L are the cross-sectional area of the bubble column and the liquid height, respectively. Moreover, according to the hydrodynamic parameter determination method proposed by Painmanakul et al. (2006) the bubble diameters can be correctly determined by an image analysis. This experimental approach can be applied to determine the value of (a) in this work.

3.8.2 Mass transfer parameter determination

In this study, the experimental approach presented in (Deckwer, 1992) is used to determine the specific interfacial area (a) and the corresponding volumetric mass transfer coefficient ($k_L a$). Thus, the liquid-side mass transfer coefficient (k_L) can be calculated.

- *Volumetric mass transfer coefficient ($k_L a$)*

In the case of the gas which is relatively insoluble in the liquid, such as oxygen in water, the solubility of oxygen is very low. It can be noted that this process is the controlled liquid phase. Thus, the $k_L a$ value is used to analyze the absorption process. The equation that used to determine the $k_L a$ value can be written as follows;

$$\frac{\partial C_L}{\partial t} = k_L a (C_L^S - C_L) \quad (3.4)$$

where C_L is the dissolved oxygen concentration, and C_L^S is the saturated oxygen concentration in the liquid. Notably, sodium sulfite (Na_2SO_3) was used in this research in order to decrease the amount of dissolved oxygen in water before analyzing at any flow rate. The oxygen concentration in the liquid phase is measured by the UNISENSE oxygen micro-sensor which is a miniaturized Clark-type oxygen sensor with an internal reference and a guard cathode.

- *Liquid-side mass transfer coefficient (k_L)*

The liquid-side mass transfer coefficient (k_L) was performed to understand the effects of surfactants molecules on the bubble column. The k_L values were obtained from the volumetric mass transfer coefficient ($k_L a$) and the interfacial area (a) was deduced from the bubble diameter (d_B). Thus, the optimal type and concentration of surfactant likely to be selected in this research by considering the k_L value in order to enhance the efficiency of the bubble column. The local liquid-side mass transfer coefficient is simply determined by:

$$k_L = \frac{k_L a}{a} \quad (3.5)$$

3.8.3 Removal efficiency

Benzene removal efficiency ($\%Eff$) indicated the performance of the absorption process occurred in the small bubble column. Note that the area (A) under curve obtained from gas chromatography was used in this study. The efficiency of removal can be calculated using the following equation:

$$Eff(\%) = \frac{C_{inlet} - C_{outlet}}{C_{inlet}} \times 100 = \frac{A_{inlet} - A_{outlet}}{A_{inlet}} \times 100 \quad (3.6)$$

3.9 Experimental Procedures

3.9.1 Selection of optimal diffuser (rigid and flexible) in Bubble column

The objective of this research was to compare two types of diffuser applied with the different gas flow rates. The flow diagram and the summary of variables concerning to

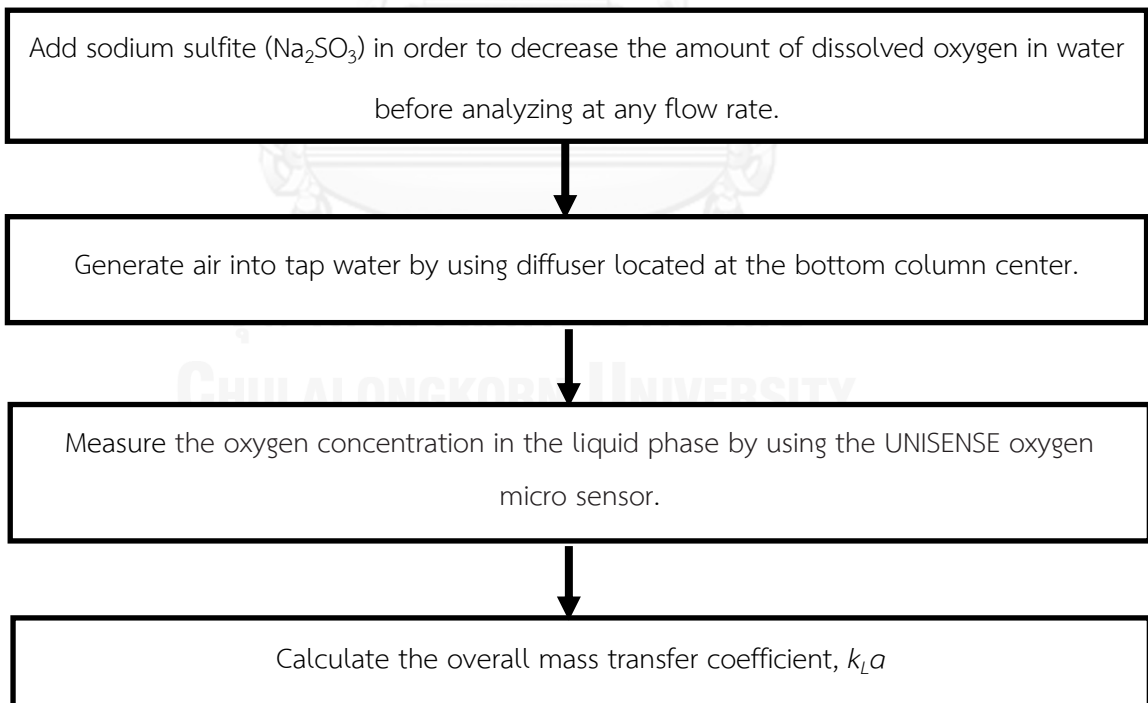


Figure 3. 7 Flow diagram for selection of optimal diffuser in bubble column

Table 3. 4 Variable of study benzene absorption in water

Fixed Variables	Parameter
Temperature	Room temperature
Liquid phase (absorbent)	Water
Independent Variables	Parameter
Gas flow rates	0.1, 0.2, 1.0, 1.5, and 2.0 L/min.
Dependent Variables	Parameter
Mass transfer parameter	$k_L a$

3.9.2. Study the effect of absorbents at different concentrations

The objective of this research is to study the effect of surfactants and concentration with the different applied gas flow rates. The flow diagram and the summary variables in this research are presented in Figure 3.8 and Table 3.5, respectively.

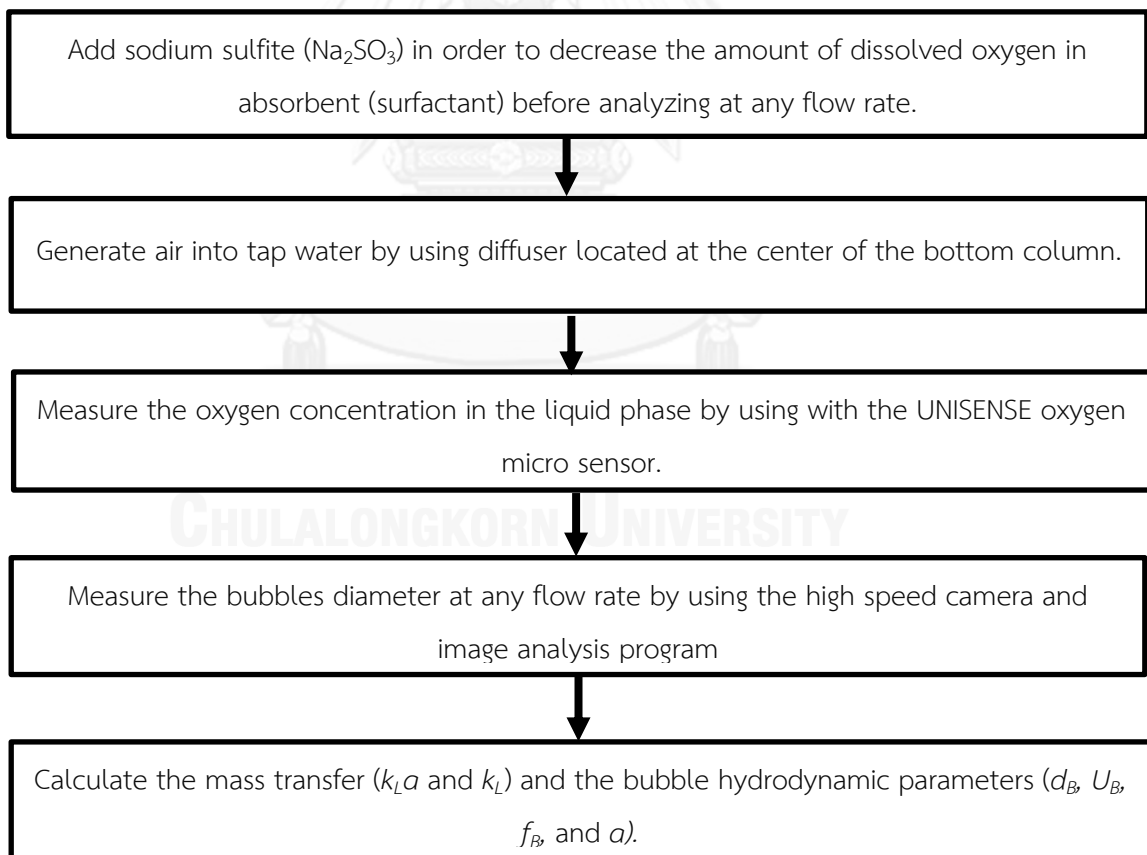


Figure 3. 8 Flow diagram for study the effect of absorbents at different concentrations

Table 3. 5 Variable of study benzene absorption in water

Fixed Variables	Parameter
Temperature	Room temperature
Liquid phase (absorbent)	Surfactant
Independent Variables	Parameter
Gas flow rates	0.1, 0.2, 1.0, 1.5, and 2.0 L/min.
Concentration	0.1 and 1.0 cmc
Dependent Variables	Parameter
Mass transfer parameter	$k_L a$ and k_L
Hydrodynamic parameter	d_B , U_B , f_B , and a

3.9.3 The effect of absorbents and concentrations on hydrophobic VOCs absorption process

The objective of this research is to study the effect of surfactants and concentration on hydrophobic VOCs absorption process applied with the different gas flow rates. The flow diagram in this research is presented in Figure 3.9. Moreover, the summary of variables concerning in this study can be presented in Table 3.6.

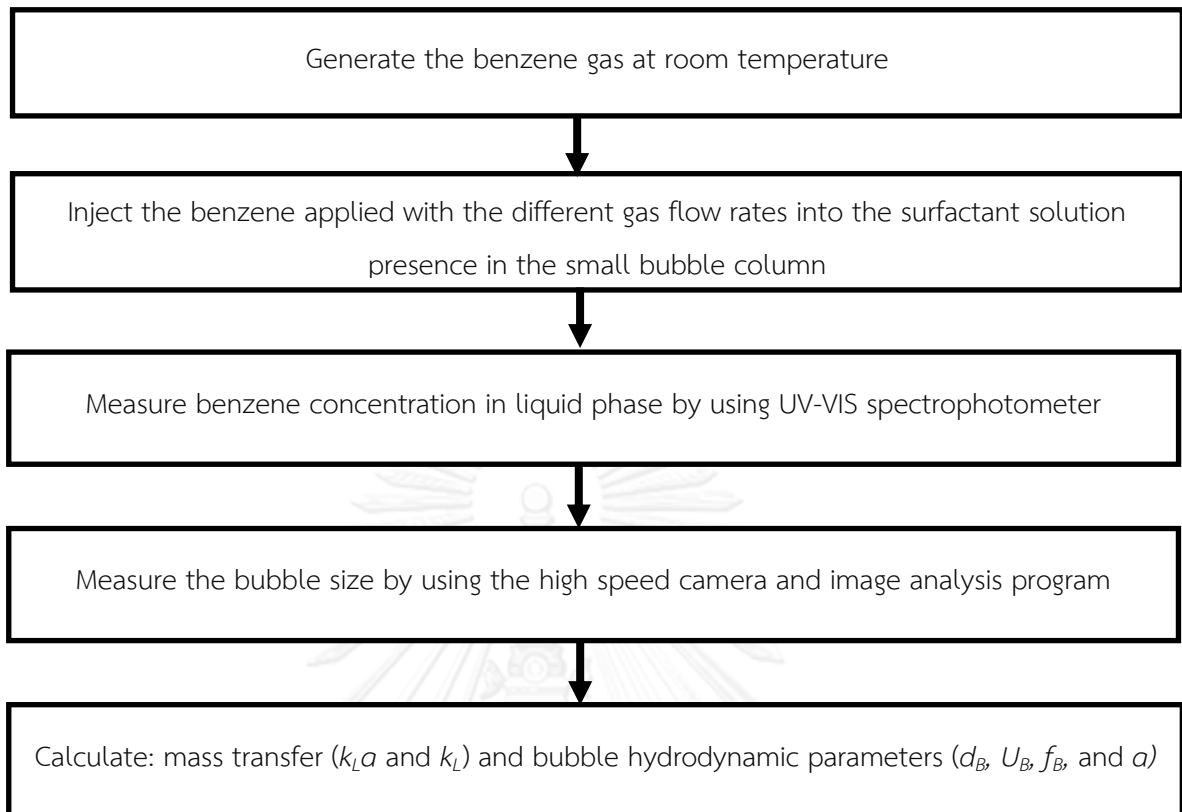


Figure 3. 9 Flow diagram for the effect of absorbents and concentrations on hydrophobic VOCs absorption process

Table 3. 6 Variable of study benzene absorption in liquid phases

Fixed Variables	Parameter
Volatile organic compounds	Benzene
Temperature	Room temperature
Liquid phase (absorbent)	Tap water and surfactant
Independent Variables	Parameter
Gas flow rates	1.0, 1.5, and 2.0 L/min.
Concentration	0.1, 1.0, and 3.0 cmc
Dependent Variables	Parameter
Mass transfer parameter	$k_L a$ and k_L
Hydrodynamic parameter	d_B , U_B , f_B , and a

3.9.4 Liquid-side mass transfer coefficient (k_L) for aeration and hydrophobic VOCs

The objective of this research is to analyze the effect of parameters that relate to the k_L value for aeration and hydrophobic VOCs (benzene). The flow diagram of this research is presented in Figure 3.10.

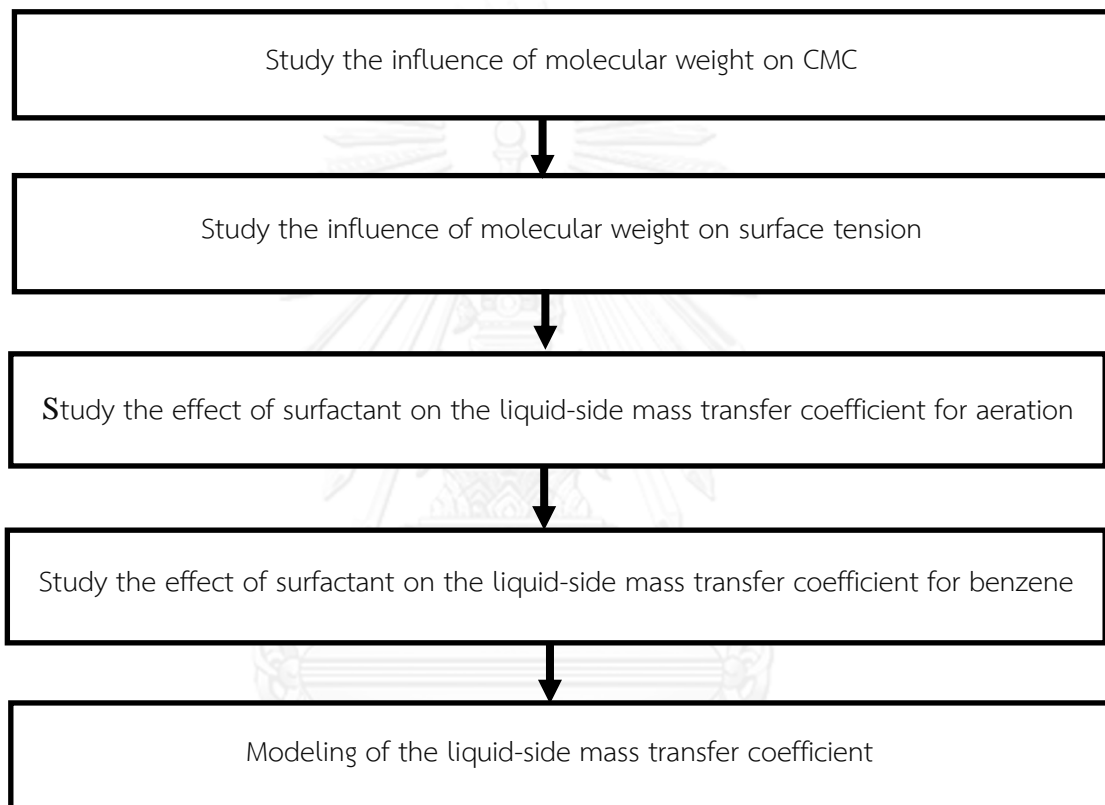


Figure 3. 10 Flow diagram for liquid-side mass transfer coefficient (k_L) for aeration and hydrophobic VOCs

3.9.5 VOCs removal efficiency

The objective of this research is to measure the removal efficiency with and without activated carbon applied with the optimal absorbent and flow rate. Moreover, the flow diagram and the summary variables of this study are shown in Figure 3.11 and in Table 3.7, respectively.

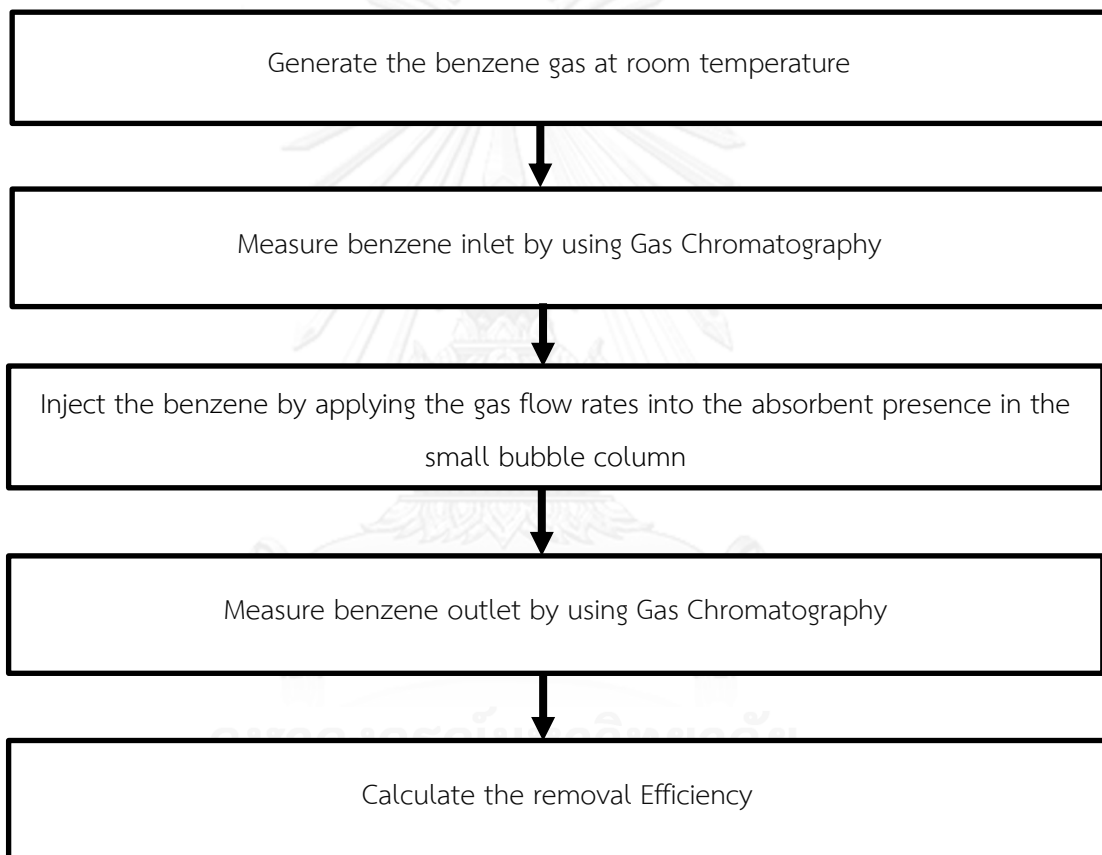


Figure 3. 11 Flow diagram for the effect of hydrophobic VOCs on hybrid processes
(absorption and adsorption)

Table 3. 7 Variable of VOCs removal efficiency

Fixed Variables	Parameter
Volatile organic compounds	Benzene
Temperature	Room temperature
Liquid phase (absorbent)	Tap water and surfactant
Independent Variables	Parameter
Time	Minute
Dependent Variables	Parameter
Removal Efficiency	% Removal efficiency

CHAPTER IV

RESULTS AND DISCUSSION

The objectives of this research were to study the effect of bubble hydrodynamic and liquid phase on mass transfer mechanism for removing the hydrophobic Volatile Organic Compounds (VOCs) in bubble column. The bubble hydrodynamic and mass transfers parameters from the gas phase to the liquid phase were the key parameters of this study. The results were consists of 5 parts as follow:

1. The effect of different gas diffusers (rigid and flexible) in bubble column
2. Study the effect of surfactant at difference concentrations
3. The effect of surfactant and concentrations on hydrophobic VOCs absorption process
4. Liquid-side mass transfer coefficient for aeration and hydrophobic VOCs
5. VOCs Removal efficiency

It can be noted that these results can possibly provide the optimal design criteria and operating condition for enabling the hydrophobic VOCs treatment efficiency in a bubble column.

4.1 The effect of different gas diffusers (rigid and flexible) in bubble column

In this section, the volumetric mass transfer coefficient ($k_L a$) is studied in order to analyze the influence of 2 types of gas diffusers: rigid and flexible. Figure 4.1 shows the variation of the volumetric mass transfer coefficient ($k_L a$) with the different gas flow rates in tap water for different gas diffusers.

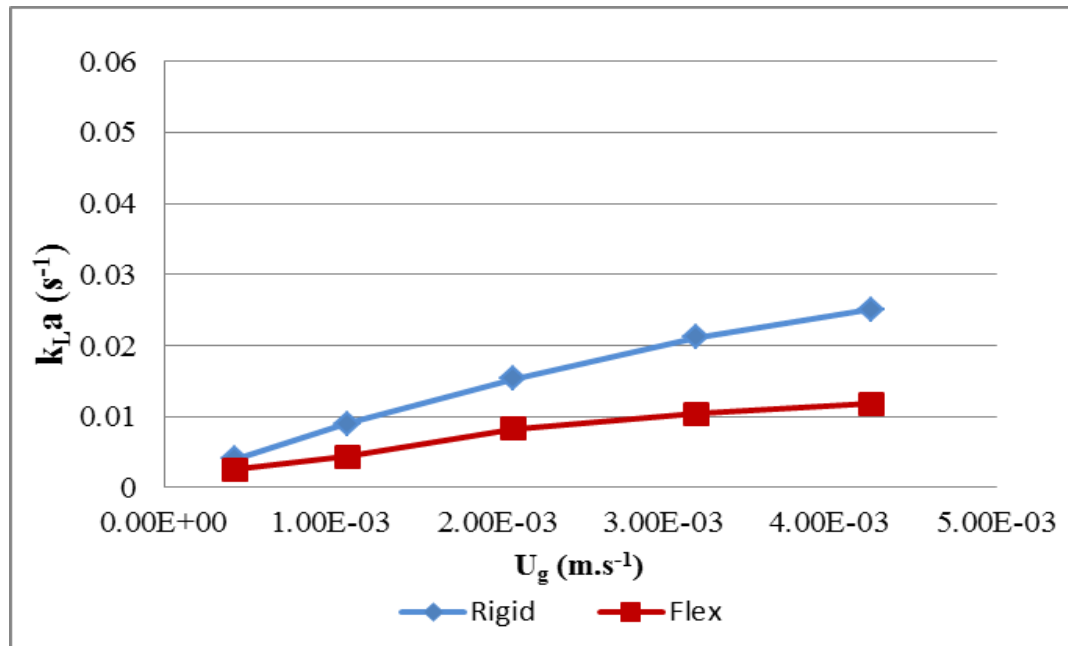


Figure 4. 1 Volumetric mass transfer coefficient versus gas flow rate in tap water

Figure 4.1 indicates that, in any liquid phase, the volumetric mass transfer coefficient increased with the superficial gas velocity ($U_g = Q_g/a_{\text{column}}$). The values of k_La coefficients varied between 0.0026 and 0.0251 s^{-1} and superficial gas velocity vary between 0.000425 and 0.00425 $m.s^{-1}$. The volumetric mass transfer coefficient, k_La increases with the superficial gas velocity in both of two gas diffusers. The overall following trends are found that the k_La values of rigid are greater than the k_La values of flexible. However, the k_La value shows the mass transfer efficiency from gas to liquid phase. In this regard, rigid is applied into next step.

To understand properly these phenomena, the liquid-side mass transfer coefficient (k_L) and surface interfacial area (a) that was deduced from the bubble diameter (d_B) has to be considered separately.

4.2 Study the effect of absorbents at difference concentrations

4.2.1. Volumetric mass transfer coefficient ($k_L a$)

Figure 4.2 presents the oxygen concentration in liquid phase at different experimental times. The gas flow rate used in this work is $1.5 \text{ L}\cdot\text{min}^{-1}$ ($U_g = 0.0032 \text{ m}\cdot\text{s}^{-1}$), and the experimental times were 550 second.

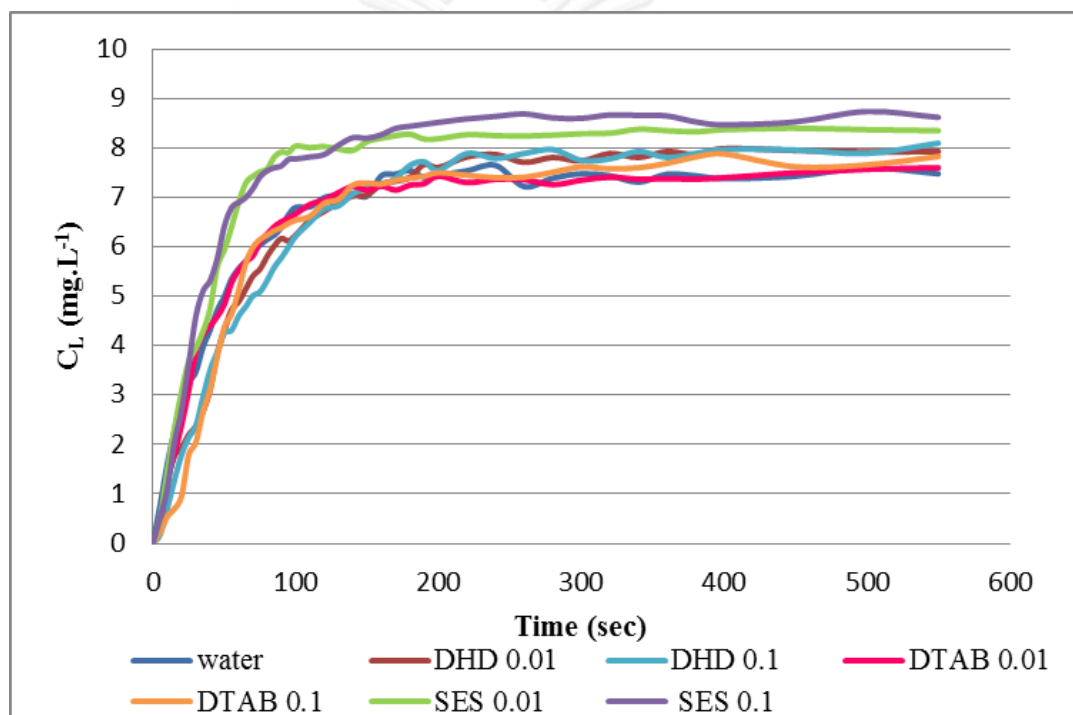


Figure 4. 2 The oxygen concentration in liquid phase at different experimental times

For this work, the volumetric mass transfer coefficient was deduced from the oxygen concentration in liquid phase (C_L) and the oxygen saturation C_L^S that were measured by the UNISENSE oxygen microsensor. Note that, during the experimental run, sufficient time is available to reach the oxygen saturation in the liquid. The equation that used to determine $k_L a$ value can be written as follows:

$$\frac{\partial C_L}{\partial t} = K_L a (C_L^S - C_L) \quad (4.1)$$

or, in its integral form by

$$\ln[C_L^S - C_L] = \ln C_L^S - K_L a \cdot t \quad (4.2)$$

Thus, the local volumetric mass transfer coefficient $k_L a$ is deduced from the slope of the curve relating the variation of $\ln[C_L^S - C_L]$ with t .

In this section, the volumetric mass transfer coefficient ($k_L a$) is determined and applied in order to provide a better understanding on the influence of surfactant molecules on the VOCs absorption in a bubble column. Figure 4.3 presents the variation of the volumetric mass transfer coefficient ($k_L a$) with the gas flow rate for the different liquid phases.

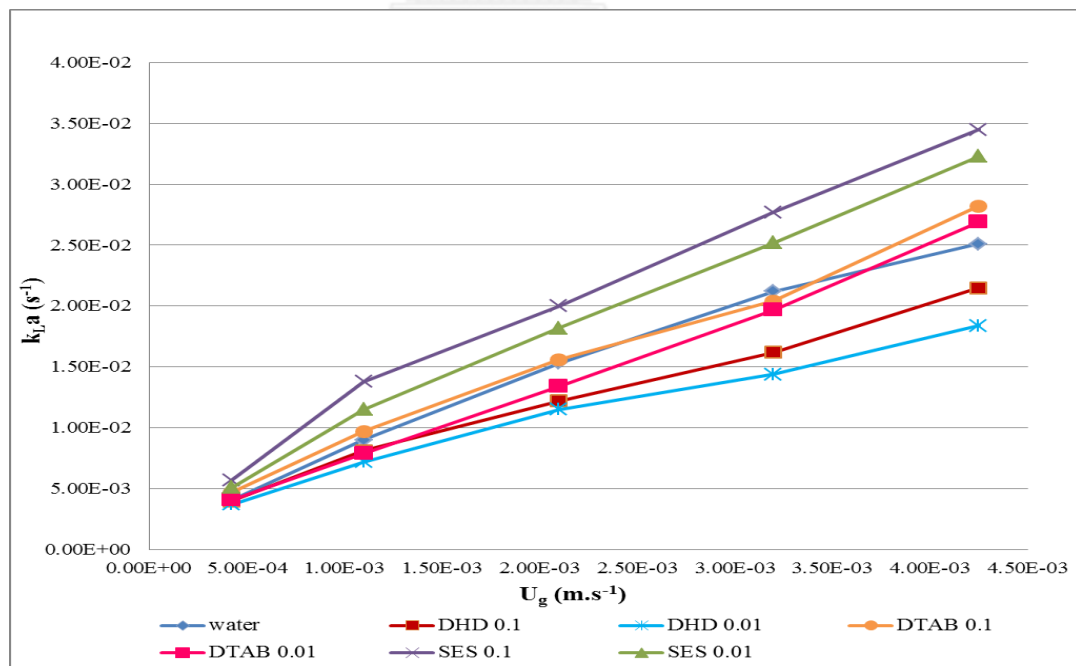


Figure 4. 3 Volumetric mass transfer coefficient versus gas flow rate for different liquid phases (tap water and surfactant solutions)

Figure 4.3 indicates that, in any liquid phase, the volumetric mass transfer coefficient increased with the superficial gas velocity. The values of $k_L a$ coefficients vary between 0.0041 and 0.0345 s^{-1} and superficial gas velocity vary between 0.000425 and 0.00425 $m.s^{-1}$. It was observed that the concentrations of surfactant solutions affected the $k_L a$ values, especially anionic surfactants, but in the effect of cationic and anionic is not change significantly. Moreover, the $k_L a$ values of anionic surfactants (SES) were greater than cationic (DTAB) and non-ionic surfactants (DHD) at 0.01 and 0.1 CMC. In this study, the trend obtained is summarized as follows:

$$k_{La} \text{ 0.1 CMC SES} > k_{La} \text{ 0.01 CMC SES} > k_{La} \text{ 0.1 CMC DTAB} \cong k_{La} \text{ WATER} > k_{La} \text{ 0.01 CMC DTAB} > k_{La} \text{ 0.1 CMC DHD} \\ > k_{La} \text{ 0.01 CMC DHD}$$

These results show that the type and the concentration of surfactants had a direct effect on gas-liquid mass transfer. To well understand these phenomena, the liquid-side mass transfer coefficient (k_L) and interfacial area (a) have to be considered separately.

4.2.2 Site distribution for air bubble

The site distribution was studied in order to observe distribution of bubble diameter that measuring in approximately at half the height of the bubble column. For this section, water and anionic (0.1 CMC) was chosen as sample absorbent applied with the superficial gas velocity at 0.0032 $m.s^{-1}$ which classifies 100 sorts of different bubble diameter (Figure 4.4 and 4.5).

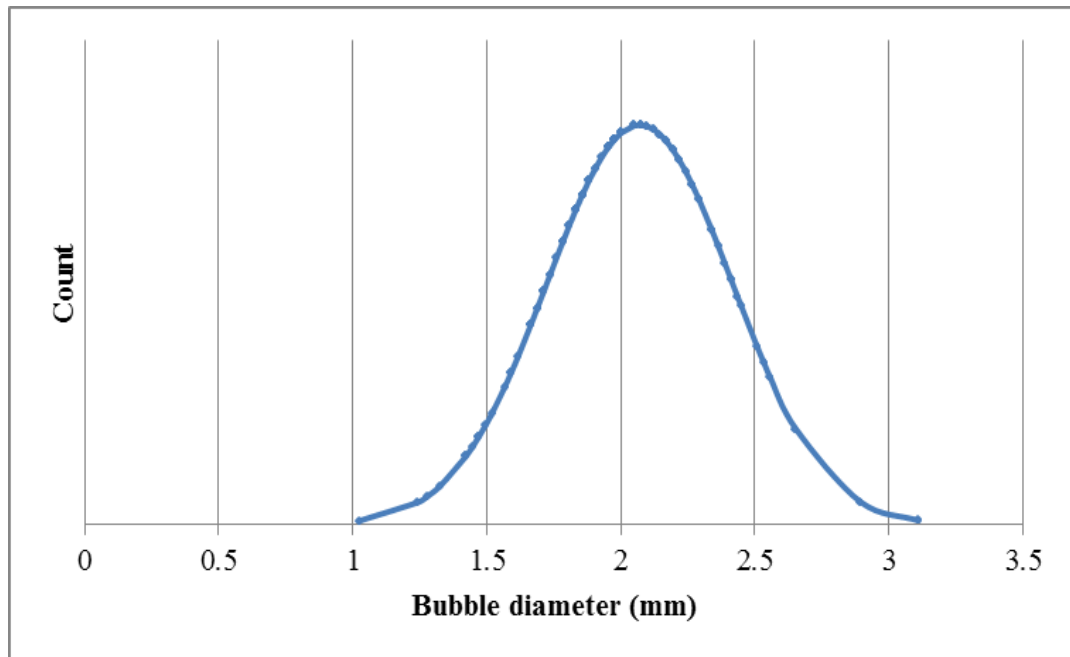


Figure 4. 4 Site distribution for aeration in water

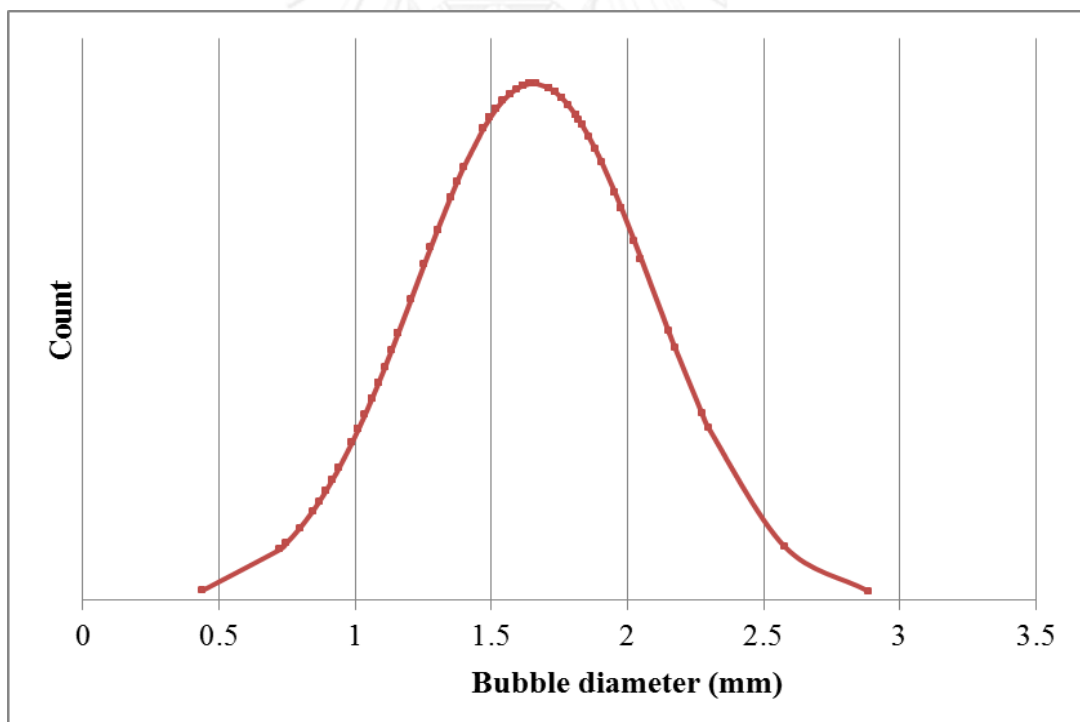


Figure 4. 5 Site distribution for aeration in anionic solution

4.2.3 Bubble diameter (d_B)

Figure 4.6 shows the variation of the generated bubble diameter with the superficial gas velocity in tap water for different liquid phases (tap water, aqueous solutions with anionic, cationic, and non-ionic surfactant). Notably, the rigid diffuser is applied due to the overall mass transfer coefficient as previously described.

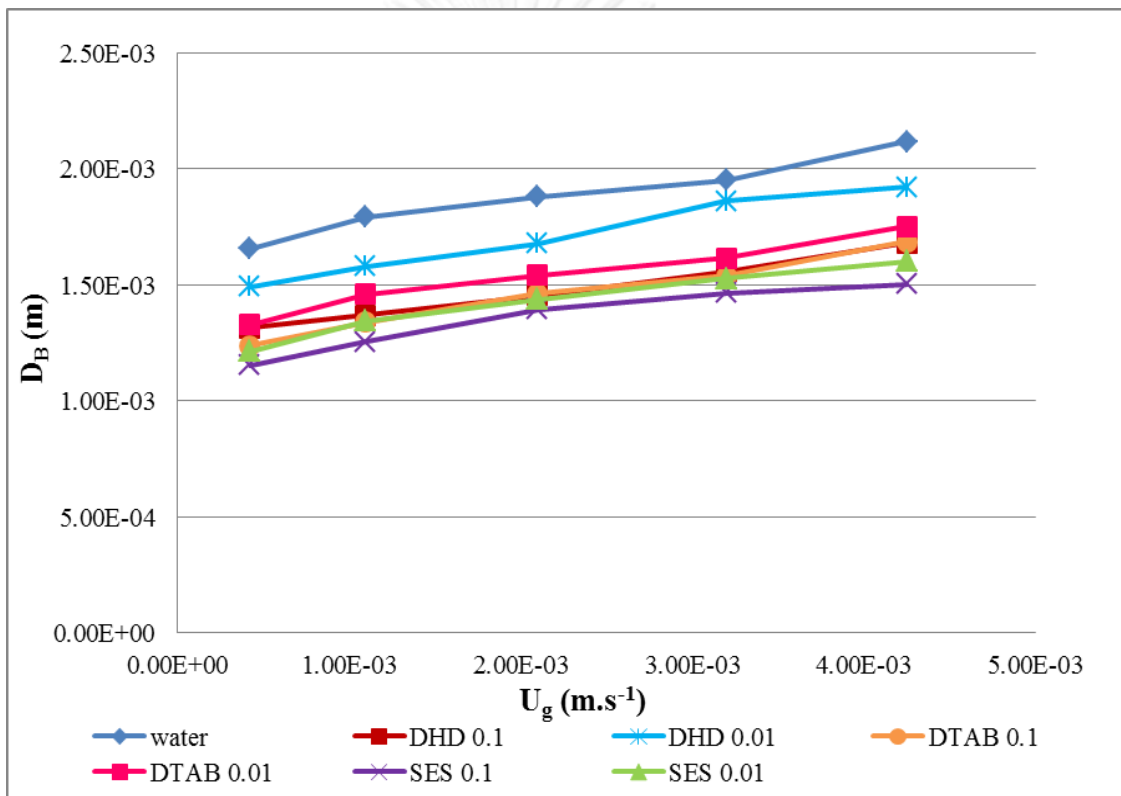


Figure 4. 6 Bubble diameter versus superficial gas velocity

Whatever the liquid properties, the bubble diameters vary between 0.0012 and 0.0021 m for superficial gas velocities varying between 0.000425 and 0.00425 ms⁻¹. At high superficial gas velocities ($U_G > 0.001$ ms⁻¹), for a given superficial gas velocity, the order below is observed:

$$d_{B \text{ anionic}} < d_{B \text{ cationic}} < d_{B \text{ non-ionic}} < d_{B \text{ water}}$$

The differences in terms of bubble diameters are directly linked to static surface tension values as expressed in Laplace's law ($\Delta P = 2\sigma_L/D_B$) and the σ_L values of each absorbents were shown in Table 3.3. In fact, in this range of superficial gas velocities, the bubble diameter is no longer only controlled by the force balance at detachment, but also by the power dissipated in the liquid phase, conditioning the bubble break up and coalescence.

Regarding in the Figure 4.6, it was observed that the calculated bubble diameter of water and anionic surfactant in this part was close to the median from the size distribution. It can probably be concluded that measuring the bubble diameter at half of the height of the bubble column is accuracy.

4.2.4 Specific interfacial area (a)

The variations of the specific interfacial area with the superficial gas velocity were plotted in Figure 4.7 for the different liquid phases.

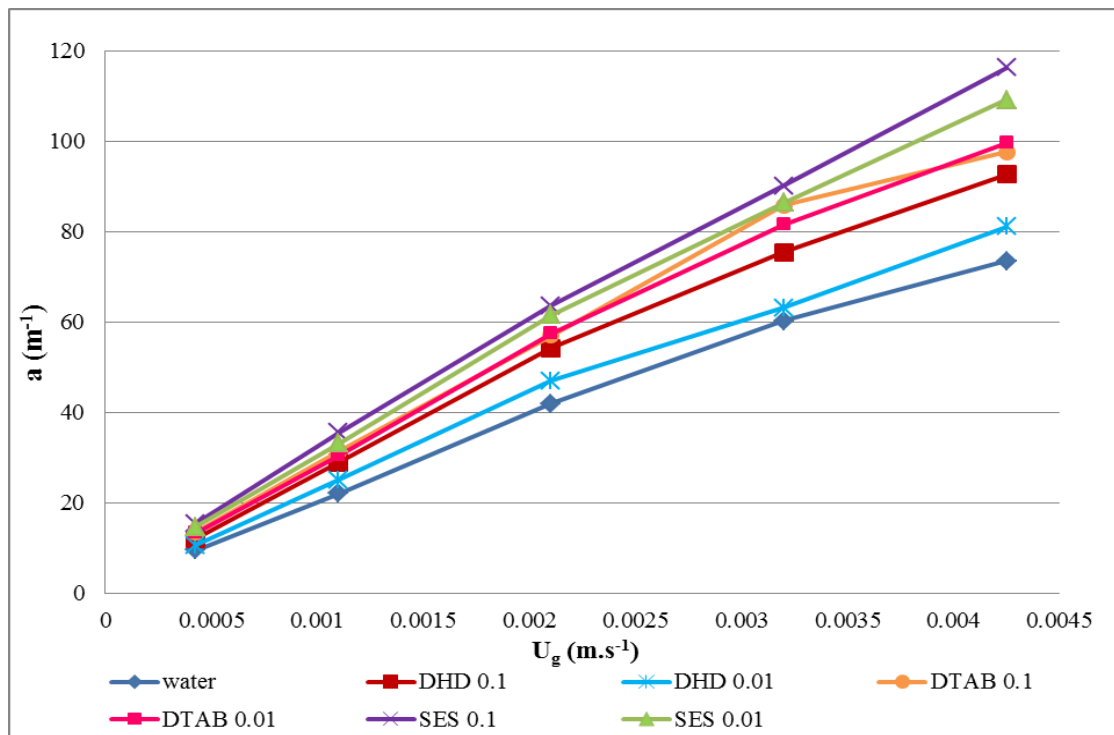


Figure 4. 7 Specific interfacial area versus superficial gas velocity

According to Figure 4.7, this observation would indicate that whatever the liquid phases, the specific interfacial area increases roughly linearly with the superficial gas velocity. Their values vary between 10.7 and 116.3 m⁻¹ for superficial gas velocities varying between 0.000425 and 0.00425 ms⁻¹. The specific interfacial areas related to surfactant solutions are significantly larger than those of water. The following overall trend is found:

$$a_{\text{water}} < a_{\text{non-ionic}} < a_{\text{cationic}} < a_{\text{anionic}}$$

These results show that an increase of the superficial gas velocities has a directly effect on the number of bubbles in the column (N_b), which also directly affect the specific interfacial area. From the trend, it showed that the specific interfacial area of surfactant solution is greater than those of water which relate to the equation 3.5. Moreover, it was

found that the concentration of surfactant solutions and surface tension (Table 3.3) has a directly effected on the specific interfacial area as well. In conclusion, the increasing of the specific interfacial area directly affects the mass transfer performance. Moreover, an addition of surfactant solution was able to decrease the bubble diameter or increase specific interfacial area.

However, the influence of surfactant molecules on k_L values will be considered, in the next section, in order to obtain the optimal values of $k_L a$ and thus the suitable bubble column design and operation.

4.2.5 Liquid-side mass transfer coefficient (k_L)

Figure 4.8 illustrates the variation of the liquid-side mass transfer coefficient (k_L) with the superficial gas velocity for the different liquid phases.

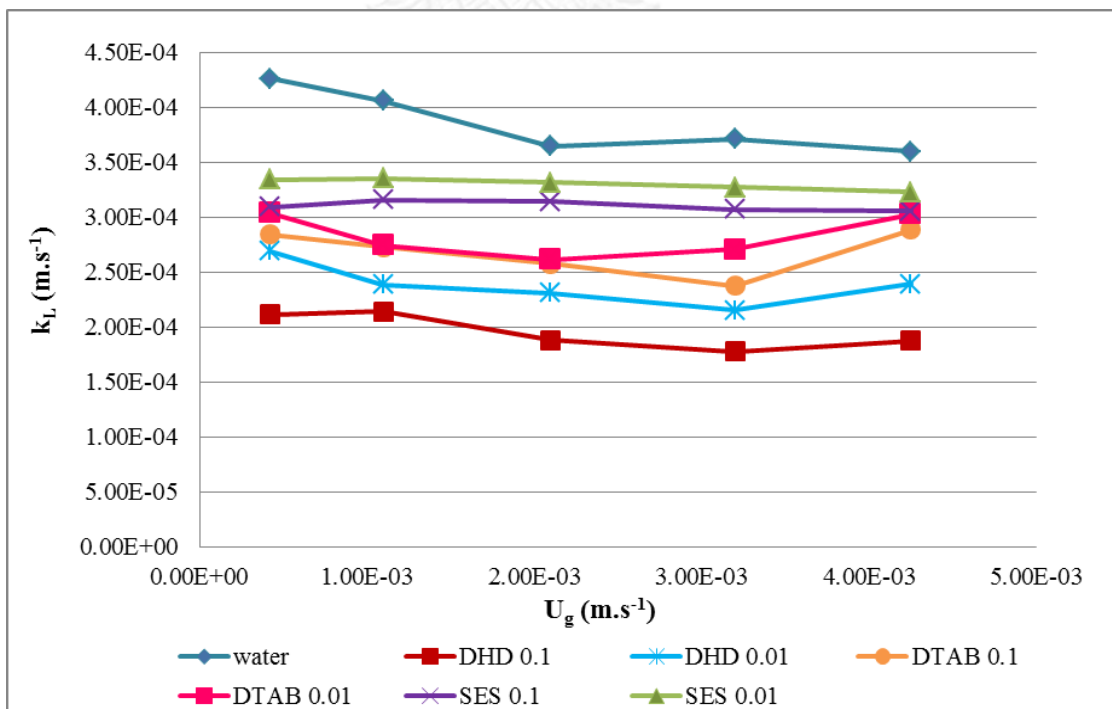


Figure 4. 8 Liquid-side mass transfer coefficient versus superficial gas velocity

According to Figure 4.8, it can be indicated that whatever the superficial gas velocity, the liquid-side mass transfer coefficient exhibit a degree of scattering. This is because of the fact that the calculation of k_L accumulated the experimental errors which are associated with measurements of both $k_L a$ and a . The liquid-side mass transfer coefficient of all surfactant solutions was significantly less than those of water. Therefore, these results clearly indicated that the presence of surfactants at the bubble interface can effect on the mass transfer mechanism by modifying the composition or the thickness of liquid film around the bubbles. An addition of anionic surfactant (SES) provided the highest the volumetric mass transfer coefficient and the specific interfacial area. Consequently the calculated liquid-side mass transfer coefficient was close to the liquid-side mass transfer coefficient of water: these were higher than those obtained with cationic and nonionic surfactants. Moreover, the results showed that whatever the surfactant types, the quantity of surfactant had a direct impact on the liquid-side mass transfer coefficient, which the liquid-side mass transfer coefficient at 0.01 CMC was greater than at 0.1 CMC. Therefore, each factor (MW, CMC, surface tension, and concentration), which affected the k_L values, were studied in the next step in order to provide a better understanding on the phenomena of surfactant molecule on air bubbles surface.

Due to the propose of this research aimed to apply this process for the treatment of benzene, studying the effect of absorbent in terms of mass transfer mechanism has to be analyzed in order to choose the suitable liquid phase.

4.3 The effect of absorbents and concentrations on hydrophobic VOCs absorption process

4.3.1 Pre-test the effect of each absorbent on benzene absorption process

Due to the characteristic of air (oxygen) and benzene is different, studying of their absorption on each liquid phases have to be required. Figure 4.9 shows the variation of the volumetric mass transfer coefficient ($k_L a$) with the different liquid phases. The solution surfactants 1.0 CMC applied with gas flow rate at $1.5 \text{ L}\cdot\text{min}^{-1}$ was applied in this section.

From the previous part (oxygen absorption), there were four liquid phases that were compared, and the anionic surfactant has the highest performance to absorb oxygen. For this part, it was found that the optimal surfactant from aeration is not appropriate for benzene absorption. This is because anionic surfactant has a negative charge on their polar head group, while benzene is non-polar. Thus, it was expected that non-ionic, which contain no specific charge, might well absorb benzene than in case of anionic surfactant. As show in Figure 4.9, the result shows that non-ionic (dehydol) has the lowest $k_L a$ value. For this reason, other type of non-ionic surfactant would be tested. Tween 80 is the commercial non-ionic surfactant that was analyzed in this study, and their result shows that its $k_L a$ value was higher than the $k_L a$ value of dehydol and anionic, respectively. Moreover, from Table 4.2, the saturated concentration of benzene in liquid phase (C_L^S) of Tween 80 was higher than those of other liquid phases, and the overall following trend was found:

$$C_L^S_{\text{Tween80}} > C_L^S_{\text{Anionic}} > C_L^S_{\text{Dehydol}} > C_L^S_{\text{Water}}$$

Thus, there were three liquid phases (water anionic, and Tween 80) that were applied into the next step.

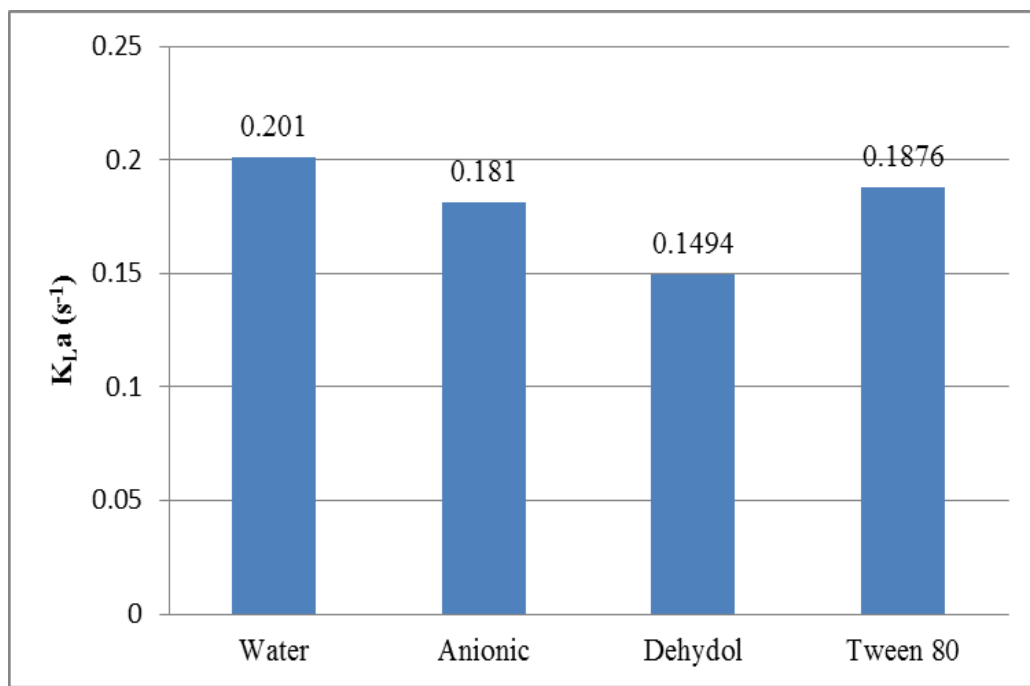


Figure 4. 9 The volumetric mass transfer coefficient (k_La) for the different liquid phases

Table 4. 1 The saturation concentration of benzene in liquid phase

Absorbent	Saturated concentration in liquid phase , C_L^S ($mg.L^{-1}$)
Water	878.5
Anionic 1.0 CMC	1107.9
Non-ionic (Dehydol) 1.0 CMC	1031.5
Non-ionic (Tween80) 1.0 CMC	1179.8

4.3.2 Volumetric mass transfer coefficient ($k_L a$)

In this section, the volumetric mass transfer coefficient ($k_L a$) is determined and applied in order to provide a better understanding on the influence of surfactant molecules on the VOCs absorption in a bubble column. Notably, there were 3 different type of liquid phase that were used in this study (water, anionic, and non-ionic surfactant). The commercial non-ionic surfactant that was chosen as absorbent is Tween 80, which was expected that it might well absorb benzene because of its structure. Figure 4.10 presents the variation of the volumetric mass transfer coefficient ($k_L a$) with the superficial gas velocity for the different liquid phases.

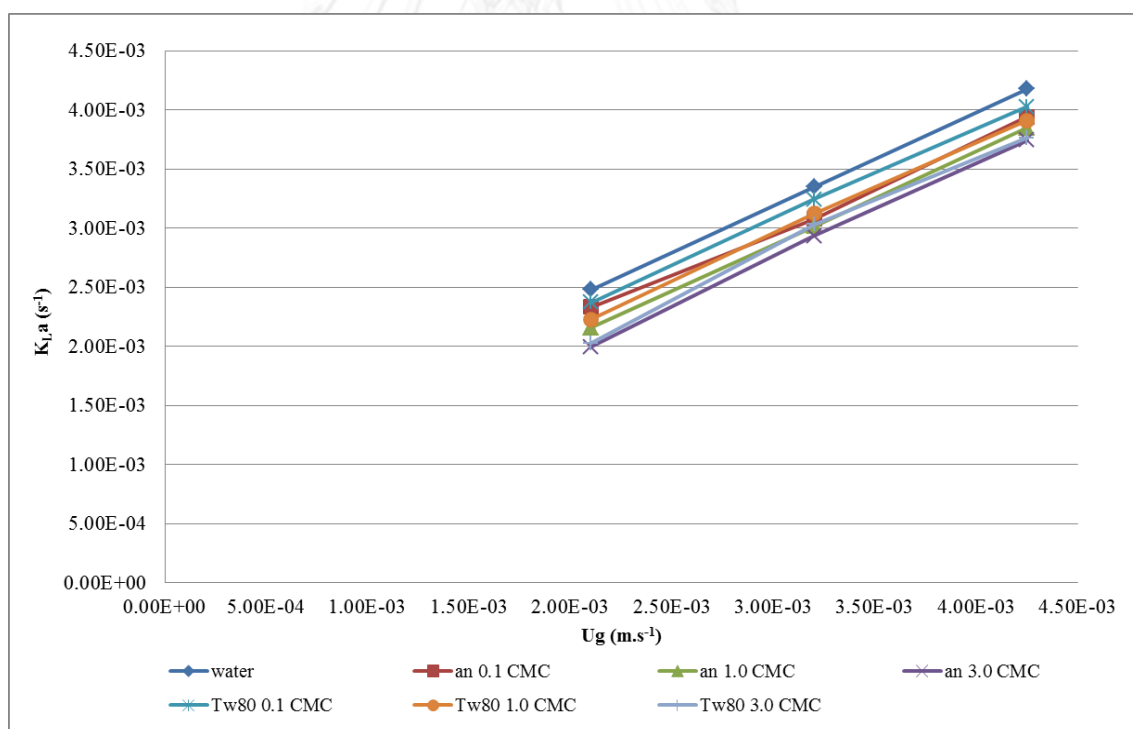


Figure 4. 10 Volumetric mass transfer coefficient versus gas flow rate for different liquid phases (tap water and surfactant solutions)

Figure 4.10 indicates that, in any liquid phase, the volumetric mass transfer coefficient increased with the superficial gas velocities. The values of $k_L a$ coefficients vary and between 0.0021 and 0.0042 ms^{-1} and the superficial velocity vary between 0.0021 and 0.0042 s^{-1} . The volumetric mass transfer coefficients of both surfactant solutions and lubricant oily-emulsion are significantly smaller than those of water. In this study, the trend obtained is summarized as follows:

$$k_{L a \text{ water}} > k_{L a \text{ Anionic}} > k_{L a \text{ Non-ionic}}$$

Concerning the surfactant solution, it can be noted that, for a given gas flow rate, the lowest $k_L a$ values are obtained with the surfactant solution at highest CMC values (3 CMC). These results correspond with the fact that presence of surfactants, at different concentration or even in small quantities, can have significant effects on the mass transfer mechanism (Painmanakul et al., 2005).

Moreover, this work has studied the saturation concentration in liquid phase. It was found that the saturated concentration of benzene in water is less than those in anionic and non-ionic surfactant, respectively. As in Table 4.3, it can be stated that non-ionic surfactant rather absorb benzene higher than other liquid phase, which related to the benzene removal efficiency.

Table 4. 2 The saturation concentration of benzene in liquid phase

Absorbent	CMC	Saturated concentration in liquid phase, C_L^S (mg.L ⁻¹)
water	-	878.5
Anionic (SES)	0.1	914.2
	1.0	1107.9
	3.0	1196.4
Non-ionic (Tween80)	0.1	998.3
	1.0	1179.8
	3.0	1397.1

4.3.2 Site distribution for hydrophobic VOCs

Similar to the aeration part, the site distribution of water and non-ionic surfactant (1.0 CMC) was studied (Figures 4.11 and 4.12). Note that the superficial gas velocity used is 0.0032 m.s^{-1} .

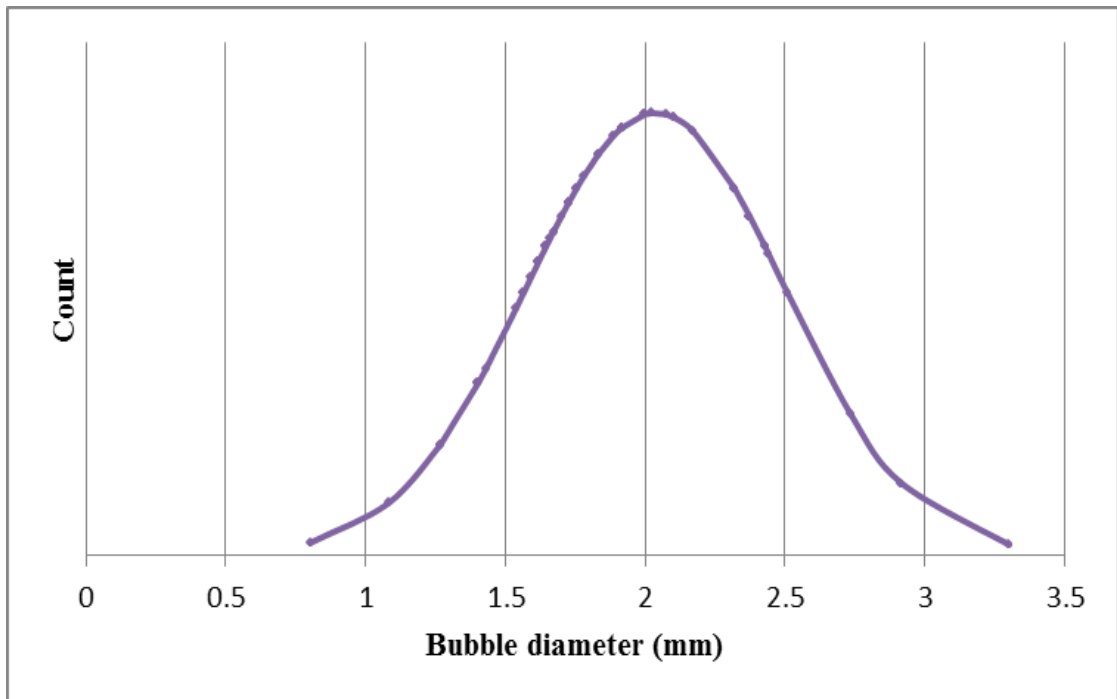


Figure 4. 11 Site distribution for hydrophobic VOCs in water

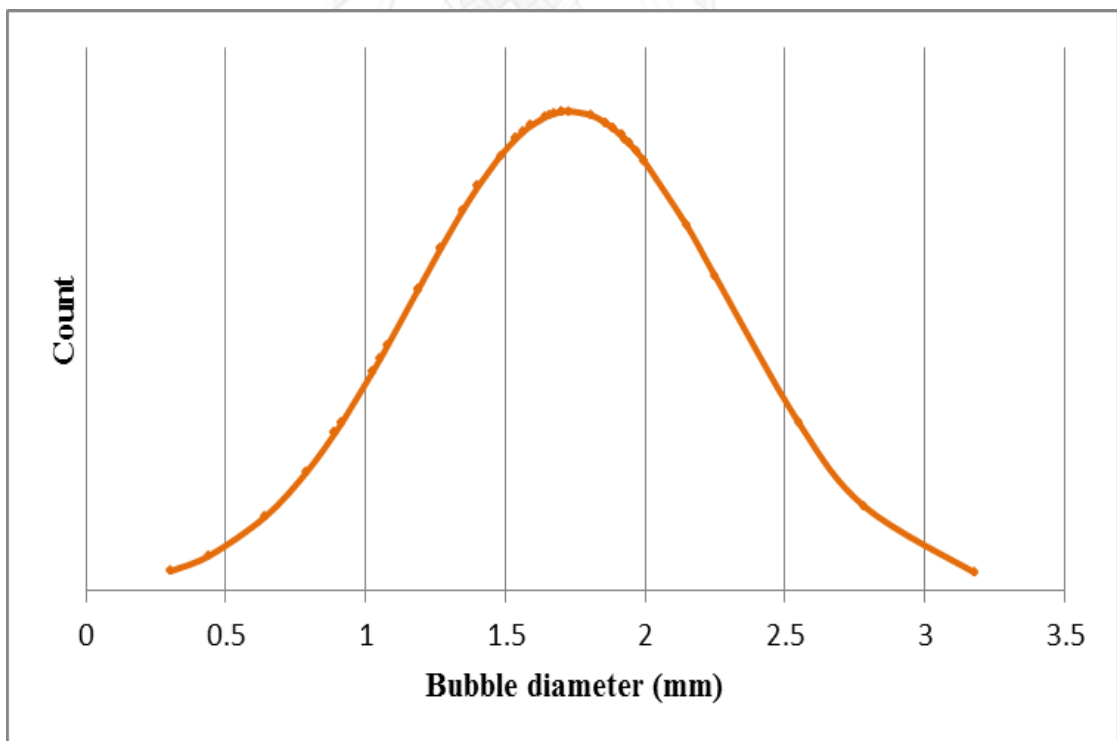


Figure 4. 12 Site distribution for hydrophobic VOCs in non-ionic surfactant solution

4.3.3 Bubble diameter (D_B)

Figure 4.13 shows the variation of the generated bubble diameter with different gas flow rates in tap water for different liquid phases (tap water and aqueous solutions with non-ionic and cationic surfactant).

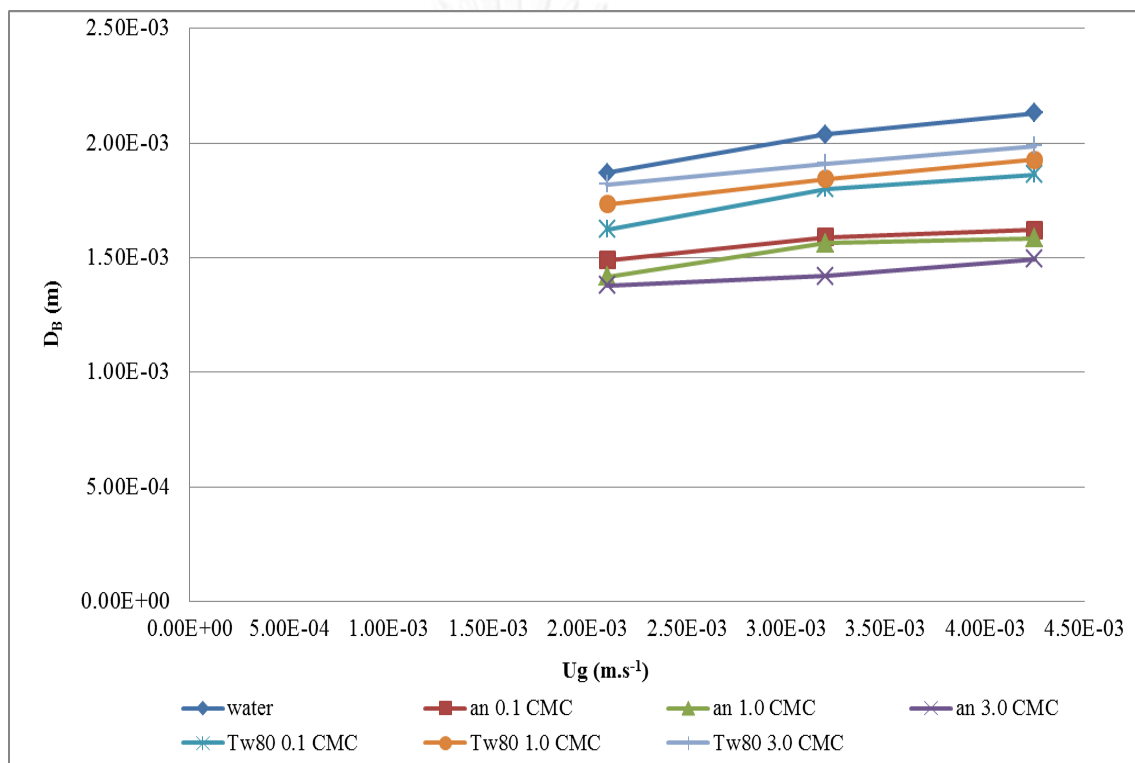


Figure 4. 13 Bubble diameters versus superficial gas velocity for different liquid phases (tap water and surfactant solutions)

According to Figure 4.13, the bubble diameter obtained from the experiment varies between 0.0014 and 0.0021 mm, while the superficial gas velocity can change between 0.0021 and 0.0042 m.s⁻¹. It can be noted that, at low gas flow rates, the bubble diameters are roughly constant and start to slightly increase at high gas flow rates ($U_G > 0.0032$ m.s⁻¹). The same trend line as obtained from the previous experiments can also be observed.

Due to Laplace's equation ($\Delta P = 2\sigma L/D_B$), the bubble diameter is directly related to static surface tension as presented in Table 3.3. In this study, the following overall trend is found as follows:

$$d_{B \text{ 3.0 CMC anionic}} < d_{B \text{ 1.0 CMC anionic}} < d_{B \text{ 0.1 CMC anionic}} < d_{B \text{ 3.0 CMC non-ionic}} < d_{B \text{ 1.0 CMC non-ionic}} < d_{B \text{ 0.1 CMC non-ionic}} < d_{B \text{ water}}$$

As proposed by (Loubière & Hébrard, 2003), these results should be due to the differences observed in terms of dynamic surface tensions, and to their consequences on the balance between the surface tension and the buoyancy forces during the bubble growth and detachment. At high gas flow rates, the differences in terms of bubble diameters are directly linked to static surface tension values. In fact, in this range of gas flow rates, the bubble diameter is no more controlled by the force balance at detachment, but rather by the power dissipated in the liquid, conditioning the bubble break up and coalescence phenomena.

Over the whole bubble diameter range, the terminal rising bubble velocities are nearly constant and vary between 17 and 20 $\text{cm}\cdot\text{s}^{-1}$ and are within the range of the U_B values of (Grace & Wairegi, 1986) corresponding to the contaminated and pure systems as shown in Figure 2.5. Moreover, it can be noted that the presence of contaminants can affect the bubble hydrodynamic parameters, especially the contamination of surfactant molecules.

Similar to the previous experiment, the local interfacial area (a) can be determined by using the experimental results of d_B and, U_B values.

4.3.3 The local interfacial area (a)

Figure 4.15 presents the relation between the interfacial area and the superficial gas velocity for different liquid phases applied in these experiments.

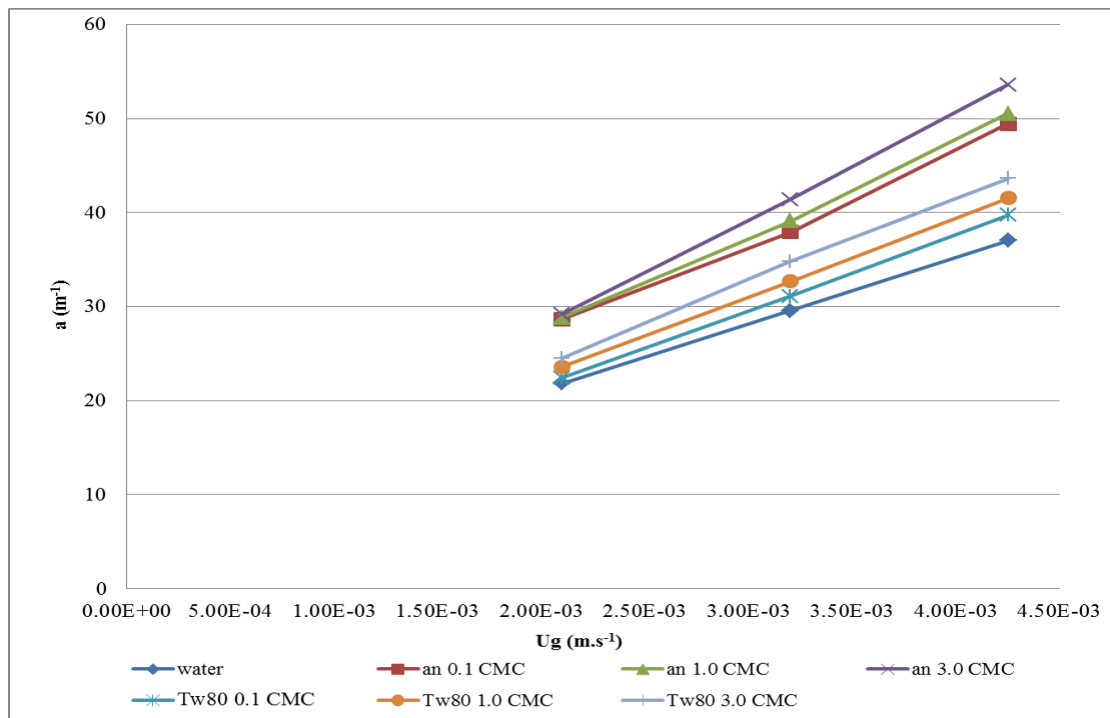


Figure 4. 14 Interfacial area versus superficial gas velocity for different liquid phases

According to Figure 4.15, regardless of the liquid phases, the interfacial area roughly increases linearly with the superficial gas velocity. Their values vary between 21.8 and 53.6 m⁻¹, whereas the superficial gas velocity change between 0.0021 and 0.0042 m.s⁻¹.

Moreover, the highest and lowest of a values can be obtained with anionic 3.0 CMC and tap water, respectively. It can be stated that the interfacial area is directly linked to the bubble diameter and thus the static surface tension of liquid phases under the test. Low values of σ_L are associated with high values of a (Sardeing, Painmanakul, & Hébrard,

2006), (Painmanakul et al., 2005), and (Loubie`re & He`brard, 2004). In this study, the following overall trend is thus found as follows:

$$a_{3.0 \text{ CMC anionic}} > a_{1.0 \text{ CMC anionic}} > a_{0.1 \text{ CMC anionic}} > a_{3.0 \text{ CMC non-ionic}} > a_{1.0 \text{ CMC non-ionic}} \\ > a_{0.1 \text{ CMC non-ionic}} > a_{\text{water}}$$

Furthermore, the difference among the values obtained from tap water and another absorbent can be observed at high gas flow rates. These results may possibly be related to the prevention of bubble coalescence phenomena provided by some contaminant molecules presence in the liquid phase (Deckwer, 1992).

4.3.4 Liquid-side mass transfer coefficient (k_L)

In order to enhance a better understanding of these phenomena, the liquid-side mass transfer coefficient (k_L) has to be considered separately. In this study, the k_L coefficient can be calculated from the experimental values of the volumetric mass transfer coefficient (Figure 4.16) and the experimental values of the interfacial area (Fig. 4.15) by using equation 3.5. Figure 4.16 shows the variation of the liquid-side mass transfer coefficient (k_L) with the gas flow rate for the different liquid phases.

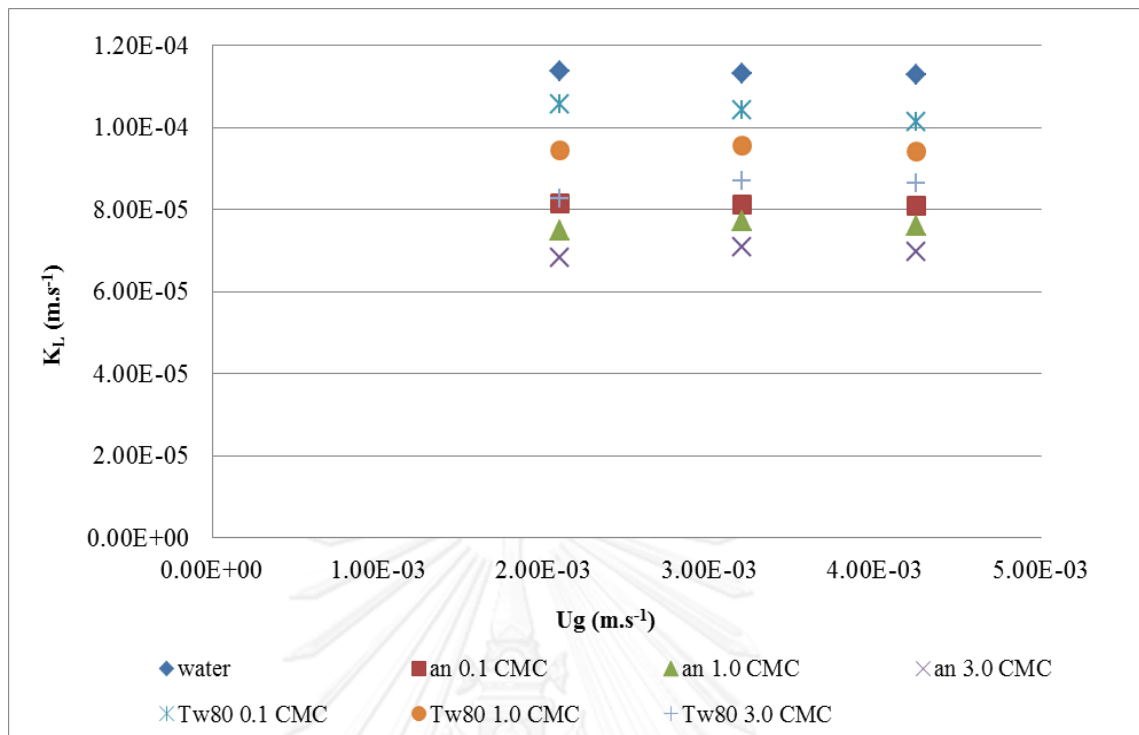


Figure 4. 15 Liquid-side mass transfer coefficient versus gas flow rate for different liquid phases (tap water and surfactant solutions)

According to Fig.12, the values of k_L obtained vary between 0.0000683 and 0.00013 m.s^{-1} and the superficial gas velocity rates vary between 0.0021 and 0.0042 m.s^{-1} . In every liquid phase, the k_L values remain roughly constant with the superficial gas velocity. Moreover, it can be noted that the k_L values of both surfactant solutions are significantly smaller than those of water. These results clearly indicate that the presence of surfactants at the bubble interface disturbs the mass transfer, certainly by modifying the composition or the thickness of liquid film around the air bubbles. The overall trend of the k_L coefficient obtained is summarized as follow:

$$k_{L \text{ Water}} > k_{L \text{ 0.1 CMC TW80}} > k_{L \text{ 1.0 CMC TW80}} > k_{L \text{ 3.0 CMC TW80}} > k_{L \text{ 0.1 CMC anionic}} >$$

$$k_{L \text{ 1.0 CMC anionic}} > k_{L \text{ 3.0 CMC anionic}}$$

For a given gas flow rate, the k_L values obtained of any surfactant solutions are smaller than those of water. Moreover, the results showed that whatever the surfactant types, the quantity of surfactant had a direct impact on the liquid-side mass transfer coefficient, which the liquid-side mass transfer coefficient at 0.1 CMC was greater than at 1.0 and 3.0 CMC, respectively. According to Fig. 13, the trend of k_L values in this part is different from the previous part (Figure 4.8). This is because the trend of $k_L a$ values decrease. Thus it affects to the k_L values which are calculated from the measurement of both $k_L a$ and a (equation 3.5). Moreover, it was found that the k_L values of non-ionic surfactant (Tween 80) are higher than the k_L values of anionic surfactant. It can be explained that an addition of anionic surfactant was able to decrease the bubble diameter or increase specific interfacial area greater than in case of non-ionic surfactant that affect the calculation of k_L values.

However, this section aims to choose the suitable absorbent in order to apply with the granular activated carbon to enhance the removal efficiency of benzene. Non-ionic surfactant 1.0 CMC was chosen as absorbent applied with gas flow rate at $1.5 \text{ L}\cdot\text{min}^{-1}$ ($U_g = 0.0032 \text{ m}\cdot\text{s}^{-1}$). This is because the structure of non-ionic surfactant is non-polar group, which is appropriate for hydrophobic VOCs or benzene. Furthermore, considering its k_L value, it can be stated that the presence of non-ionic surfactant at the bubble interface disturbs the mass transfer, certainly by modifying the composition or the thickness of liquid film around the air bubbles lower than in case of anionic surfactant. Besides, it was found that an addition of non-ionic surfactant 3.0 CMC at high gas flow rate generated the great amount of bubbles and overflowed from the bubble column.

Although the absorption reactor filled with the surfactant solutions can provide more oxygen dissolution and hydrophobic VOCs removal efficiencies than that filled with water, it has a direct effect to the decrease in k_L values. In order to provide a better understanding on these phenomena, it is necessary to study the effect of absorbent on an aeration and benzene absorption by considering the k_L value

4.4 Liquid-side mass transfer coefficient (k_L) for aeration and hydrophobic VOCs

Due to their effect relate to measurements of d_B , a , and $k_L a$ that associated with the k_L value. In order to enhance a better understanding of these phenomena, the effect of molecular weight on CMC and surface tension has to be considered.

4.4.1 The influence of molecular weight on CMC

The CMC value and molecular weight of each surfactant in this work and (Sardeing et al., 2006) were compared (Table 4.5). It can be observed that high molecular weight used less surfactant quantity than low molecular weight to generate micelle. As previously mentioned, it can be concluded that the CMC value varied inversely with molecular weight.

Table 4. 3 Comparing the CMC value and molecular weight of each surfactant

Surfactant type	This work			Painmanakul, 2006		
	Name	MW (g/mol)	CMC (mg/L)	Name	MW (g/mol)	CMC (mg/L)
Non-ionic	DHD	406.6	25.21	FOH	382	400
Cationic	DTAB	308.38	4245	LDBAB	400	900
Anionic	SES	232.27	2879	SLS	700	1900

4.4.2 The influence of molecular weight on surface tension

The surface tension and molecular weight of each surfactant in this work and (Sardeing et al., 2006) were compared (Table 4.6). It can be indicated that low molecular weight tended to reduce the σ_L value which was higher than high molecular weight. It was because the low molecular weight attached on air bubble surface was greater than the high molecular weight. Thus, it can be stated that the σ_L value varied depending on the molecular weight.

Table 4. 4 The surface tension and molecular weight of each surfactant

Surfactant type	This work			Painmanakul, 2006		
	MW (g/mol)	σ_L (mN/m)		MW (g/mol)	σ_L (mN/m)	
		0.01 cmc	0.1 cmc		0.01 cmc	0.1 cmc
Non-ionic	406.6	57.5	48.1	382	45.1	30.4
Cationic	308.38	59.2	41.4	400	42.4	27.6
Anionic	232.27	58	37.4	700	60.45	39.7

4.4.3 The effect of surfactant on the liquid-side mass transfer coefficient (k_L) for aeration

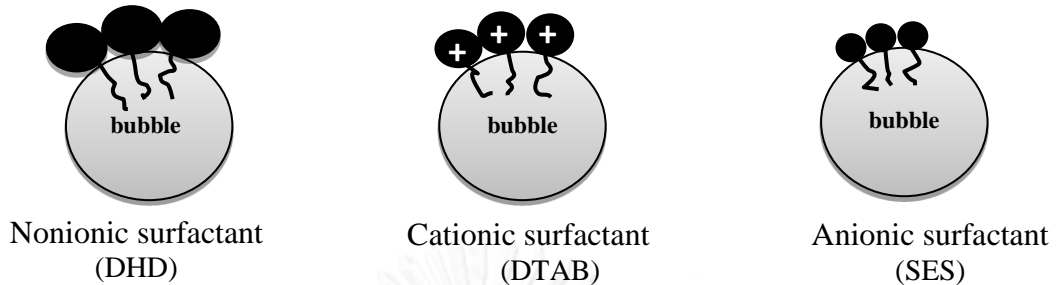


Figure 4. 16 Attachment of each surfactant molecule on air bubbles surface

According to Figure 4.8, it was observed that the k_L values of water were higher than those of anionic, cationic, and non-ionic surfactant solution, respectively. This can be explained by the effect of each surfactant that presence on bubble surface was shown in Figure 4.17. It can be observed that the presence of surfactant can directly effect to the mass transfer by disturbs the composition of bubble surface. Considering addition of anionic surfactant, it was higher attached on bubble surface when compared with other surfactants because it has the lowest molecular weight. Thus its arrangement on the bubble surface was higher neatly than in case of cationic and non-ionic surfactant solution, respectively. Therefore, it can compress or decrease the bubble size greater than other surfactant.

In terms of cationic surfactant and non-ionic surfactant, despite cationic surfactants molecular weight which was close to the anionic surfactant, k_L values of cationic surfactants were significantly lower than the anionic surfactant; while, they were close to k_L values of the non-ionic surfactant that had high molecular weight. It can be explained that the charge of surfactant had probably affected on the bubble surface. As the gas

bubble in aqueous solution had a negative charge (Jia, Ren, & Hu, 2013), the positive charge of cationic surfactant should be attached on bubble surface, which were explained by dipole-dipole interaction.

To understand properly these phenomena, the k_L and d_B , has to be considered.

Figure 4.18 show the variation of k_L values with bubble diameter (d_B) for aeration.

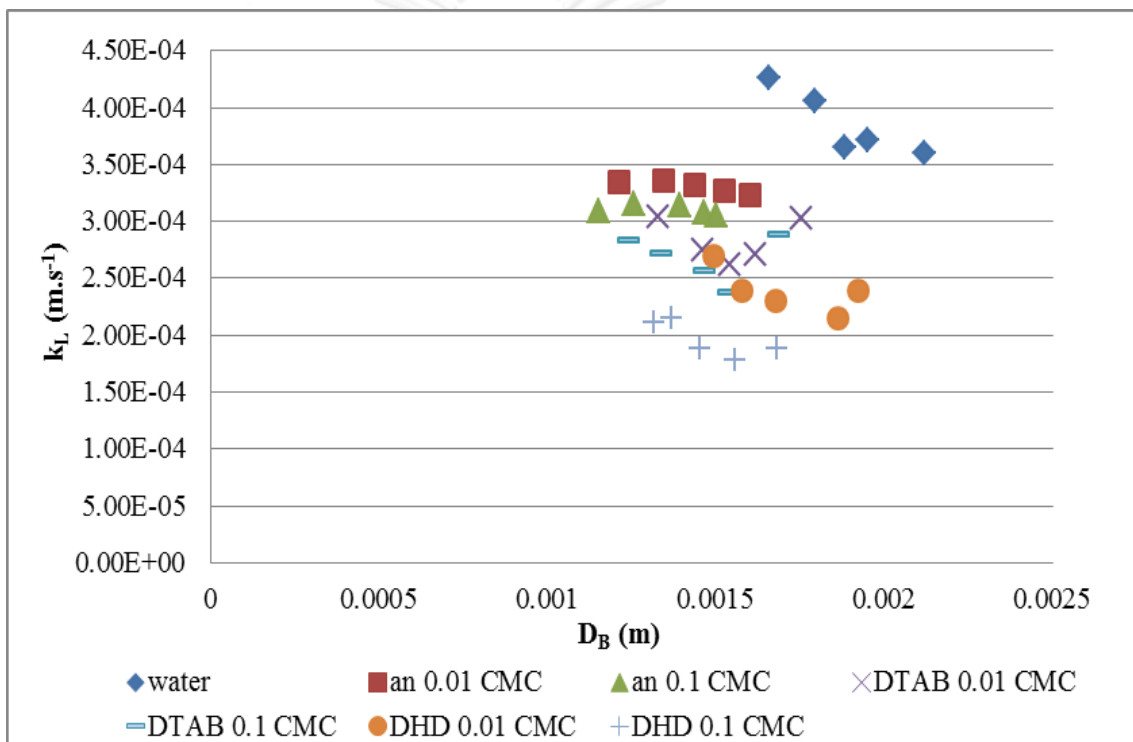


Figure 4. 17 liquid-side mass transfer coefficient versus bubble for aeration part

As shown in Figure 4.18, the results indicate that the presence of surfactant, even in little small quantities can have more significant effect, not only on d_B values, but also on the calculated k_L values. Moreover, it was found that the k_L tend to decrease with the increase of concentration. This is because the presence of surfactant at the bubble

interface disturbs the mass transfer, certainly by modifying the composition or the thickness of liquid film around the air bubbles.

4.4.4 *The effect of surfactant on the liquid-side mass transfer coefficient (k_L) for benzene*

Regarding in Figure 4.19, the k_L values obtained with the high surfactant concentration are smaller than those for another lower concentration which is similar to the aeration part. These results confirm that filling surfactant in the absorption reactor has a direct effect on the decrease in k_L values. Concerning the effect of each surfactant on bubble surface is shown in Figure 4.13, it was observed that non-ionic surfactant is suitable for benzene treatment, even though anionic surfactant was able to reduce the bubble size greater than those of non-ionic surfactant. This can possibly relate to their structure is no specific charge, while the structure of anionic surfactant has a negative charge on their polar head group. Another observation is that hydrophilic-lipophilic balance (HLB) of non-ionic surfactant is less than those in anionic surfactant as shown in Table 4.7. The HLB value for a given surfactant is the relative degree to which the surfactant is water soluble or oil/non-polar soluble. The lower HLB value is the more lipophilic whereas the higher HLB value is the more hydrophilic. It can be stated that non-ionic surfactant is more lipophilic than in case of anionic surfactant. From these reasons, it can be concluded that non-ionic surfactant is appropriate for benzene treatment. When comparison the k_L values between k_L values from aeration part and k_L values benzene part, it was obviously that the trend of k_L value in the aeration part is higher than those in benzene part. This is probably because the diffusion coefficient of oxygen in water ($2.1 \times 10^{-5} \text{ cm}^2 \cdot \text{s}^{-1}$, (Cussler, 1997)) is

higher than the diffusion of coefficient of benzene in water ($1.02 \times 10^{-5} \text{ cm}^2 \cdot \text{s}^{-1}$, (Cussler, 1997)). This result directly affect to the decrease of k_L values that obtained from the benzene part. Thus, these results confirm that the types and concentrations of surfactants significantly affect the liquid-side mass transfer.

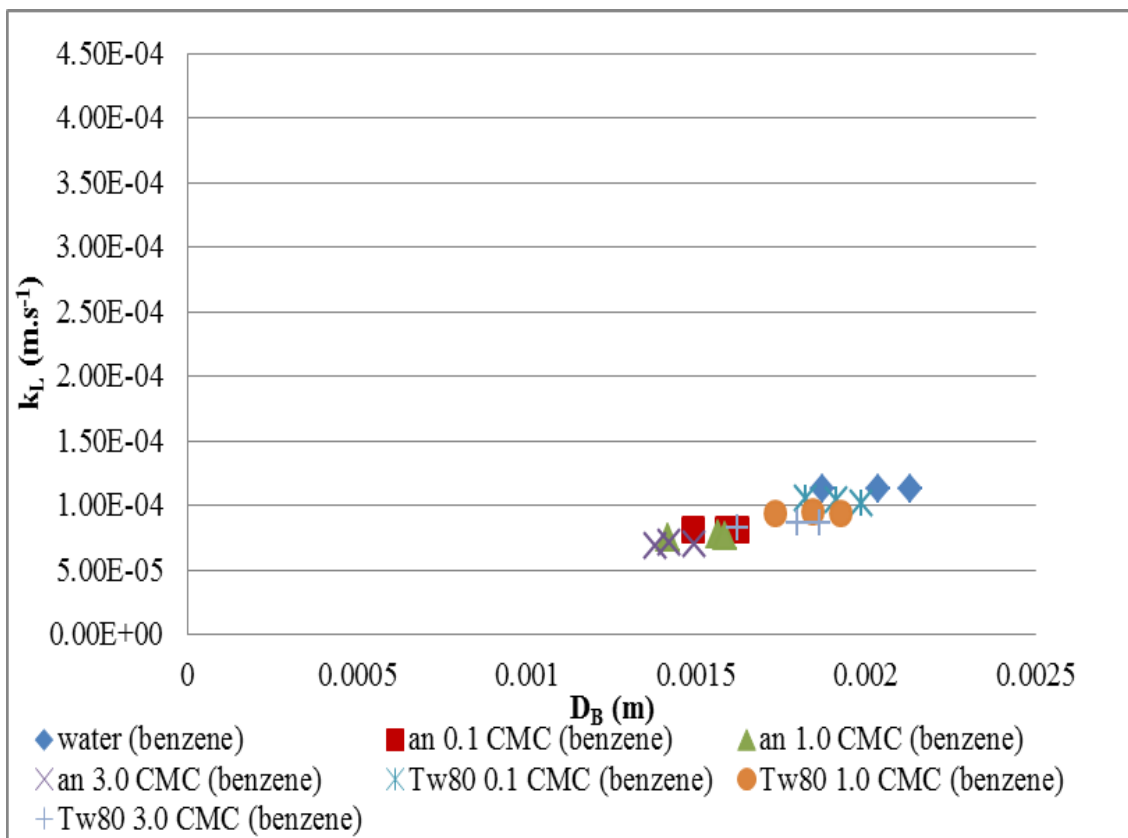


Figure 4. 18 Experimental liquid-side mass transfer coefficient versus bubble for hydrophobic VOCs part

Table 4. 5 The characteristic of each absorbent

Absorbent	CMC (mg.L ⁻¹)	Surface tension	HLB
		(mN.m ⁻¹)	
water	-	-	-
anionic	0.1	58	42 (Flick, 1993)
	1.0	37.4	
	3.0	33. 2	
Non-ionic	0.1	59.3	15 (Schramm, Stasiuk, & Marangoni, 2003)
	1.0	44.2	
	3.0	43.5	

4.4.5 Modeling of the liquid-side mass transfer coefficient

The variation of k_L values with bubble diameter (d_B) of both aeration and hydrophobic VOCs part are shown in Figure 4.20. According to (Sardeing et al., 2006), three zones appear and are considered in this research for analyzing the variation of the k_L values with the bubble diameter:

- Zone A : $d_B < 1.0$ mm.

(Frössling, 1938) proposed that the k_L value depends on bubble geometry.

- Zone B : $1.0 < d_B < 3.0$ mm.

(Sardeing et al., 2006) proposed that the k_L value depends on bubble geometry and physical-chemical properties of surfactant.

- Zone C : $d_B > 3.0$ mm.

(Calderbank & Moo-Young, 1961) proposed that the k_L value depends on physical-chemical properties of surfactant.

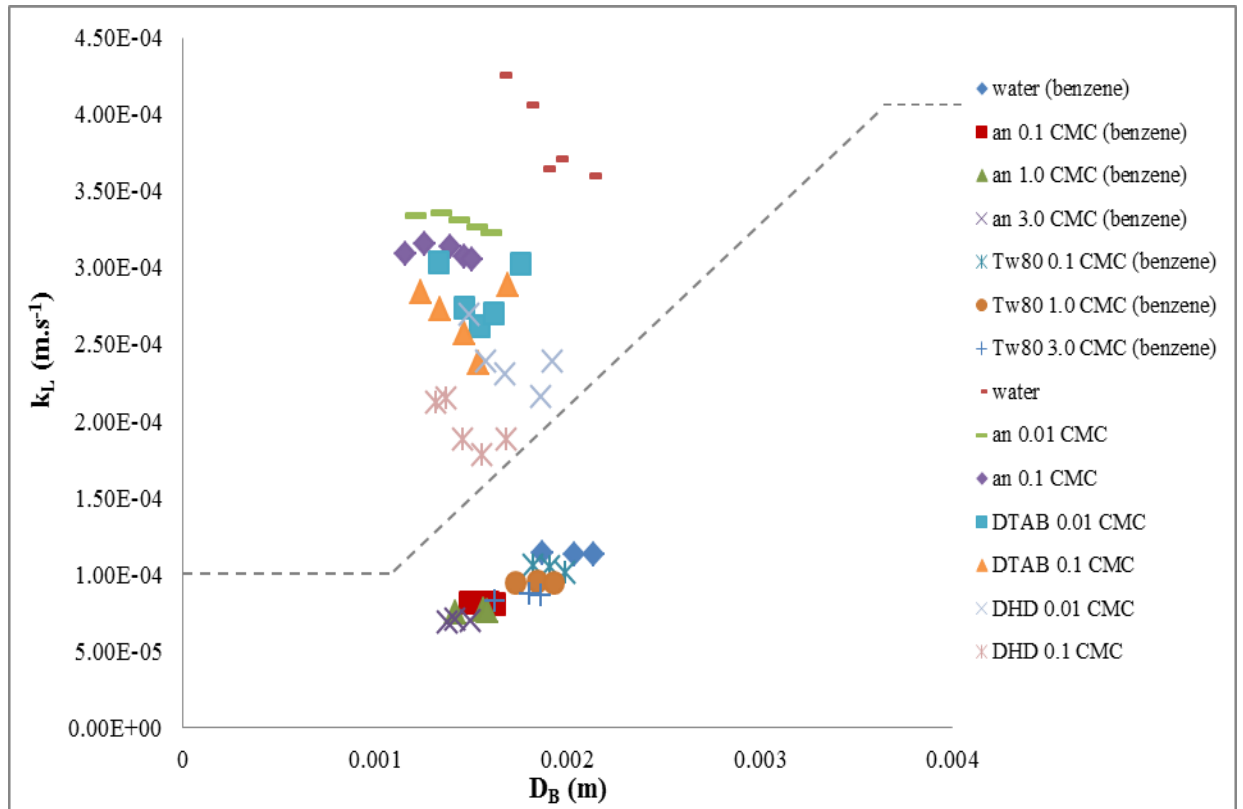


Figure 4. 19 Liquid-side mass transfer coefficient predicted by the models proposed versus the bubble diameters for the different liquid phases

Regarding in Figure 4.20, It can be noted that the results in this study. it was obvious that both the k_L values in aeration and hydrophobic VOCs part values were categorized into zone B for $1.5 < d_b < 3.5$ mm. Therefore, it can probably conclude that these results agree with the model of the k_L coefficients proposed by (Sardeing et al., 2006). For this bubble diameter range in zone B, in the case of water, the k_L values increase. However, in this same range of bubble diameter, the k_L increase is less in the presence of surfactant and becomes nearly zero when the surfactant concentration is very

high. It can be stated that the surfactants have an effect on k_L for this bubble diameter range. In order to determine the liquid-side mass transfer coefficient in the presence of surfactant for bubble diameters between 1.5 and 3.5 mm, the correlation from (Sardeing et al., 2006) model can be used to determine for this work as shown in equation 4.1.

$$\frac{k_L^{Zone B} - k_L^{rigid}}{k_L^{Zone C} - k_L^{rigid}} = (1 - Se) \left(\frac{d_B - d_B^1}{d_B^0 - d_B^1} \right) \quad (4.1)$$

where d_B^1 is equal to 1.5 mm and d_B^0 is equal to 3.5 mm.

The term k_L^{rigid} is proposed by Calderbank and Moo-Young (1961, rigid case),

$$k_L^{rigid} = 0.31 \left(\frac{g\mu_L}{\rho_L} \right)^{1/3} Sc^{-2/3}.$$

The term $k_L^{Zone C}$ is the liquid-side mass transfer coefficient for a bubble diameter of 3.5 mm. It depends on the surfactant concentration and type.

According to equation 4.1, there are many parameters that have to be concerned.

The experimental values and the values predicted by equation 4.1 cannot be done in this study. In the future, it is essential to continue studying the model prediction.

In the next section, an appropriate amount of surfactants and bubble hydrodynamic condition from the previous part were studied in order to obtain the fine absorption performance of hydrophobic VOCs in bubble column by considering in term of VOCs removal efficiency.

4.5 VOCs Removal efficiency

4.5.1 Removal efficiency for benzene absorption

Figure 4.21 presents hydrophobic VOCs removal efficiency obtained with in different liquid phases (tap water and aqueous solutions of surfactants containing with 1.0 CMC) applied with the gas flow rate at $1.5 \text{ L}\cdot\text{min}^{-1}$ ($U_g = 0.0032 \text{ m}\cdot\text{s}^{-1}$). In this work, VOCs removal efficiency was determined by using the equation 3.6.

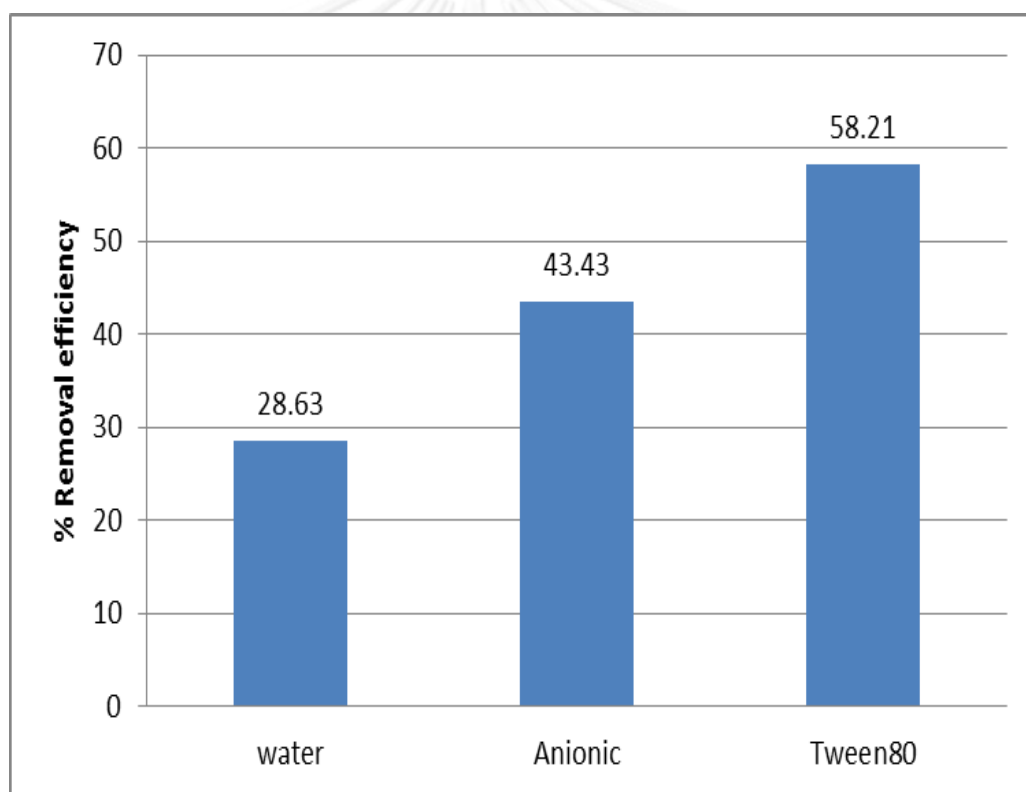


Figure 4. 20 VOCs removal efficiency

According to Figure 4.21, it was observed that % benzene removal efficiency of non-ionic surfactant (Tween80) was greater than those obtained in anionic and water. This coincides with the fact that non-polar and hydrophobic compounds such as benzene are

quite insoluble in water. Due to the chemical rule, the hydrophobic (non-polar) VOCs had higher solubility in non-polar solvent than in polar solvent, and water.

However, no single method can be used in all cases: most of methods are specific in nature. In order to enhance the benzene removal efficiency, the adsorption process was work together with absorption process.

4.5.2 The effect of the hybrid process combining absorption and adsorption process for treatment of benzene

In this research, granular activated carbon was chosen as adsorbent because their structure that is extreme porous with a very large surface area to curtain contaminant accumulate on their surface. Consequently, it was expected that benzene gas is well-adsorbed by granular activated carbon. Thus GAC was applied with the optimal aqueous solution of surfactant from the previous part and with water as well. Note that the mass of GAC used are 25, 50, 75 and 100 g, and the VOCs concentrations obtained in this study are measured by UV-Visible spectrophotometer. The variation of the absorbance with time is shown in Figure 4.22.

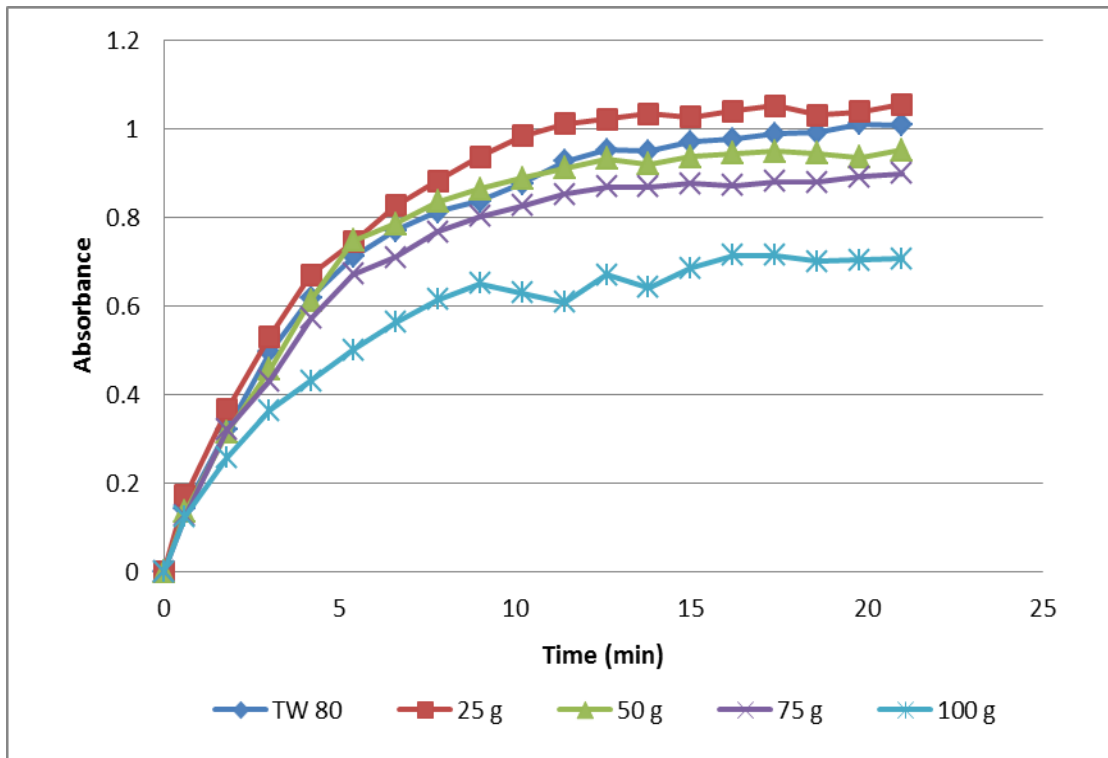


Figure 4. 21 Absorbance versus time for non-ionic surfactant

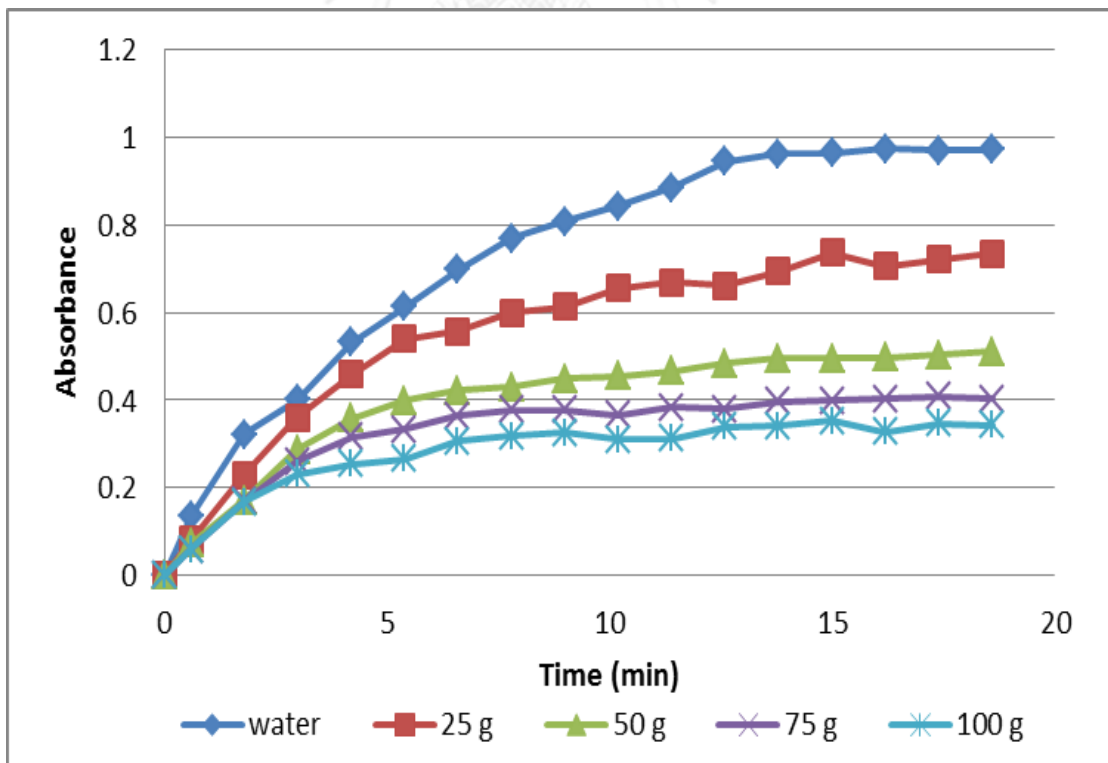


Figure 4. 22 Absorbance versus time for water

According to Figures 4.22 and 4.23, the results show that mass of GAC has effect on benzene absorption. The absorbance values are rather high for non-ionic surfactant even in using high GAC mass, while the absorbance values are rather low with the increasing of GAC for water. It can be stated that non-ionic surfactant is not appropriate for working with GAC. This is because non-ionic surfactant might cover at the surface of GAC, and was adsorbed into GAC as well, which decrease the adsorption efficiency of benzene. This phenomenon was shown in Figure 4.24. Moreover, it was observed that the absorbance values tend to decrease with the increase of the mass of GAC. This is probably because the rate of adsorption is greater than the rate of absorption rate. Notably, the volumetric mass transfer coefficient or the rate of adsorption was deduced from the difference of absorbance value between only tap water and tap water combined with GAC then the relation between concentrations of benzene in liquid phase with time was plotted, and the k_{LS} was found from the slope. Regarding in Table 4.6, these results confirm that the transfer rate of benzene from gas phase to liquid phase is less than the transfer rate of benzene from liquid phase to solid phase. The mechanism of this process is shown in Figure 4.25.

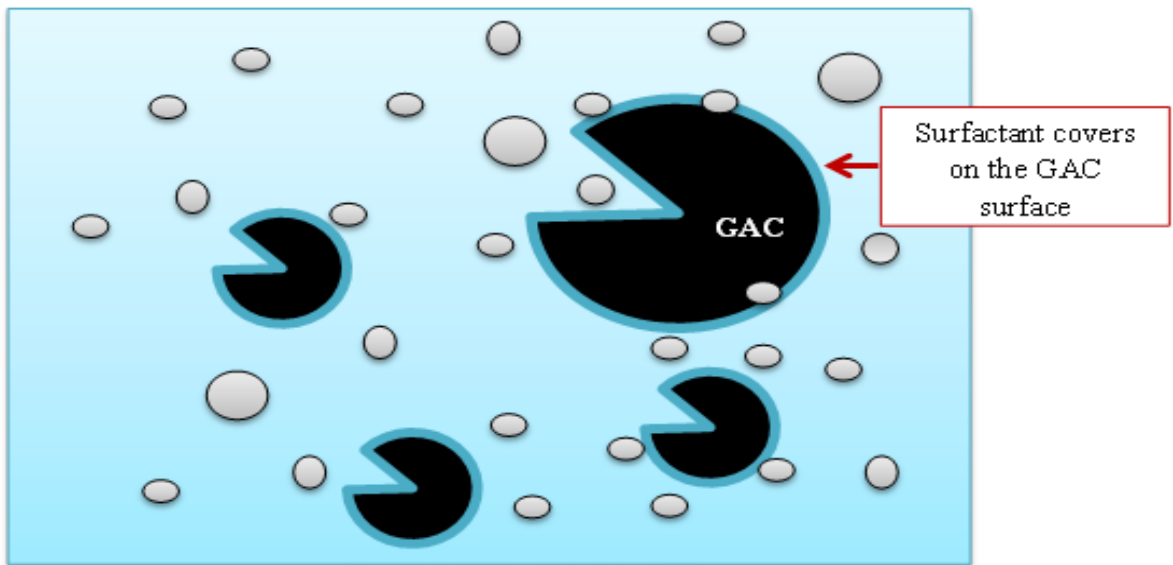


Figure 4. 23 Effect of surfactant (non-ionic) on GAC adsorption

Table 4. 6 The volumetric mass transfer coefficient in different phase

Transfer	The overall mass transfer coefficient (min^{-1})
Benzene gas to liquid phase	0.201
liquid phase to solid phase	0.2601

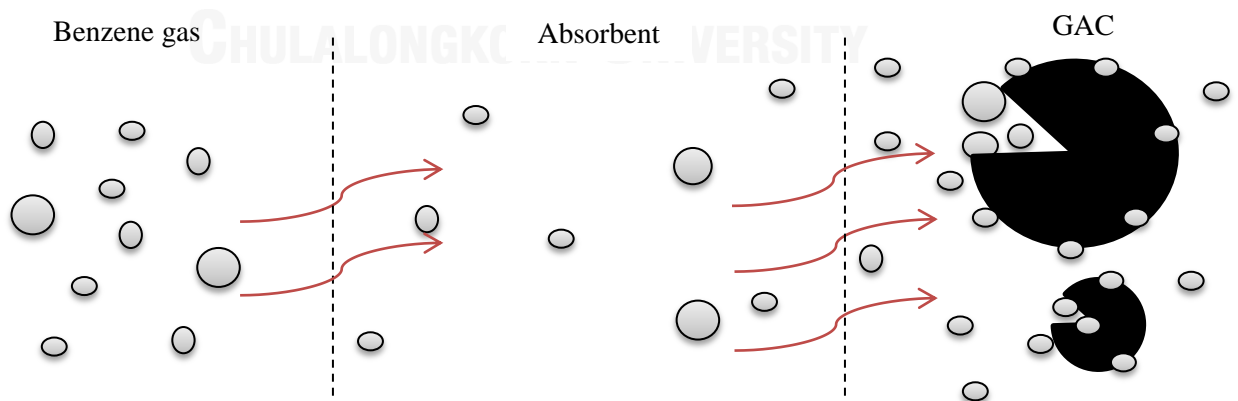


Figure 4. 24 Mechanism for benzene absorption and adsorption

4.5.3 VOCs Removal efficiency of hybrid process (absorption and adsorption)

Figure 4.26 shows the VOCs removal efficiency which was analyzed by using Gas Chromatography

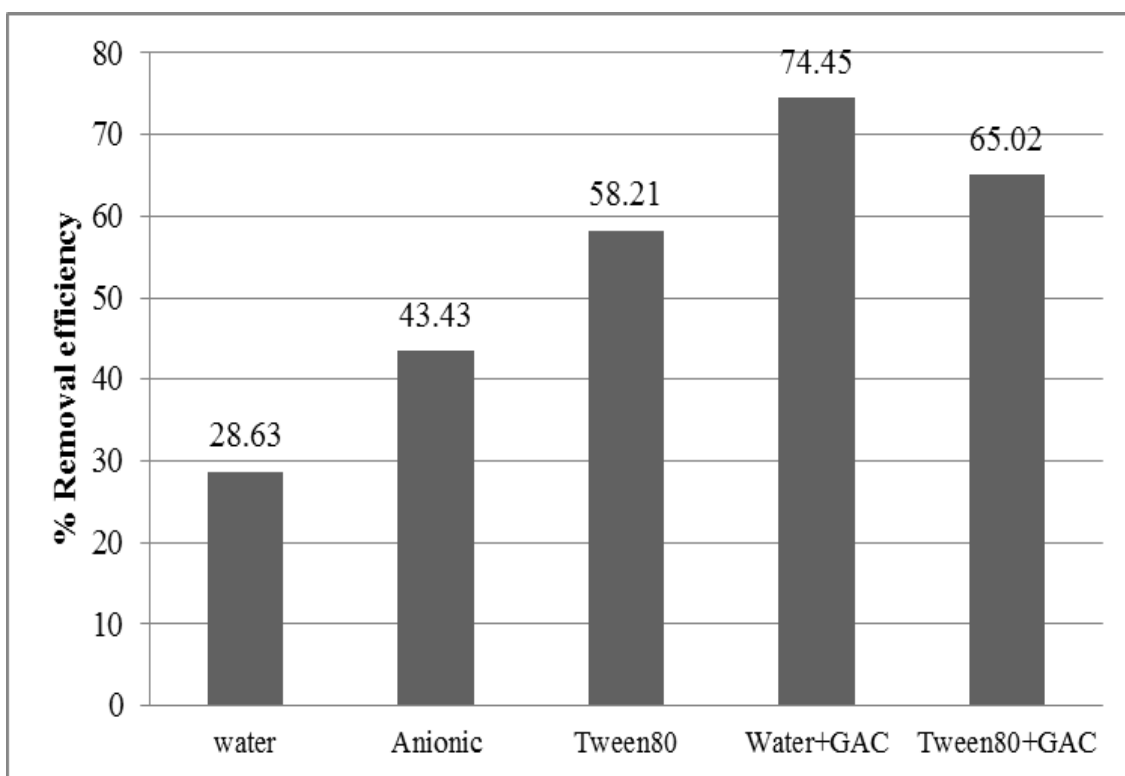


Figure 4. 25 The VOCs removal efficiency

According to Figure 4.26, it was shown that VOCs removal efficiencies range between 28.63% - 74.45%. The highest value of VOCs removal efficiency was observed at water worked together with GAC (75 g), and another observation was that these results confirm that the addition of GAC into liquid phase can improve the removal efficiency of benzene. Moreover, % removal efficiency of hybrid processes obtained is higher than those obtained in others absorbent.

In this study, the rigid diffuser with the gas superficial velocity at ($U_g = 0.0032 \text{ m.s}^{-1}$) and water combined with GAC (75 g) are suggested in order to reduce VOCs desorption mechanism, and maintain the suitable absorption efficiency. In practice, the physical and chemical properties of absorbance, the reactor configuration/maintenance are critical factors that can affect and limit the apparent absorption performance.



CHAPTER V

CONCLUSIONS AND RECOMMENDATIONS

5.1 Conclusions

The objective of this paper is to study the effect of bubble hydrodynamic and liquid phase on mass transfer mechanism in bubble column, and to apply this process into a purification process for benzene. To fulfill this purpose, the effects of gas diffusers, gas flow rates, and absorbents (tap water, aqueous solution with anionic, cationic, and non-ionic surfactant) are analyzed by using the benzene as hydrophobic VOCs. In this study, the following results have been obtained:

- The rigid diffuser is chosen as the optimal gas diffusers due to the smallest bubble sizes generated. This leads to the highest interfacial area (a) for mass transfer mechanism that occurs for VOCs absorption in a bubble column.
- The different types of diffusers and surfactant molecules presence in liquid phase can affect the bubble size, interfacial area, liquid-side mass transfer and volumetric mass transfer.
- An addition of anionic surfactant (SES) with low concentration (0.01 and 0.1 CMC) can also increase the $k_L a$ coefficient compared with another absorbent.
- In any gas flow rate, the bubble sizes obtained from surfactant solutions at different concentrations are lower than those obtained from tap water. These results are associated with the increase of interfacial area.

- In any gas flow rate, the liquid-side mass transfer coefficients (k_L) are roughly constant for a given liquid phase. The k_L coefficients of non-ionic and anionic surfactant as absorbents are smaller than those of tap water.
- For the benzene absorption, the volumetric mass transfer coefficient ($k_L a$) increases with the superficial gas velocity regardless of the liquid phases, and the $k_L a$ coefficients of anionic and non-ionic surfactants at different concentrations are smaller than those of tap water.
- An additional of GAC in liquid phase enhances the benzene removal efficiency.
- Using non-ionic surfactant combined with GAC is not appropriate for benzene removal because the non-ionic surfactant might cover at the surface of GAC, which directly affect to the adsorption efficiency of benzene.
- The combination of absorption and adsorption can apply into a purification process for benzene.

5.2 Recommendations for future work

For future research, it is essential to study the effect of various types of Volatile Organic Compounds (VOCs) in order to provide a better understanding on bubble hydrodynamic phenomena and mass transfer mechanism for absorption process in a bubble column. Moreover, it is evident that the results observed in the bubble column have to be validated in a tall bubble column and at higher superficial velocities. Finally, the theoretical models or correlations should be considered to compare the experimental results of bubble hydrodynamic and mass transfer parameters and predict the absorption efficiency obtained in a bubble column.

REFERENCES

- Asenjo, N. G., Alvarez, P., Granda, M., Blanco, C., Santamaria, R., & Menendez, R. (2011). High performance activated carbon for benzene/toluene adsorption from industrial wastewater. *J Hazard Mater*, *192*(3), 1525-1532. doi: 10.1016/j.jhazmat.2011.06.072
- Bouaifi, M., Hebrard, G., Bastoul, D., & Roustan, M. (2001). A comparative study of gas hold-up, bubble size, interfacial area and mass transfer coefficients in stirred gas-liquid reactors and bubble columns. *Chemical Engineering and Processing*, *40*, 97-111.
- Calderbank, P. H., & Moo-Young, M. B. (1961). The continuous phase heat and mass-transfer properties of dispersions. *Chemical Engineering Science*, *16*, 39-54.
- Cussler, E. L. (1997). *Diffusion: Mass Transfer in Fluid Systems New York: Cambridge University Press*, 2.
- Deckwer, W. D., Trad, D.E., Cottrell, V. (1992). *Bubble Column Reactors. Wiley, Chichester*, 239-254.
- EPA, U. S. (1989). *Design Manual: Fine Pore Aeration Systems. EPA Center for Environmental Research Information. Cincinnati, Ohio*, EPA/625/621-689/023.
- EPA, U. S. (1998). *Carcinogenic Effects of Benzene: An Update. Office of Research and Development, Washington, DC*, EPA/600/P-697/001A.
- Flick, E. W. (1993). *Industrial Surfactants. An Industrial Guide*, 2, 93.
- Frössling, N. (1938). Über die Verdunstung fallender Tropfen. *Gerlands Beiträge zur Geophysik*, *52*, 170-216.
- Grace, J. R., & Wairegi, T. (1986). Properties and characteristics of drops and bubbles. *Encyclop. Fluid Mech.*, *3*, 43-57.
- Heymes, F., Demoustier, P. M., Charbit, F., Fanlo, J.-L., & Moulin, P. (2007). Treatment of gas containing hydrophobic VOCs by a hybrid absorption-pervaporation process: The case of toluene. *Chemical Engineering Science*, *62*(9), 2576-2589. doi: 10.1016/j.ces.2007.02.001
- Jia, W., Ren, S., & Hu, B. (2013). Effect of Water Chemistry on Zeta Potential of Air Bubbles. *Electrochemical Science*, *8*.
- Kantarci, N., Borak, F., & Ulgen, K. O. (2005). Bubble column reactors. *Process Biochemistry*, *40*(7), 2263-2283. doi: 10.1016/j.procbio.2004.10.004

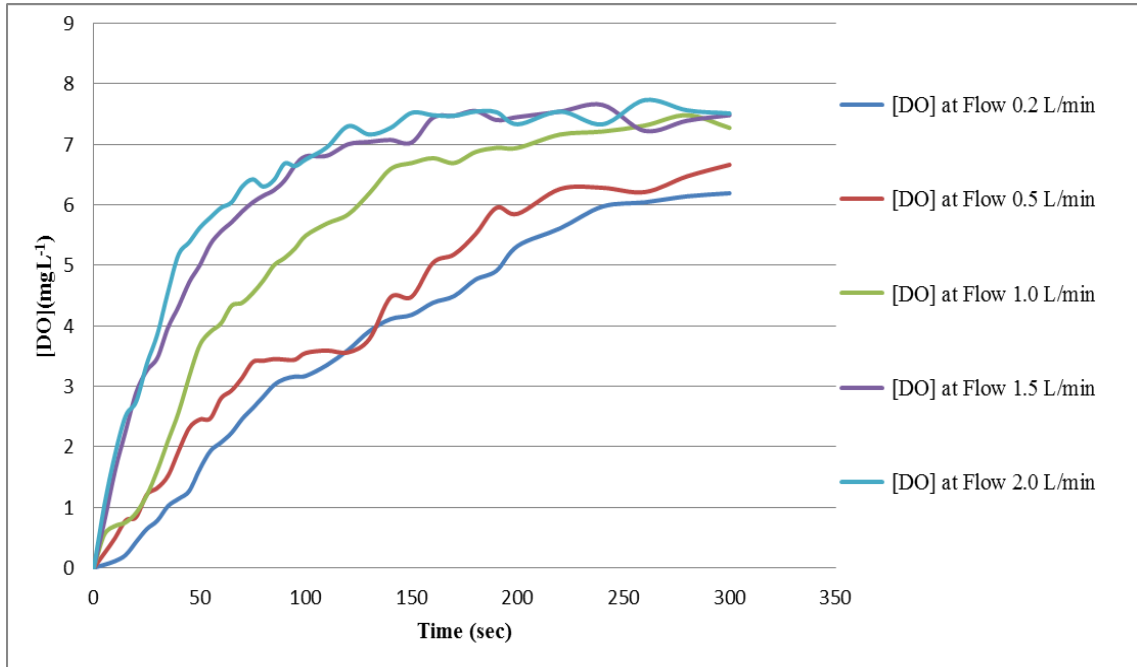
- Loubie`re, K., & Hébrard, G. (2004). Influence of liquid surface tension (surfactants) on bubble formation at rigid and flexible orifices. *Chemical Engineering and Processing*, *43*, 1361–1369.
- Loubière, K., & Hébrard, G. (2003). Bubble formation from a flexible hole submerged in an inviscid liquid. *Chemical Engineering Science*, *58*(1), 135-148. doi: 10.1016/s0009-2509(02)00468-2
- Painmanakul, P., Loubiere, K., Hebrard, G., & Buffiere, P. (2004). Study of different membrane spargers used in waste water treatment: characterisation and performance. *Chemical Engineering and Processing: Process Intensification*, *43*(11), 1347-1359. doi: 10.1016/j.cep.2003.09.009
- Painmanakul, P., Loubière, K., Hébrard, G., Mietton-Peuchot, M., & Roustan, M. (2005). Effect of surfactants on liquid-side mass transfer coefficients. *Chemical Engineering Science*, *60*(22), 6480-6491. doi: 10.1016/j.ces.2005.04.053
- Pavoni, B., Drusian, D., Giacometti, A., & Zanette, M. (2006). Assessment of organic chlorinated compound removal from aqueous matrices by adsorption on activated carbon. *Water Res*, *40*(19), 3571-3579. doi: 10.1016/j.watres.2006.05.027
- Ross, D. (1996). Metabolic basis of benzene toxicity. *HAEMATOLOGY*, *57*, 111-118.
- Sardeing, R., Painmanakul, P., & Hébrard, G. (2006). Effect of surfactants on liquid-side mass transfer coefficients in gas–liquid systems: A first step to modeling. *Chemical Engineering Science*, *61*(19), 6249-6260. doi: 10.1016/j.ces.2006.05.051
- Schramm, L. L., Stasiuk, E. N., & Marangoni, D. G. (2003). Surfactants and their applications. *Annu. Rep. Prog. Chem.*, *99*, 3-48. doi: 10.1039/b208499f
- Seeger, A., Affeld, K., Kertzsch, U., Goubergrits, L., Wellnhofer, E. (2001). Assessment of Flow Structures in Bubble Columns by X-ray Based Particle Tracking Velocimetry. *4th International Symposium on Particle Image Velocimetry Göttingen, Germany*.
- Shepherd, A. (2001). Activated Carbon Adsorption For Treatment of VOCs Emission *The 13th Annual EnviroExpo, Boston Massachusetts*.
- U.S., A. C. o. E. (2001). Adsorption Design Guide. Design Guide No. 1110-1-2. *Department of the Army, U.S. Army Corps of Engineers. Washington, DC*.
- Whitman, W. G., Lewis, W. K. (1924). Principles of Gas Absorption. *INDUSTRIAL AND ENGINEERING CHEMISTRY*, 1215-1220.



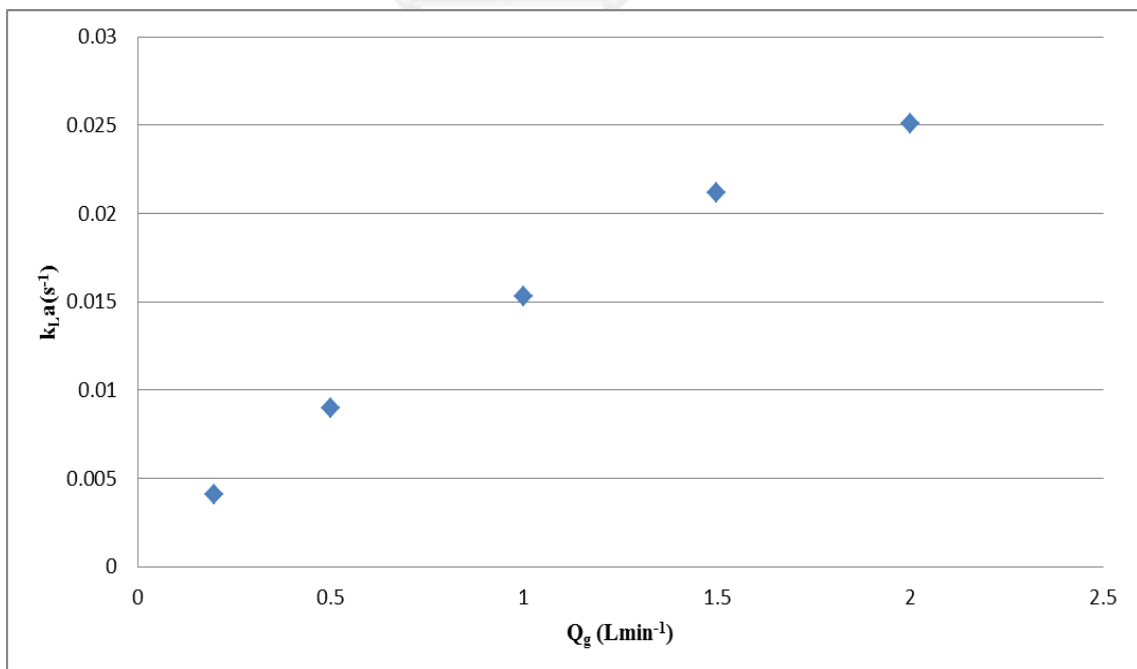
APPENDIX

จุฬาลงกรณ์มหาวิทยาลัย
CHULALONGKORN UNIVERSITY

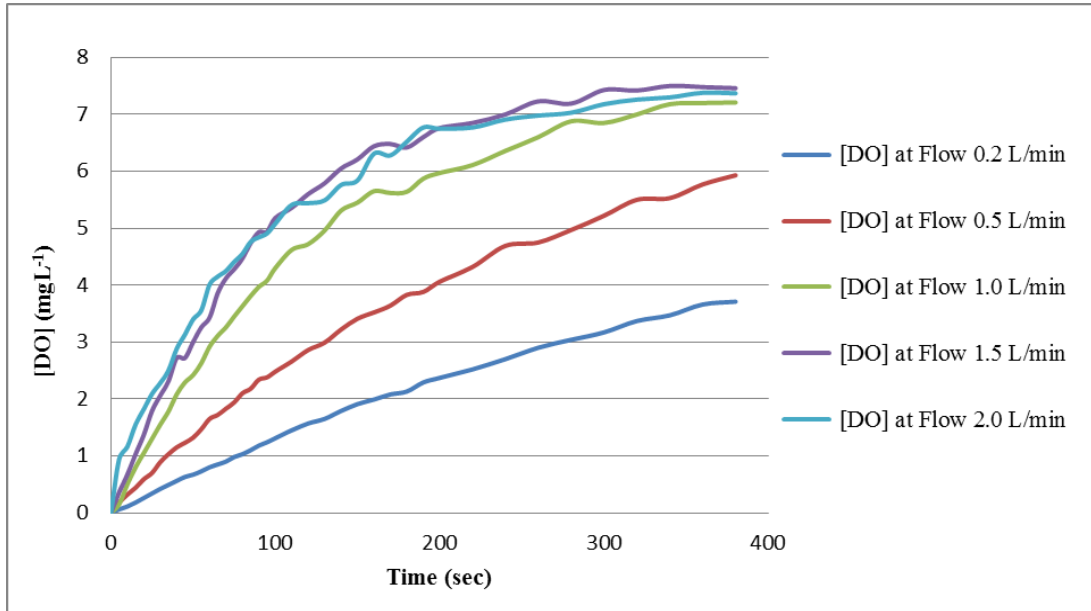
Concentration of dissolved oxygen in water for rigid diffuser



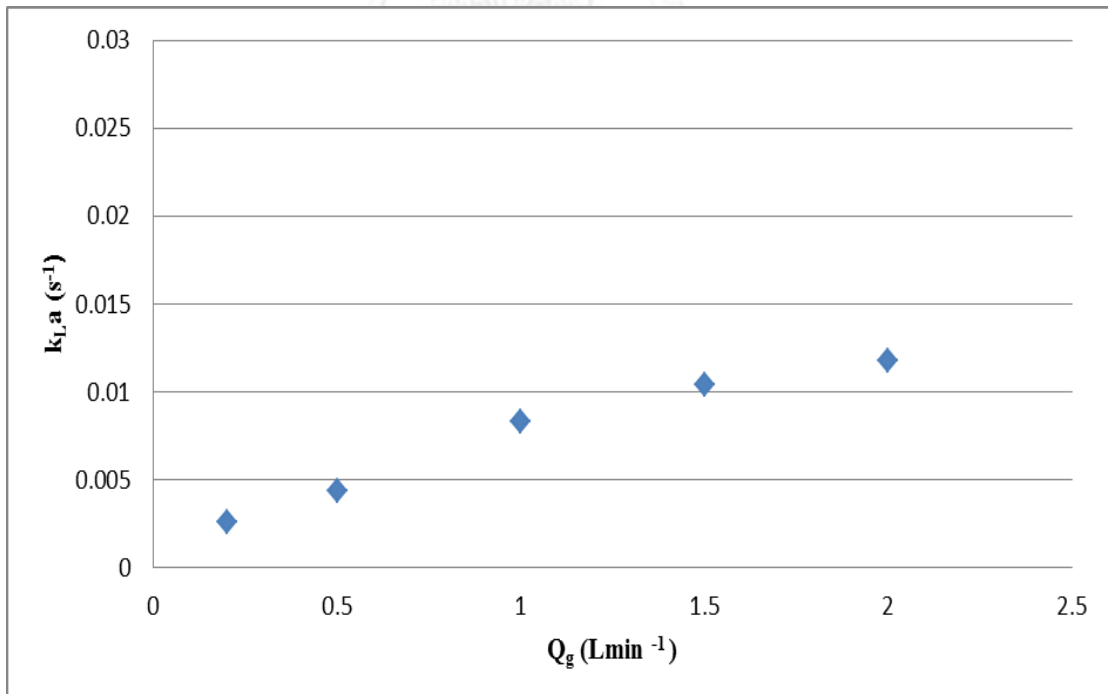
$k_L a$ versus Q_g



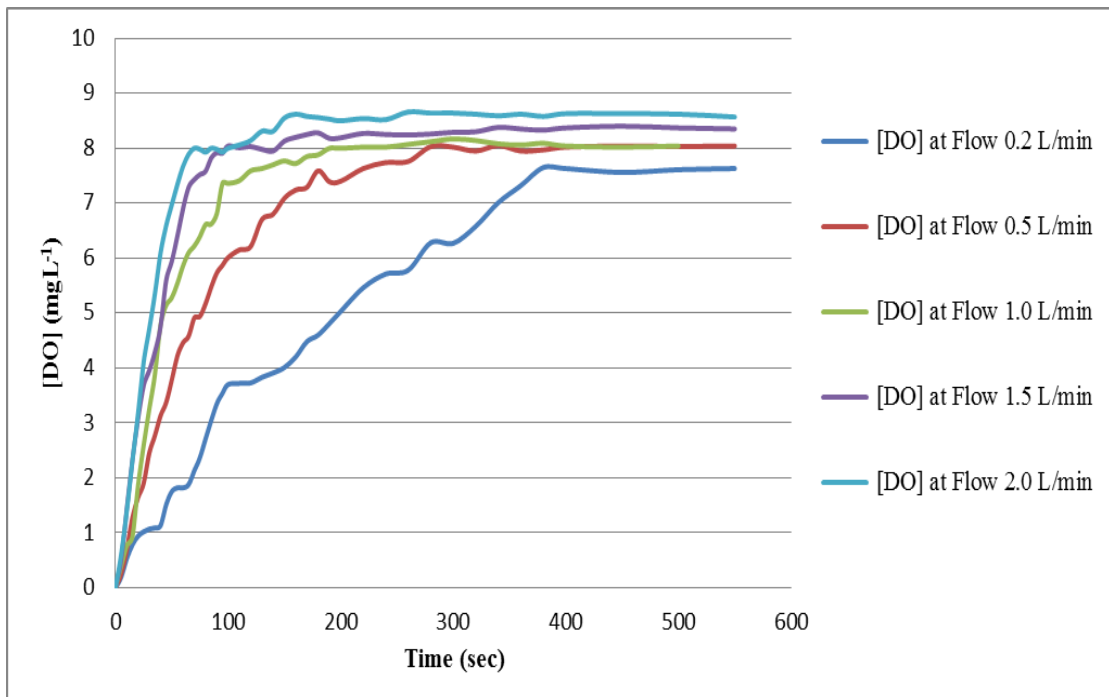
Concentration of dissolved oxygen in water for flexible diffuser



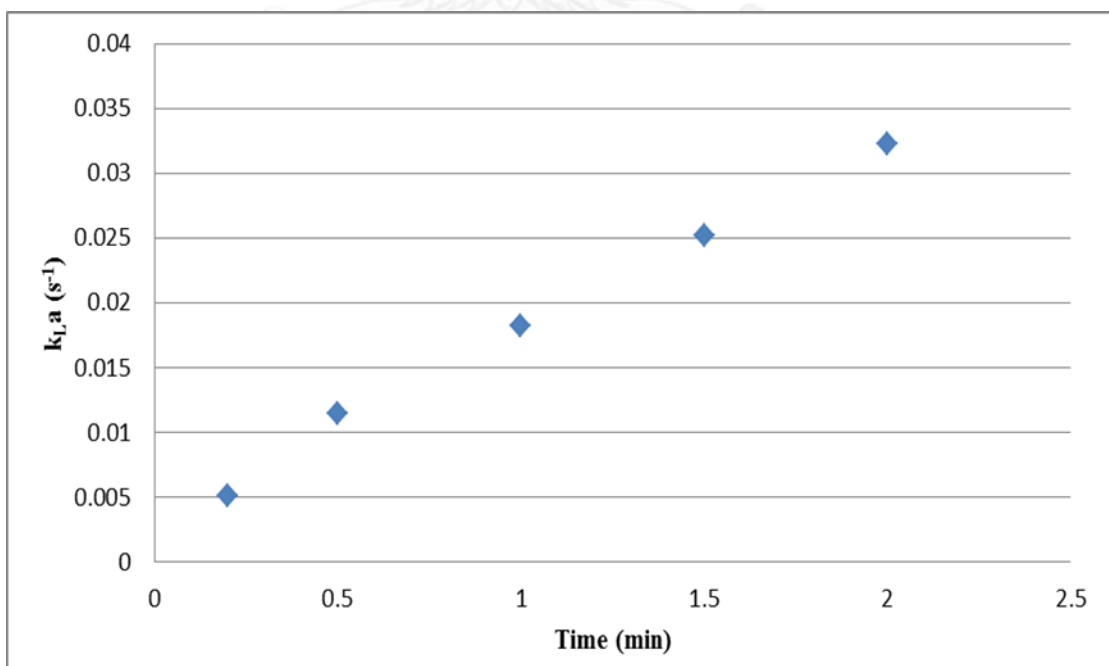
$k_L a$ versus Q_g



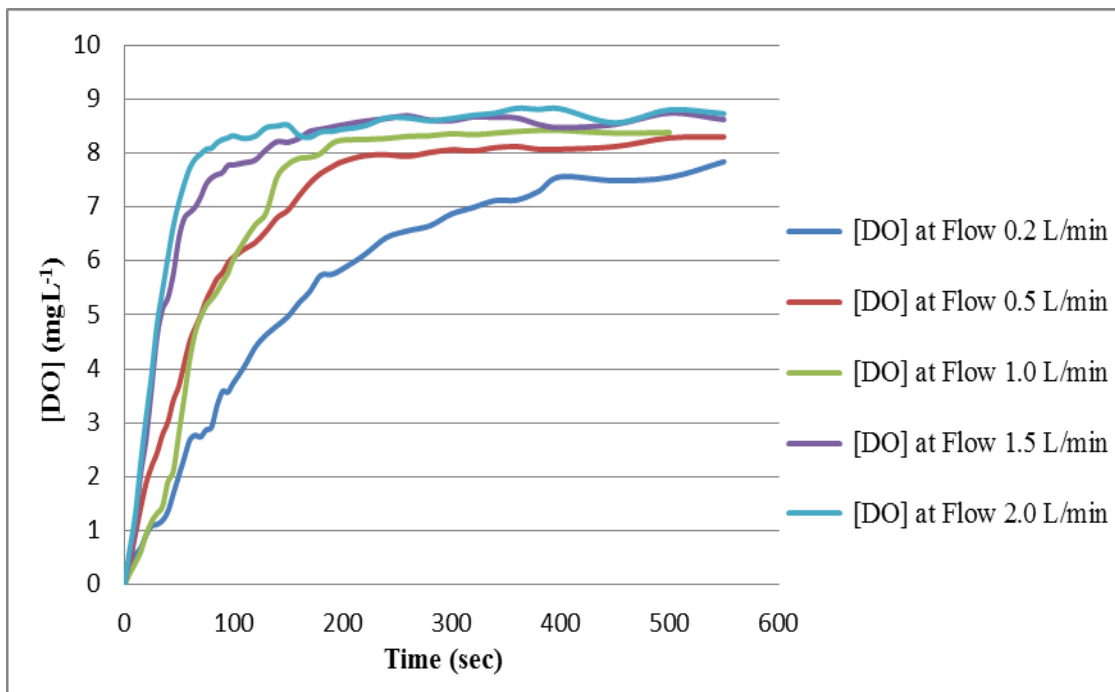
Concentration of dissolved oxygen in anionic solution at 0.01 cmc



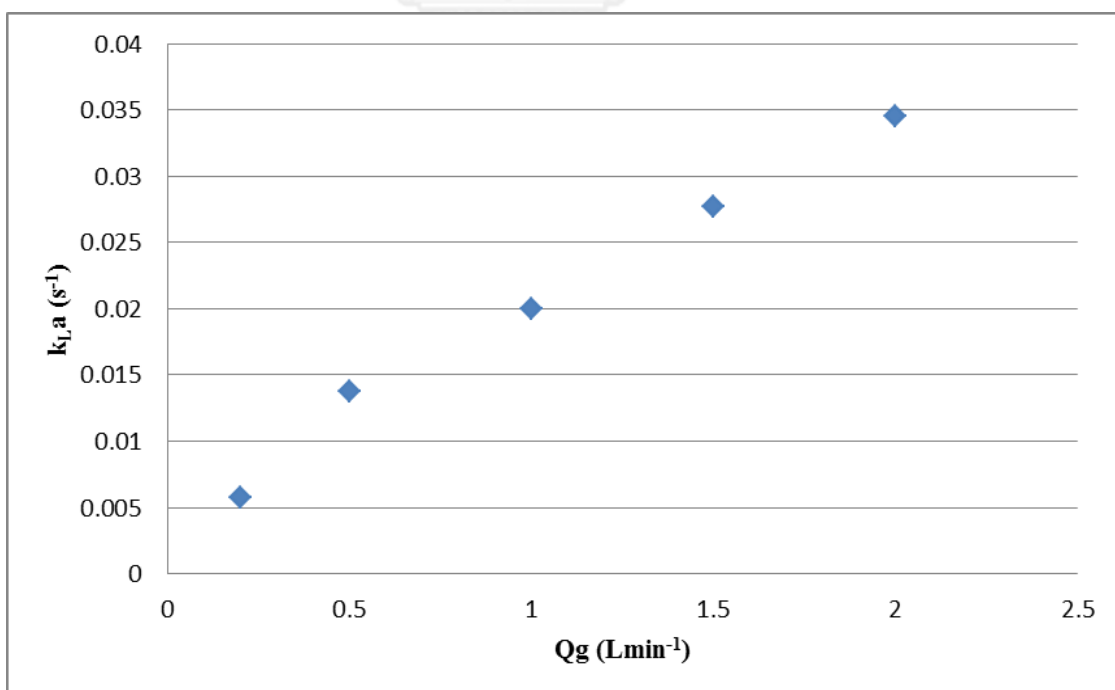
$k_L a$ versus Q_g for anionic solution at 0.01 cmc



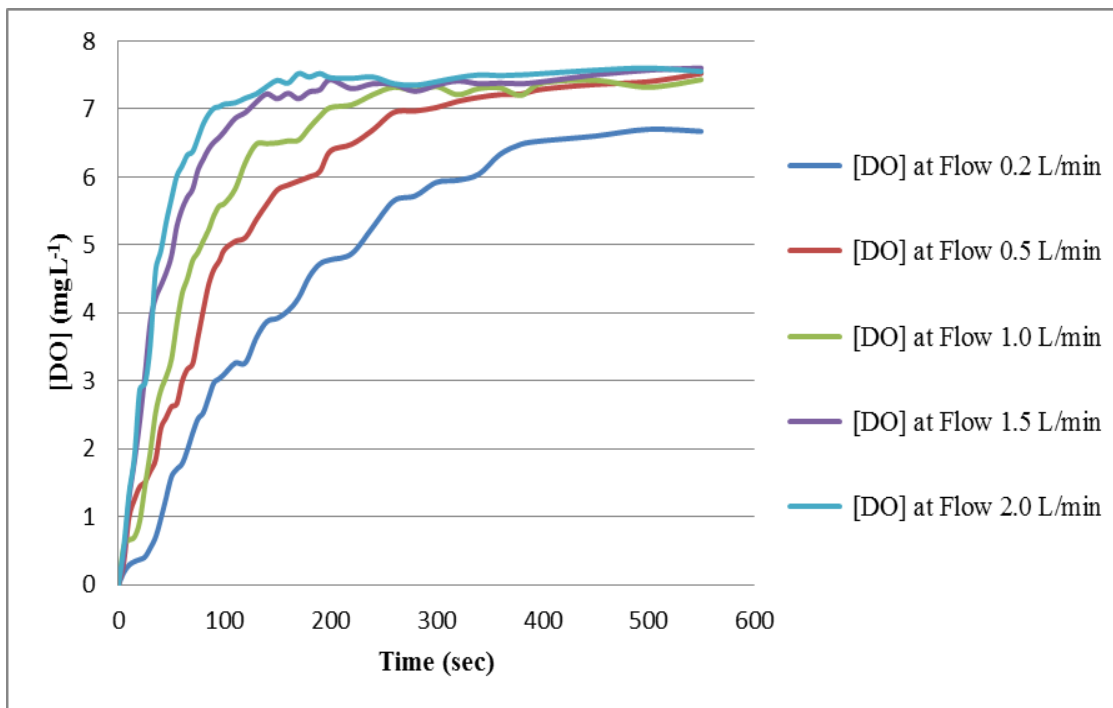
Concentration of dissolved oxygen in anionic solution at 0.1 cmc



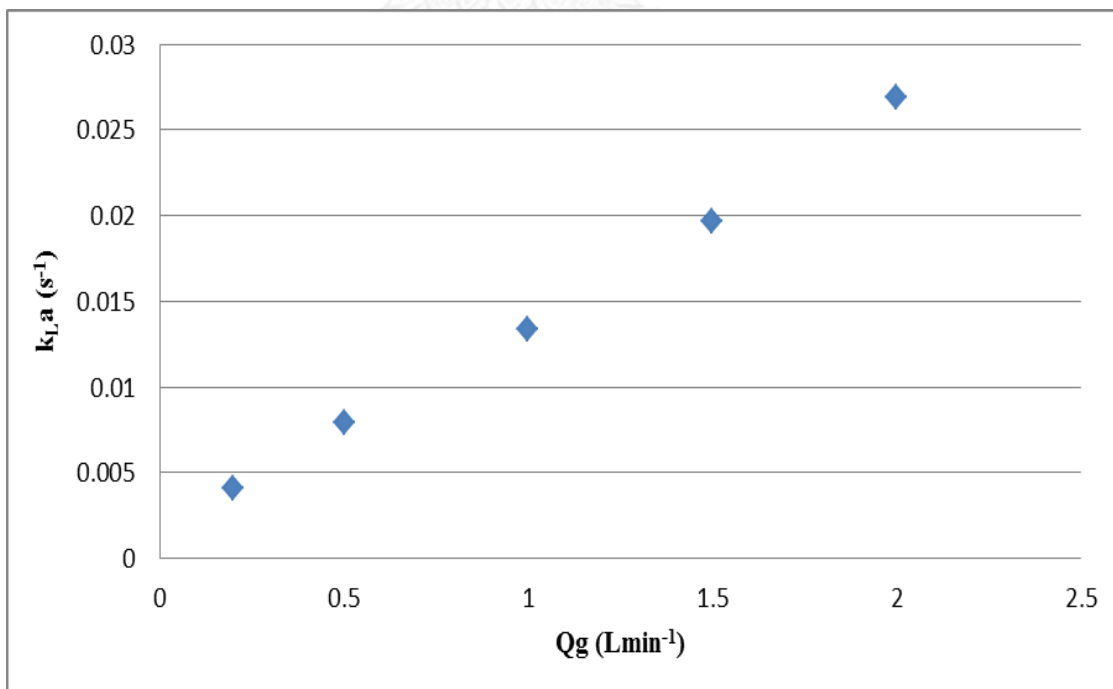
$k_L a$ versus Q_g for anionic solution at 0.1 cmc



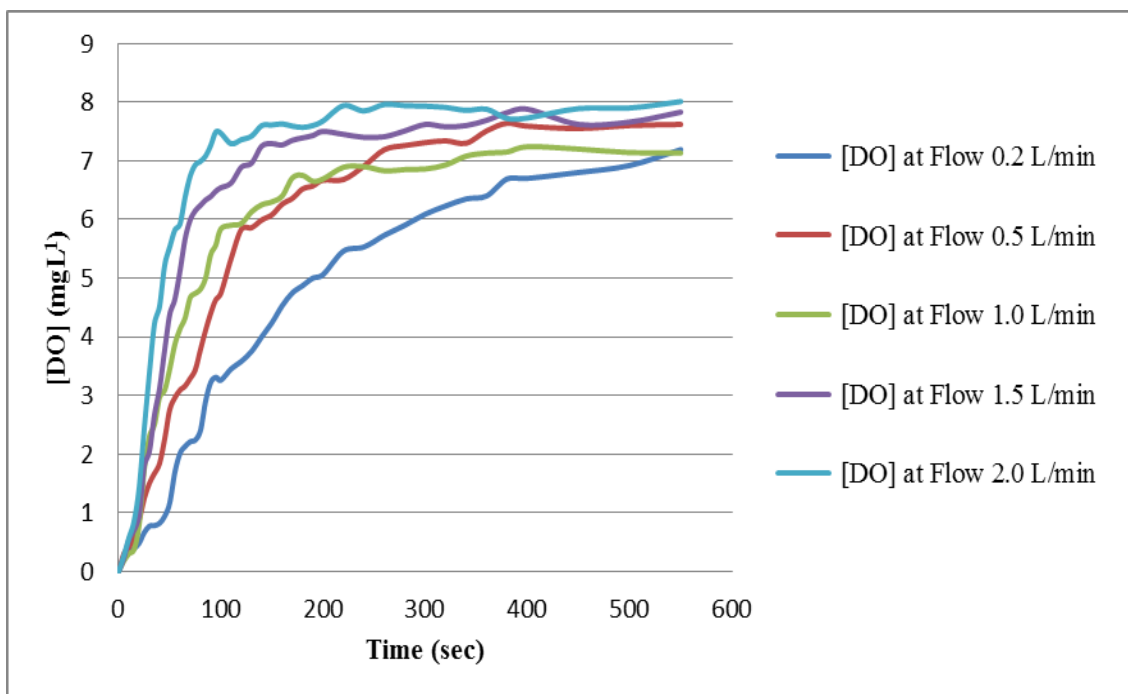
Concentration of dissolved oxygen in cationic solution at 0.01 cmc



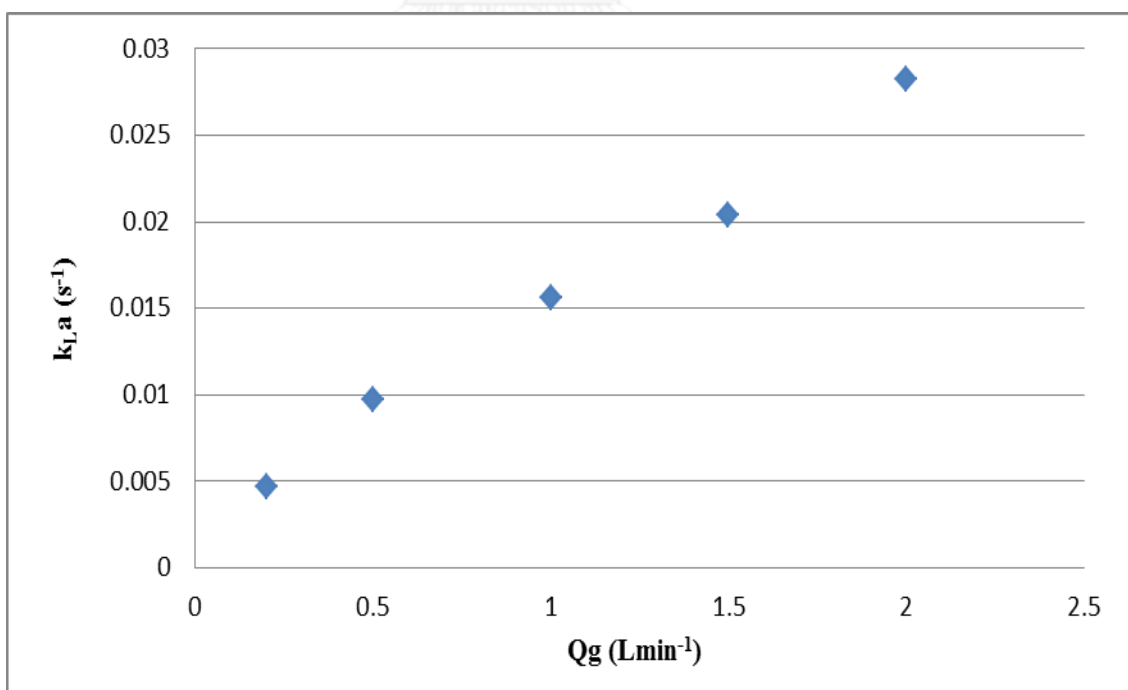
$k_L a$ versus Q_g for cationic solution at 0.01 cmc



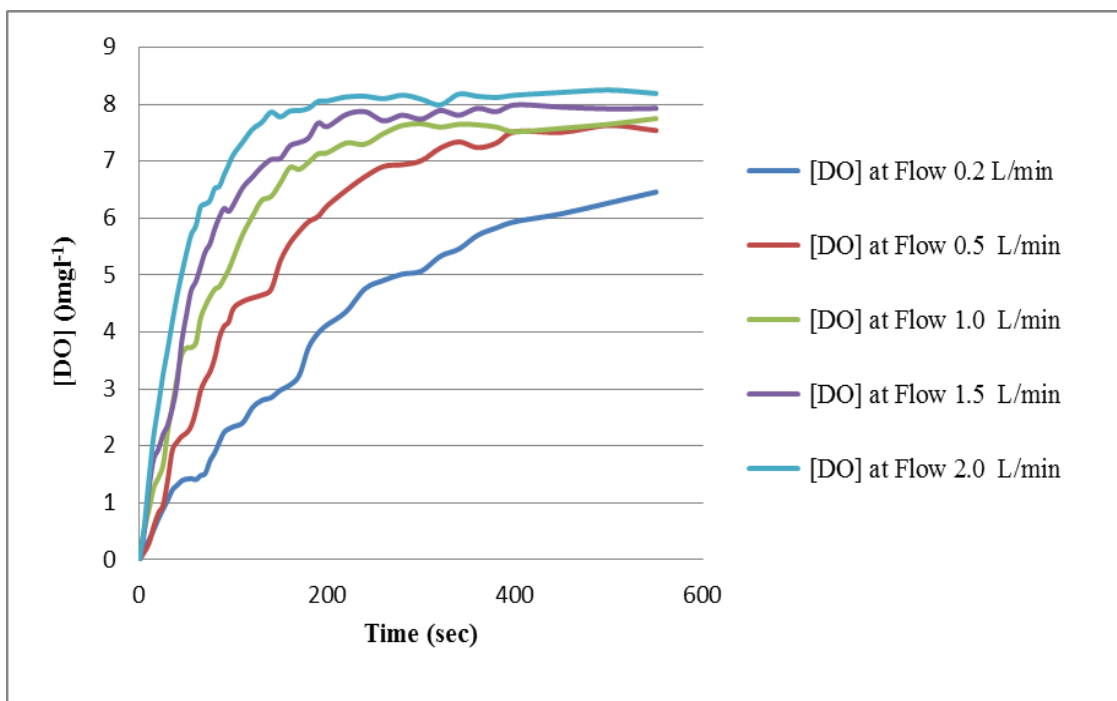
Concentration of dissolved oxygen in cationic solution at 0.1 cmc



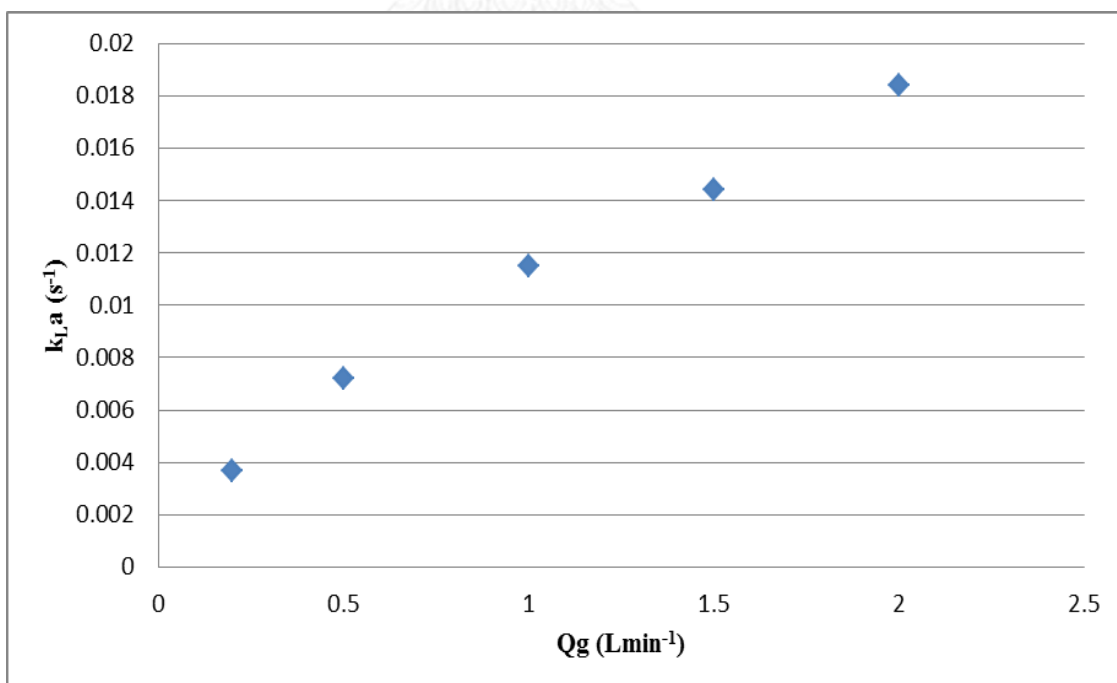
$k_L a$ versus Q_g for cationic solution at 0.1 cmc



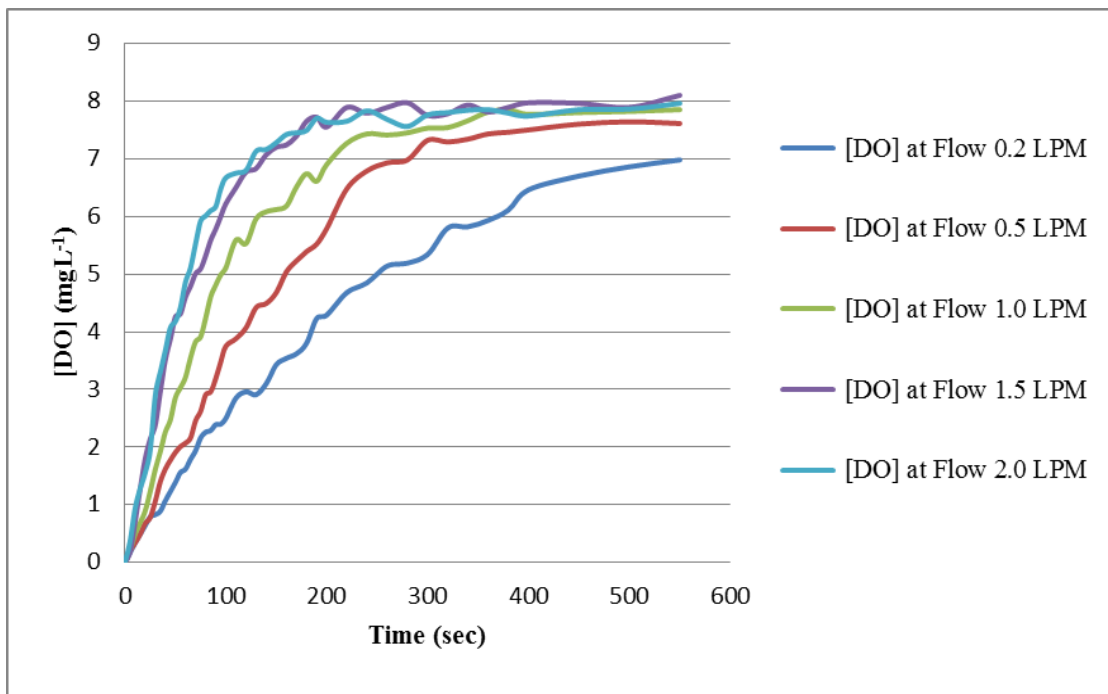
Concentration of dissolved oxygen in non-ionic solution at 0.01 cmc



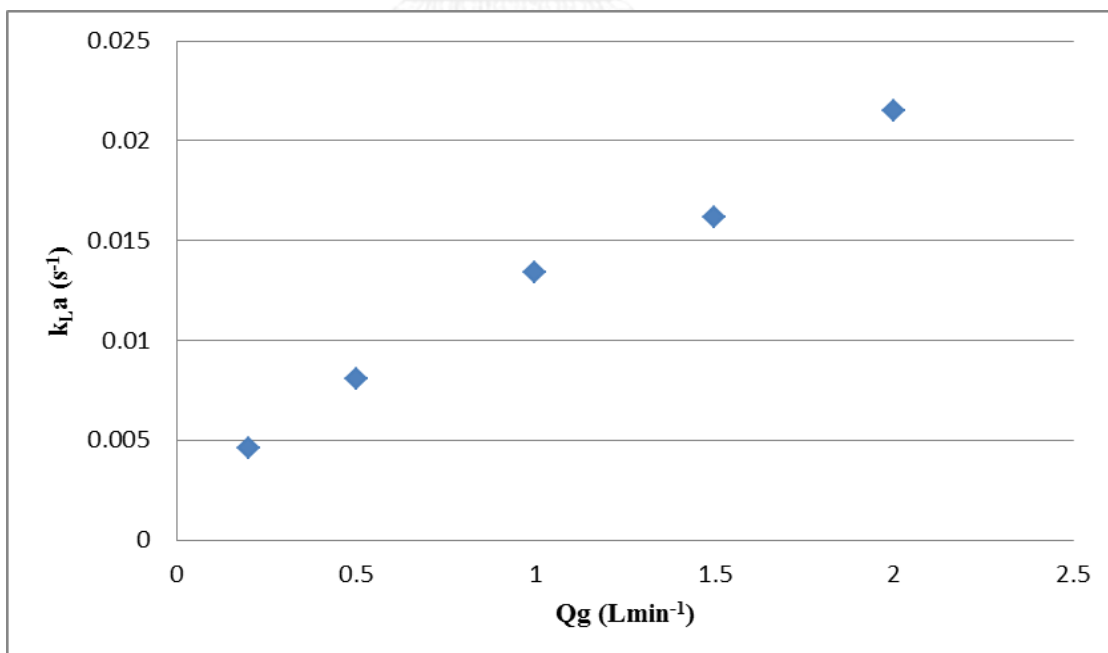
$k_L a$ versus Q_g for non-ionic solution at 0.01 cmc



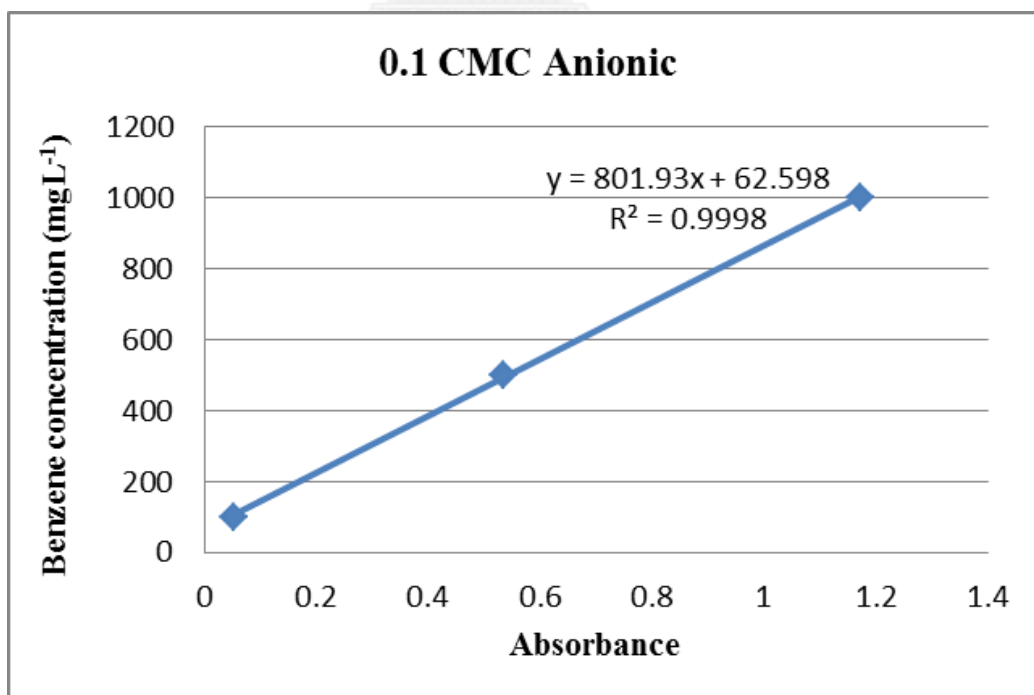
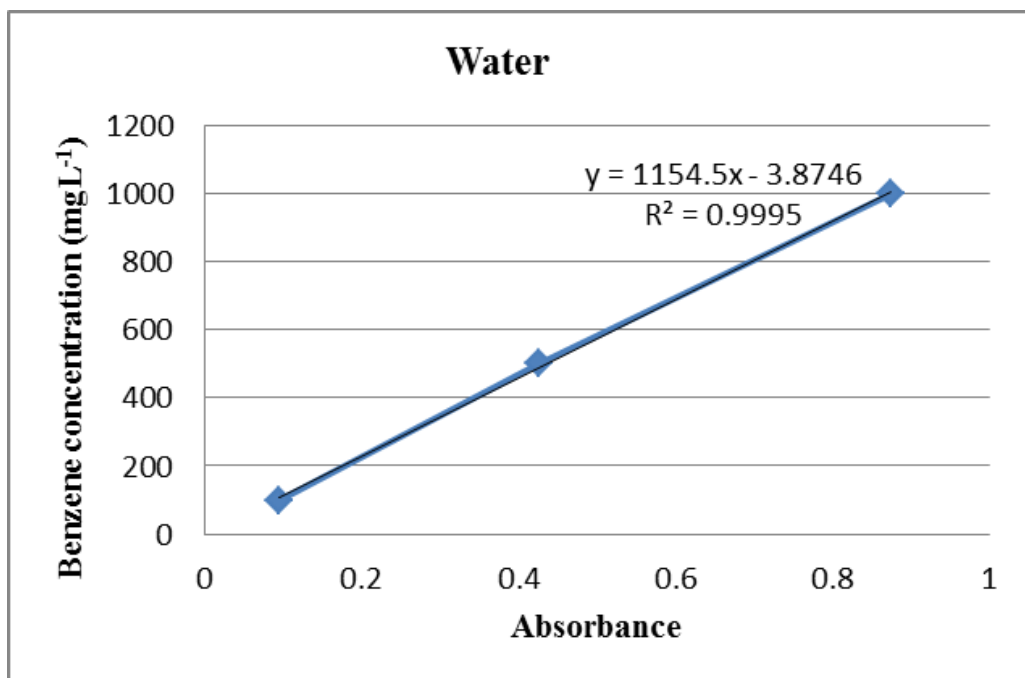
Concentration of dissolved oxygen in non-ionic solution at 0.1 cmc

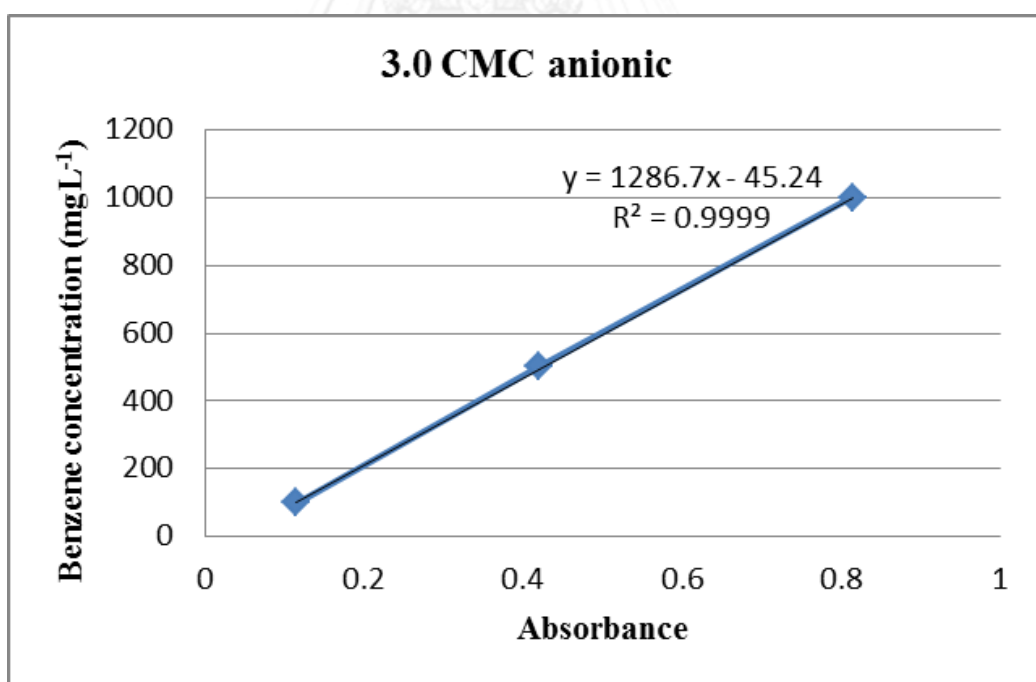
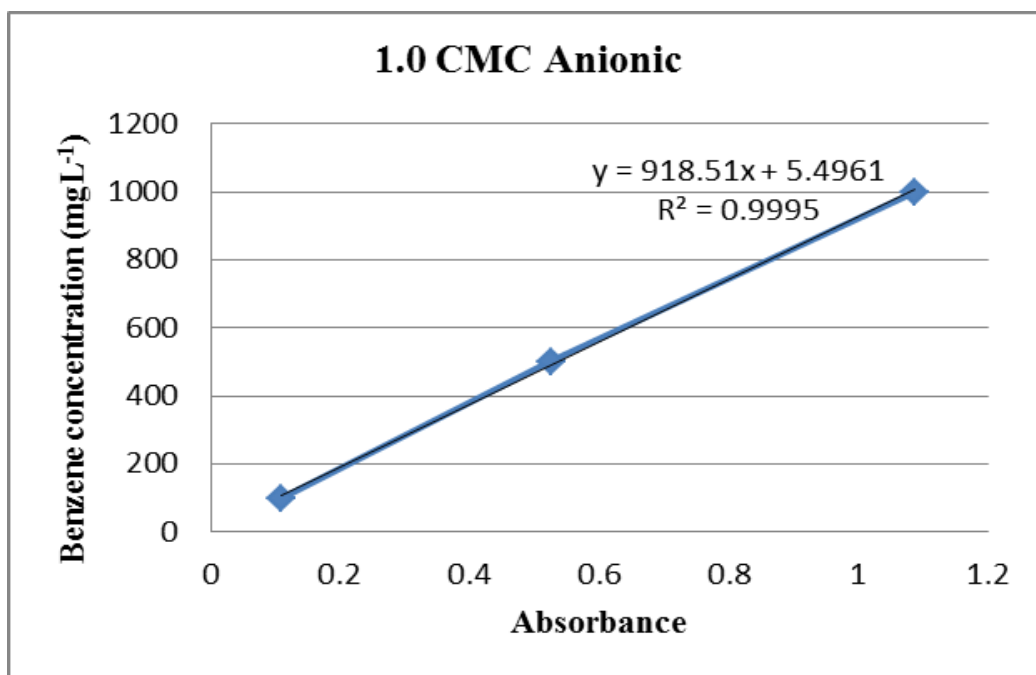


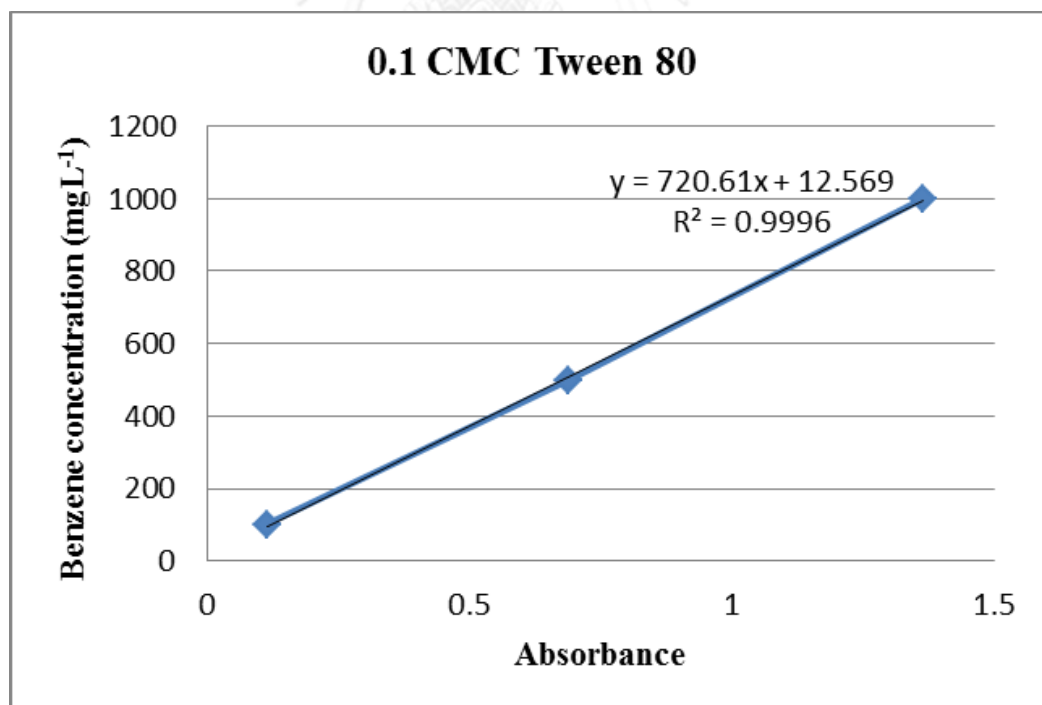
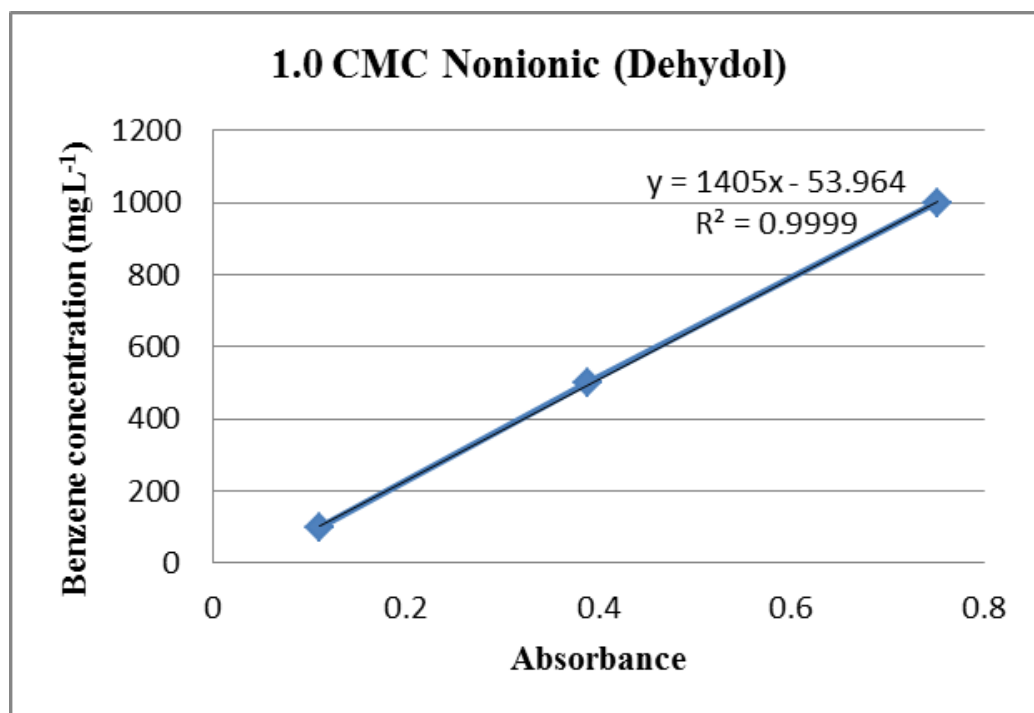
$k_L a$ versus Q_g for non-ionic solution at 0.1 cmc

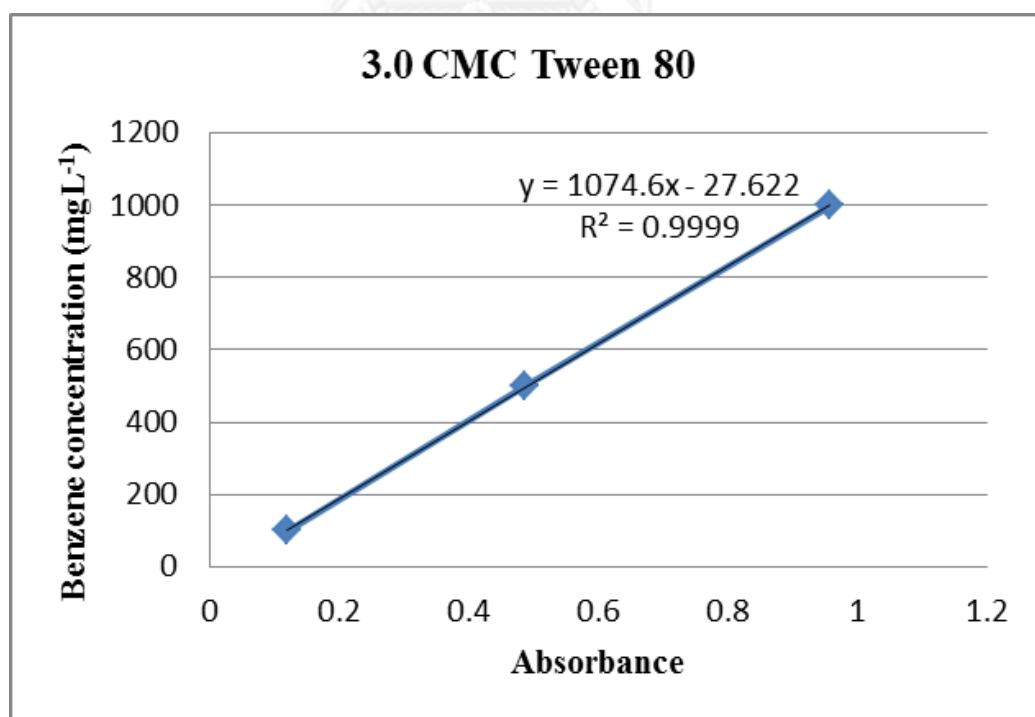
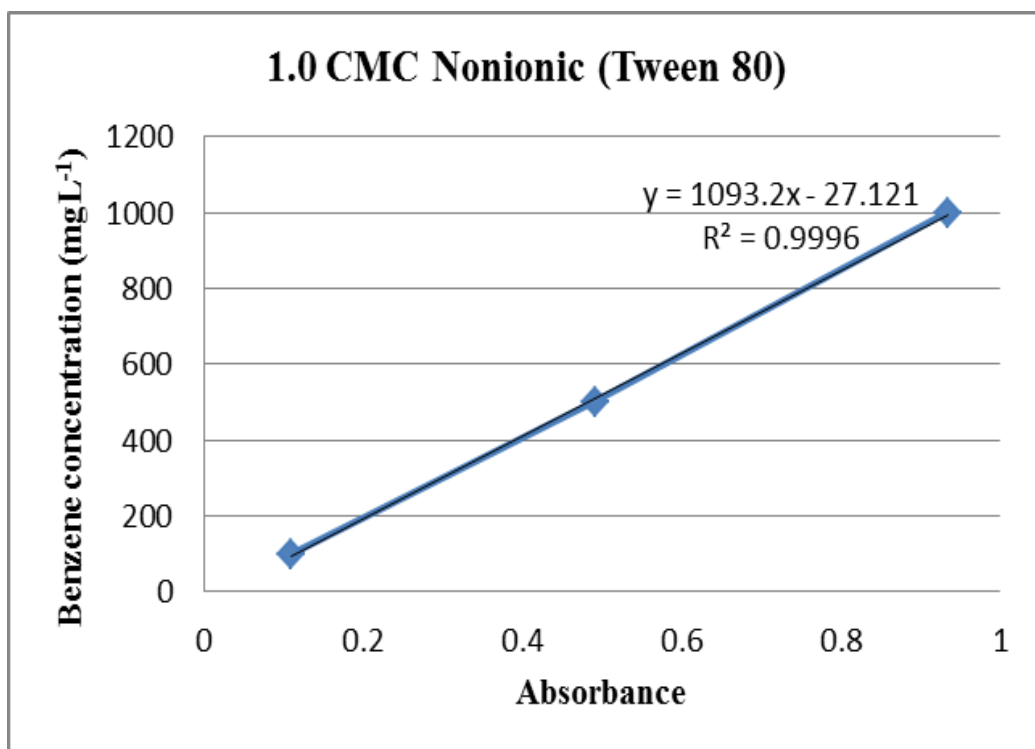


Calibration curve for benzene absorption









Site distribution of water at flow 1.5 Lmin^{-1} (aeration)

Number	d_B (mm)	Z	Normal (F%)	Curve
1	1.023948	-2.807884999	0.001205254	1.15899E-05
2	1.243948	-2.152009591	0.008283348	6.55583E-05
3	1.278063	-2.096342768	0.010802942	8.26958E-05
4	1.326291	-1.985006812	0.015490071	0.000112929
5	1.422749	-1.873670856	0.030223064	0.00019859
6	1.422749	-1.818004033	0.030223064	0.00019859
7	1.446863	-1.762337209	0.035336242	0.000225908
8	1.470977	-1.762337209	0.041138273	0.000255729
9	1.470977	-1.706668077	0.041138273	0.000255729
10	1.495092	-1.706668077	0.047690127	0.000288075
11	1.519206	-1.651001253	0.055051995	0.000322928
12	1.567435	-1.651001253	0.072444429	0.000399881
13	1.59155	-1.539665298	0.082587905	0.000441729
14	1.59155	-1.539665298	0.082587905	0.000441729
15	1.615664	-1.483998474	0.093764617	0.000485574
16	1.663893	-1.483998474	0.119393836	0.000578202
17	1.663893	-1.483998474	0.119393836	0.000578202
18	1.663893	-1.483998474	0.119393836	0.000578202
19	1.688007	-1.428329342	0.133915086	0.000626331
20	1.688007	-1.372662519	0.133915086	0.000626331
21	1.712121	-1.372662519	0.149606131	0.000675155
22	1.712121	-1.372662519	0.149606131	0.000675155
23	1.712121	-1.372662519	0.149606131	0.000675155
24	1.736236	-1.316995695	0.166479211	0.000724233
25	1.736236	-1.316995695	0.166479211	0.000724233
26	1.76035	-1.316995695	0.184533343	0.000773086
27	1.784464	-1.316995695	0.203757716	0.000821206
28	1.784464	-1.261326563	0.203757716	0.000821206

29	1.784464	-1.205659739	0.203757716	0.000821206
30	1.808579	-1.149992916	0.224129176	0.000868065
31	1.808579	-1.149992916	0.224129176	0.000868065
32	1.832693	-1.149992916	0.245609062	0.000913117
33	1.832693	-1.03865696	0.245609062	0.000913117
34	1.832693	-0.927321004	0.245609062	0.000913117
35	1.832693	-0.871651872	0.245609062	0.000913117
36	1.832693	-0.815985049	0.245609062	0.000913117
37	1.832693	-0.815985049	0.245609062	0.000913117
38	1.832693	-0.704649093	0.245609062	0.000913117
39	1.856808	-0.704649093	0.268149046	0.000955821
40	1.856808	-0.64898227	0.268149046	0.000955821
41	1.856808	-0.64898227	0.268149046	0.000955821
42	1.856808	-0.593315446	0.268149046	0.000955821
43	1.856808	-0.426312667	0.268149046	0.000955821
44	1.856808	-0.426312667	0.268149046	0.000955821
45	1.880922	-0.370643535	0.291684092	0.000995636
46	1.880922	-0.370643535	0.291684092	0.000995636
47	1.880922	-0.370643535	0.291684092	0.000995636
48	1.905036	-0.370643535	0.316139224	0.001032048
49	1.905036	-0.370643535	0.316139224	0.001032048
50	1.929151	-0.314976711	0.341427498	0.001064571
51	1.953265	-0.314976711	0.367447549	0.001092758
52	1.953265	-0.314976711	0.367447549	0.001092758
53	1.953265	-0.259307579	0.367447549	0.001092758
54	1.953265	-0.203640755	0.367447549	0.001092758
55	1.97738	-0.203640755	0.394092135	0.001116217
56	1.97738	-0.147971623	0.394092135	0.001116217
57	1.97738	-0.0923048	0.394092135	0.001116217
58	1.97738	-0.0923048	0.394092135	0.001116217
59	1.97738	-0.0923048	0.394092135	0.001116217

60	1.97738	-0.0923048	0.394092135	0.001116217
61	1.97738	-0.036637976	0.394092135	0.001116217
62	1.97738	-0.036637976	0.394092135	0.001116217
63	2.001494	-0.036637976	0.42124087	0.001134614
64	2.001494	-0.036637976	0.42124087	0.001134614
65	2.001494	0.019031156	0.42124087	0.001134614
66	2.049723	0.019031156	0.476548184	0.001155239
67	2.049723	0.130364803	0.476548184	0.001155239
68	2.073837	0.130364803	0.504440235	0.001157168
69	2.073837	0.130364803	0.504440235	0.001157168
70	2.073837	0.130364803	0.504440235	0.001157168
71	2.097952	0.186033935	0.532311742	0.001153441
72	2.097952	0.186033935	0.532311742	0.001153441
73	2.122066	0.186033935	0.560024533	0.001144116
74	2.122066	0.241700759	0.560024533	0.001144116
75	2.14618	0.241700759	0.58744621	0.001129326
76	2.170295	0.241700759	0.614448559	0.001109286
77	2.170295	0.241700759	0.614448559	0.001109286
78	2.194409	0.297367582	0.640906063	0.001084283
79	2.194409	0.353036714	0.640906063	0.001084283
80	2.218523	0.353036714	0.666704315	0.001054672
81	2.218523	0.353036714	0.666704315	0.001054672
82	2.242638	0.380870126	0.691738032	0.00102086
83	2.266752	0.408703538	0.715909342	0.000983311
84	2.266752	0.408703538	0.715909342	0.000983311
85	2.290867	0.46437267	0.739136009	0.000942517
86	2.290867	0.520039494	0.739136009	0.000942517
87	2.339095	0.575706317	0.7824759	0.000853323
88	2.339095	0.687042273	0.7824759	0.000853323
89	2.36321	0.687042273	0.802485962	0.000806004
90	2.387324	0.742711405	0.821339918	0.000757594

91	2.411438	0.742711405	0.839018643	0.000708616
92	2.411438	0.742711405	0.839018643	0.000708616
93	2.435553	0.854045052	0.855515177	0.000659568
94	2.44761	0.909714184	0.863320351	0.000635166
95	2.507896	1.140562752	0.897999522	0.000516484
96	2.53201	1.196229575	0.909907246	0.000471418
97	2.556125	1.427078143	0.920750251	0.000428183
98	2.652583	1.482747275	0.954480133	0.000277507
99	2.893726	2.125032627	0.991562925	6.66253E-05
100	3.110756	2.837895313	0.998731915	1.21416E-05

Median = 2.07

S.D. = 0.344736227

Site distribution of anionic surfactant at flow 1.5 Lmin⁻¹ (aeration)

Number	d _B (mm)	Z	Normal (F%)	Curve
1	0.439317	-3.034354731	0.001205254	1.15899E-05
2	0.723432	-2.396185652	0.008283348	6.55583E-05
3	0.747546	-2.297225934	0.010802942	8.26958E-05
4	0.795775	-2.157327669	0.015490071	0.000112929
5	0.844004	-1.877525337	0.030223064	0.00019859
6	0.868118	-1.877525337	0.030223064	0.00019859
7	0.892232	-1.807576204	0.035336242	0.000225908
8	0.892232	-1.737627072	0.041138273	0.000255729
9	0.916347	-1.737627072	0.041138273	0.000255729
10	0.916347	-1.667675039	0.047690127	0.000288075
11	0.940461	-1.597725906	0.055051995	0.000322928
12	0.940461	-1.45782474	0.072444429	0.000399881
13	0.98869	-1.387872707	0.082587905	0.000441729
14	0.98869	-1.387872707	0.082587905	0.000441729
15	1.012804	-1.317923575	0.093764617	0.000485574
16	1.012804	-1.178022409	0.119393836	0.000578202
17	1.012804	-1.178022409	0.119393836	0.000578202
18	1.012804	-1.178022409	0.119393836	0.000578202
19	1.036919	-1.108073276	0.133915086	0.000626331
20	1.061033	-1.108073276	0.133915086	0.000626331
21	1.061033	-1.038124144	0.149606131	0.000675155
22	1.061033	-1.038124144	0.149606131	0.000675155
23	1.061033	-1.038124144	0.149606131	0.000675155
24	1.085147	-0.96817211	0.166479211	0.000724233
25	1.085147	-0.96817211	0.166479211	0.000724233
26	1.085147	-0.898222978	0.184533343	0.000773086
27	1.085147	-0.828273845	0.203757716	0.000821206
28	1.109262	-0.828273845	0.203757716	0.000821206

29	1.133376	-0.828273845	0.203757716	0.000821206
30	1.15749	-0.758321812	0.224129176	0.000868065
31	1.15749	-0.758321812	0.224129176	0.000868065
32	1.15749	-0.688372679	0.245609062	0.000913117
33	1.205719	-0.688372679	0.245609062	0.000913117
34	1.253948	-0.688372679	0.245609062	0.000913117
35	1.278063	-0.688372679	0.245609062	0.000913117
36	1.302177	-0.688372679	0.245609062	0.000913117
37	1.302177	-0.688372679	0.245609062	0.000913117
38	1.350406	-0.688372679	0.245609062	0.000913117
39	1.350406	-0.618420646	0.268149046	0.000955821
40	1.37452	-0.618420646	0.268149046	0.000955821
41	1.37452	-0.618420646	0.268149046	0.000955821
42	1.398634	-0.618420646	0.268149046	0.000955821
43	1.470977	-0.618420646	0.268149046	0.000955821
44	1.470977	-0.618420646	0.268149046	0.000955821
45	1.495092	-0.548471514	0.291684092	0.000995636
46	1.495092	-0.548471514	0.291684092	0.000995636
47	1.495092	-0.548471514	0.291684092	0.000995636
48	1.495092	-0.478522381	0.316139224	0.001032048
49	1.495092	-0.478522381	0.316139224	0.001032048
50	1.519206	-0.408570348	0.341427498	0.001064571
51	1.519206	-0.338621215	0.367447549	0.001092758
52	1.519206	-0.338621215	0.367447549	0.001092758
53	1.543321	-0.338621215	0.367447549	0.001092758
54	1.567435	-0.338621215	0.367447549	0.001092758
55	1.567435	-0.268669182	0.394092135	0.001116217
56	1.59155	-0.268669182	0.394092135	0.001116217
57	1.615664	-0.268669182	0.394092135	0.001116217
58	1.615664	-0.268669182	0.394092135	0.001116217
59	1.615664	-0.268669182	0.394092135	0.001116217

60	1.615664	-0.268669182	0.394092135	0.001116217
61	1.639778	-0.268669182	0.394092135	0.001116217
62	1.639778	-0.268669182	0.394092135	0.001116217
63	1.639778	-0.198720049	0.42124087	0.001134614
64	1.639778	-0.198720049	0.42124087	0.001134614
65	1.663893	-0.198720049	0.42124087	0.001134614
66	1.663893	-0.058818884	0.476548184	0.001155239
67	1.712121	-0.058818884	0.476548184	0.001155239
68	1.712121	0.011130249	0.504440235	0.001157168
69	1.712121	0.011130249	0.504440235	0.001157168
70	1.712121	0.011130249	0.504440235	0.001157168
71	1.736236	0.081082282	0.532311742	0.001153441
72	1.736236	0.081082282	0.532311742	0.001153441
73	1.736236	0.151031415	0.560024533	0.001144116
74	1.76035	0.151031415	0.560024533	0.001144116
75	1.76035	0.220980547	0.58744621	0.001129326
76	1.76035	0.290932581	0.614448559	0.001109286
77	1.76035	0.290932581	0.614448559	0.001109286
78	1.784464	0.360881713	0.640906063	0.001084283
79	1.808579	0.360881713	0.640906063	0.001084283
80	1.808579	0.430830846	0.666704315	0.001054672
81	1.808579	0.430830846	0.666704315	0.001054672
82	1.820636	0.500782879	0.691738032	0.00102086
83	1.832693	0.570732011	0.715909342	0.000983311
84	1.832693	0.570732011	0.715909342	0.000983311
85	1.856808	0.640684045	0.739136009	0.000942517
86	1.880922	0.640684045	0.739136009	0.000942517
87	1.905036	0.78058231	0.7824759	0.000853323
88	1.953265	0.78058231	0.7824759	0.000853323
89	1.953265	0.850534343	0.802485962	0.000806004
90	1.97738	0.920483476	0.821339918	0.000757594

91	1.97738	0.990432608	0.839018643	0.000708616
92	1.97738	0.990432608	0.839018643	0.000708616
93	2.025608	1.060384641	0.855515177	0.000659568
94	2.049723	1.095359208	0.863320351	0.000635166
95	2.149723	1.27023494	0.897999522	0.000516484
96	2.173837	1.340184072	0.909907246	0.000471418
97	2.273837	1.410136106	0.920750251	0.000428183
98	2.297952	1.689938437	0.954480133	0.000277507
99	2.57618	2.389438465	0.991562925	6.66253E-05
100	2.884981	3.018992261	0.998731915	1.21416E-05

Median = 1.655649

S.D. = 0.433184408

Site distribution of water at flow 1.5 Lmin^{-1} (benzene)

Number	d_B (mm)	Z	Normal (F%)	Curve
1	0.802041	-2.674977355	0.003736715	2.4135E-05
2	1.082041	-2.06866922	0.019288569	0.000101669
3	1.267844	-1.666333969	0.047823457	0.000215526
4	1.267844	-1.666333969	0.047823457	0.000215526
5	1.402722	-1.37427101	0.084678781	0.000335998
6	1.402722	-1.37427101	0.084678781	0.000335998
7	1.429697	-1.315859718	0.094110566	0.000363461
8	1.537599	-1.082210216	0.139579565	0.00048098
9	1.564574	-1.023798924	0.152965129	0.000511493
10	1.564574	-1.023798924	0.152965129	0.000511493
11	1.591549	-0.965387631	0.167175347	0.000542088
12	1.618525	-0.906974173	0.182210228	0.000572558
13	1.618525	-0.906974173	0.182210228	0.000572558
14	1.6455	-0.84856288	0.198062285	0.00060268
15	1.6455	-0.84856288	0.198062285	0.00060268
16	1.658988	-0.819356152	0.206291622	0.00061754
17	1.672476	-0.790149423	0.214720255	0.000632226
18	1.672476	-0.790149423	0.214720255	0.000632226
19	1.699451	-0.73173813	0.232164209	0.000660961
20	1.726426	-0.673326837	0.250369691	0.000688648
21	1.726426	-0.673326837	0.250369691	0.000688648
22	1.726426	-0.673326837	0.250369691	0.000688648
23	1.726426	-0.673326837	0.250369691	0.000688648
24	1.753402	-0.614913379	0.269305963	0.000715053
25	1.753402	-0.614913379	0.269305963	0.000715053
26	1.780377	-0.556502087	0.288933834	0.000739939
27	1.834328	-0.439677336	0.33008541	0.000784273
28	1.834328	-0.439677336	0.33008541	0.000784273

29	1.888279	-0.322852585	0.373403443	0.000819995
30	1.915254	-0.264441293	0.395719948	0.000834181
31	1.915254	-0.264441293	0.395719948	0.000834181
32	1.915254	-0.264441293	0.395719948	0.000834181
33	1.996181	-0.089203084	0.464460257	0.000860434
34	1.996181	-0.089203084	0.464460257	0.000860434
35	2.023156	-0.030791792	0.487717793	0.000863455
36	2.077107	0.086032959	0.534279892	0.000860673
37	2.104082	0.144444252	0.557425162	0.000854899
38	2.104082	0.144444252	0.557425162	0.000854899
39	2.171521	0.290475731	0.614273843	0.000828177
40	2.319885	0.611741089	0.729645464	0.000716445
41	2.319885	0.611741089	0.729645464	0.000716445
42	2.373836	0.728565839	0.766866359	0.000662494
43	2.373836	0.728565839	0.766866359	0.000662494
44	2.427787	0.84539059	0.801053602	0.000604301
45	2.427787	0.84539059	0.801053602	0.000604301
46	2.441275	0.874597319	0.809103476	0.000589312
47	2.508713	1.020626633	0.846284317	0.000513154
48	2.735689	1.51211733	0.934747992	0.000275384
49	2.916615	1.903891993	0.971537874	0.000141036
50	3.302418	2.739304483	0.996921534	2.02777E-05

Median = 2.037376

S.D. = 0.461811386

Site distribution of non-ionic surfactant at flow 1.5 Lmin⁻¹ (benzene)

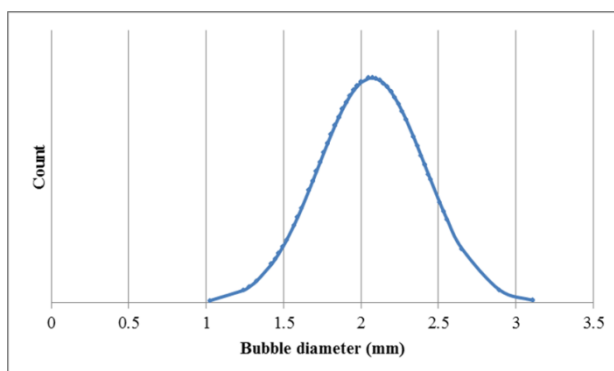
Number	d _B (mm)	Z	Normal (F%)	Curve
1	0.301824	-2.537531332	0.005581869	0.028285255
2	0.441824	-2.289216124	0.011033399	0.051501865
3	0.641824	-1.934480114	0.026527062	0.108936659
4	0.790189	-1.671328072	0.047328447	0.175073257
5	0.890189	-1.493960067	0.067593028	0.231809269
6	0.890189	-1.493960067	0.067593028	0.231809269
7	0.917164	-1.446115048	0.074072468	0.248700384
8	0.917164	-1.446115048	0.074072468	0.248700384
9	1.025066	-1.254731422	0.104788137	0.322047094
10	1.025066	-1.254731422	0.104788137	0.322047094
11	1.052041	-1.206886403	0.113737947	0.34158135
12	1.079016	-1.159041384	0.123219658	0.361472077
13	1.186918	-0.967657758	0.166607661	0.443054369
14	1.186918	-0.967657758	0.166607661	0.443054369
15	1.186918	-0.967657758	0.166607661	0.443054369
16	1.186918	-0.967657758	0.166607661	0.443054369
17	1.267844	-0.824120926	0.204935425	0.503853529
18	1.267844	-0.824120926	0.204935425	0.503853529
19	1.348771	-0.680582321	0.248067908	0.561312119
20	1.402722	-0.584890508	0.279310671	0.596348249
21	1.402722	-0.584890508	0.279310671	0.596348249
22	1.483648	-0.441353676	0.329478486	0.641928371
23	1.537599	-0.345661864	0.364798424	0.66656136
24	1.537599	-0.345661864	0.364798424	0.66656136
25	1.564574	-0.297816844	0.382921479	0.676901538
26	1.591549	-0.249971825	0.401304569	0.685830357
27	1.6455	-0.154280012	0.438694478	0.699224665
28	1.658988	-0.130356616	0.448142145	0.701609398

29	1.672476	-0.106433219	0.457619319	0.70359946
30	1.699451	-0.0585882	0.476640055	0.706382568
31	1.699451	-0.0585882	0.476640055	0.706382568
32	1.726426	-0.01074318	0.495714174	0.707555133
33	1.807353	0.132795426	0.552822414	0.701384296
34	1.861304	0.228487238	0.590366262	0.689364426
35	1.861304	0.228487238	0.590366262	0.689364426
36	1.888279	0.276332258	0.608853559	0.68108935
37	1.888279	0.276332258	0.608853559	0.68108935
38	1.915254	0.324177277	0.627098088	0.671374972
39	1.915254	0.324177277	0.627098088	0.671374972
40	1.928742	0.348100674	0.636117711	0.665997702
41	1.94223	0.37202407	0.645062536	0.660285493
42	1.94223	0.37202407	0.645062536	0.660285493
43	1.969205	0.41986909	0.662709455	0.647894733
44	1.996181	0.467715883	0.680006109	0.63428234
45	1.996181	0.467715883	0.680006109	0.63428234
46	2.150131	0.740773927	0.770584737	0.537807266
47	2.250131	0.918141932	0.820727718	0.464230389
48	2.550131	1.450245948	0.926505027	0.247217028
49	2.785008	1.866842598	0.969038214	0.123881147
50	3.178959	2.565585629	0.99484991	0.026331303

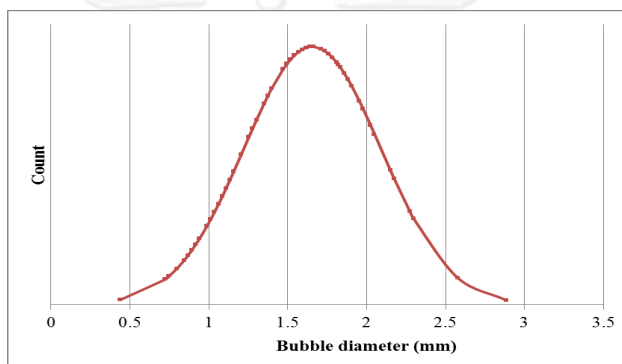
Median = 1.732483

S.D. = 0.563799541

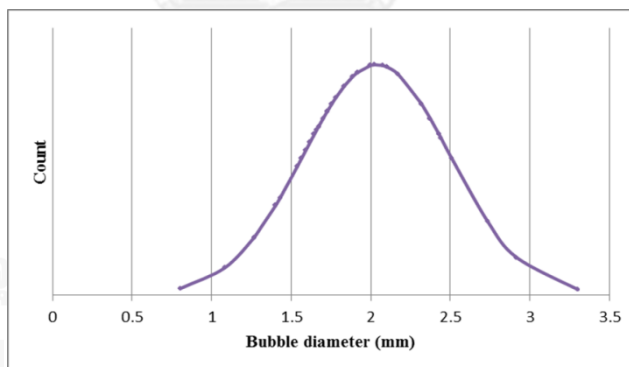
Site distribution for air bubble in water



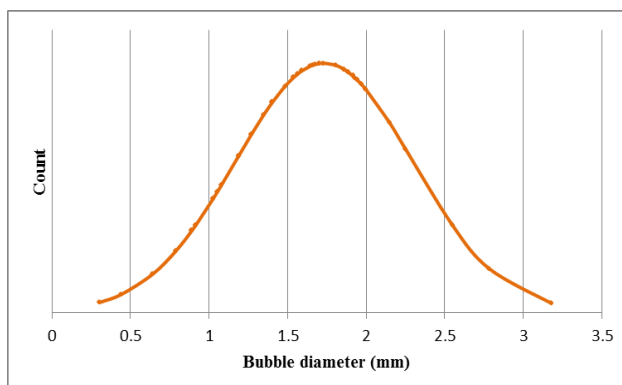
Site distribution for air bubble in anionic surfactant solution



Site distribution for hydrophobic VOCs in water



Site distribution for hydrophobic VOCs in non-ionic surfactant solution



Results from Gas Chromatography

Type	Area	Retention Time (min)
water	34433.4	3.157
	33707.2	3.150
	30668	3.164
Anionic surfactant	27404.8	3.155
	23768	3.156
	27136.2	3.166
Non-ionic surfactant (Tween80)	21751.6	3.158
	17965.3	3.163
	18137.4	3.159
Water+GAC	13778.92	3.156
	9775.96	3.163
	11818.72	3.163
Tween+GAC	18305.64	3.166
	15806.16	3.164
	14310.2	3.166

Removal efficiency

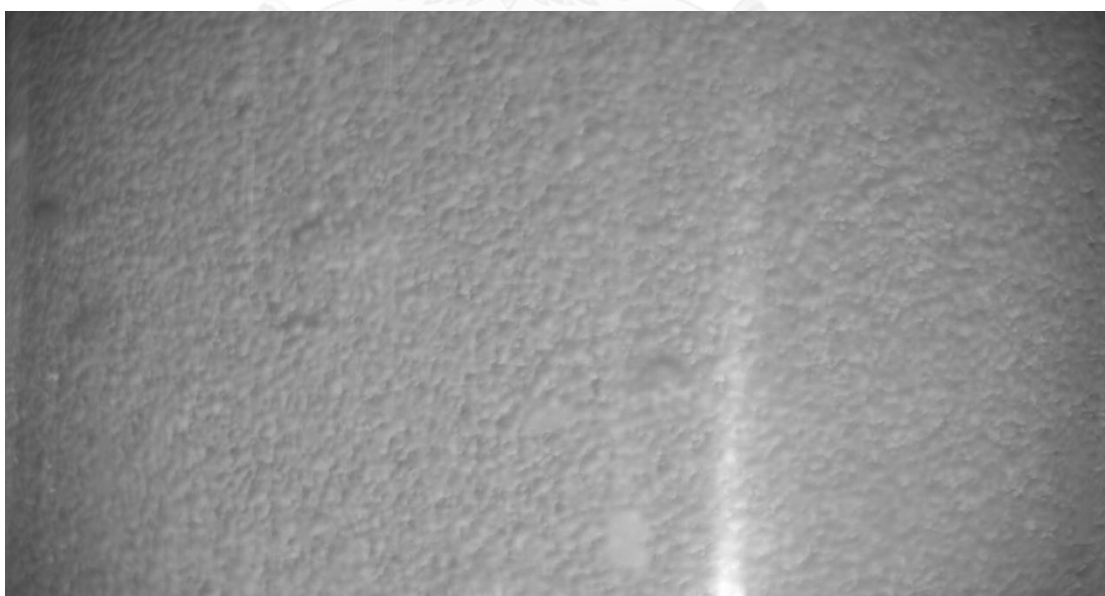
	Inlet	Water	Anionic	Tween80	Water+GAC	Tween80+GAC
Area	44294.5	34433.4	27404.8	21751.6	13778.92	18305.64
	45580.3	33707.2	23768	17965.3	9775.96	15806.16
	48563.8	30668	27136.2	18137.4	11818.72	14310.2
Average	46146.2	32936.2	26103	19284.77	11791.2	16140.66667
S.D.	2190.186	1997.596	2026.624	2138.073	2001.621893	2018.614929
% Removal efficiency		28.62641	43.43413	58.20942	74.44816691	65.02276099

Bubble diameter

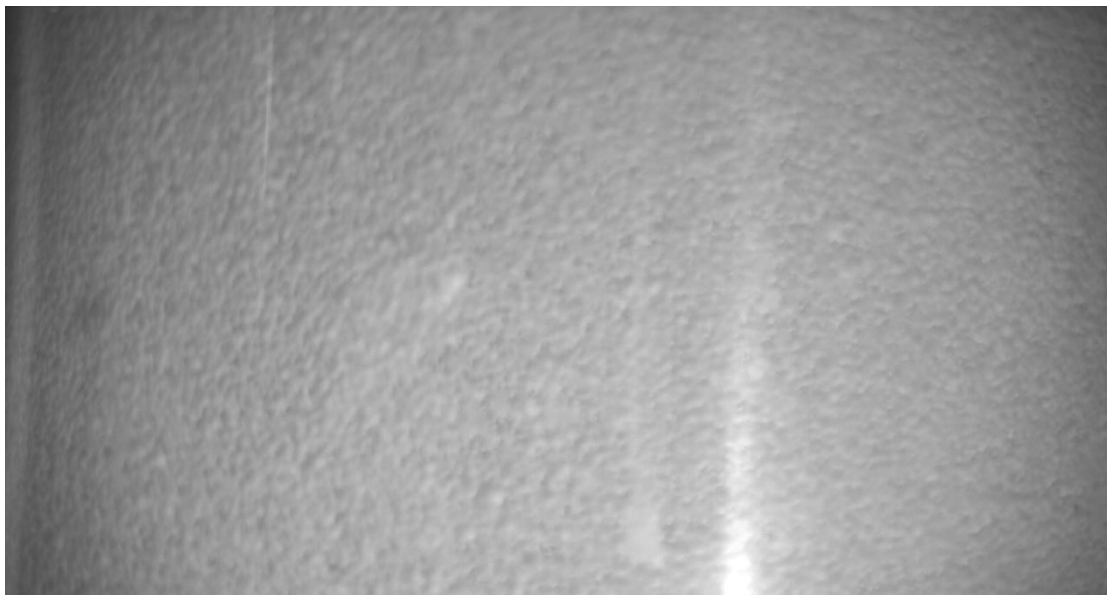
Benzene generated in water at flow 1.5 Lmin^{-1}



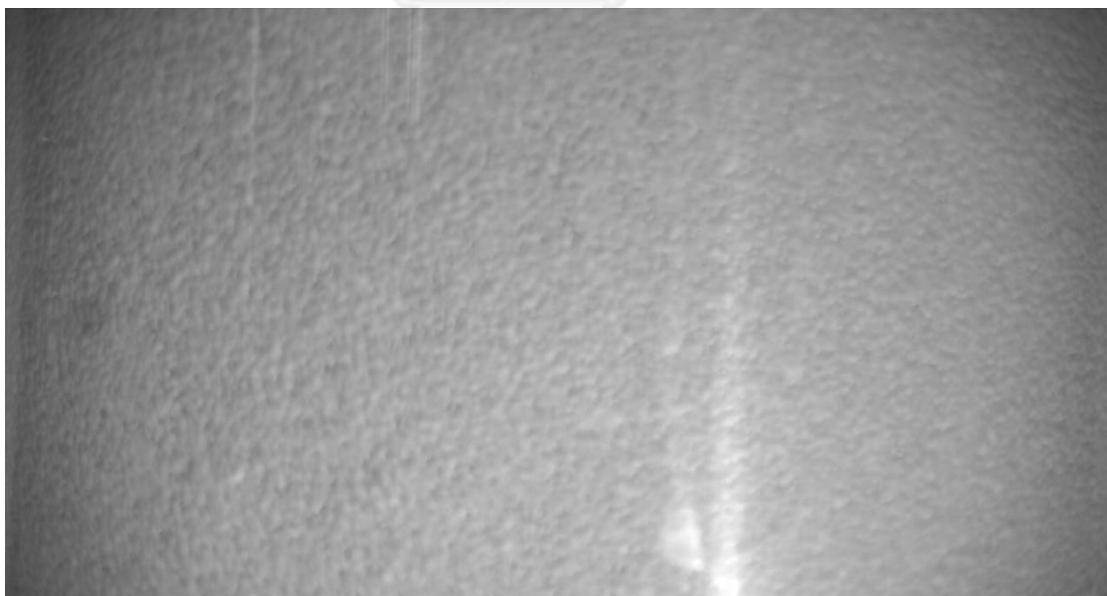
Benzene generated in anionic surfactant 0.1 CMC at flow 1.5 Lmin^{-1}



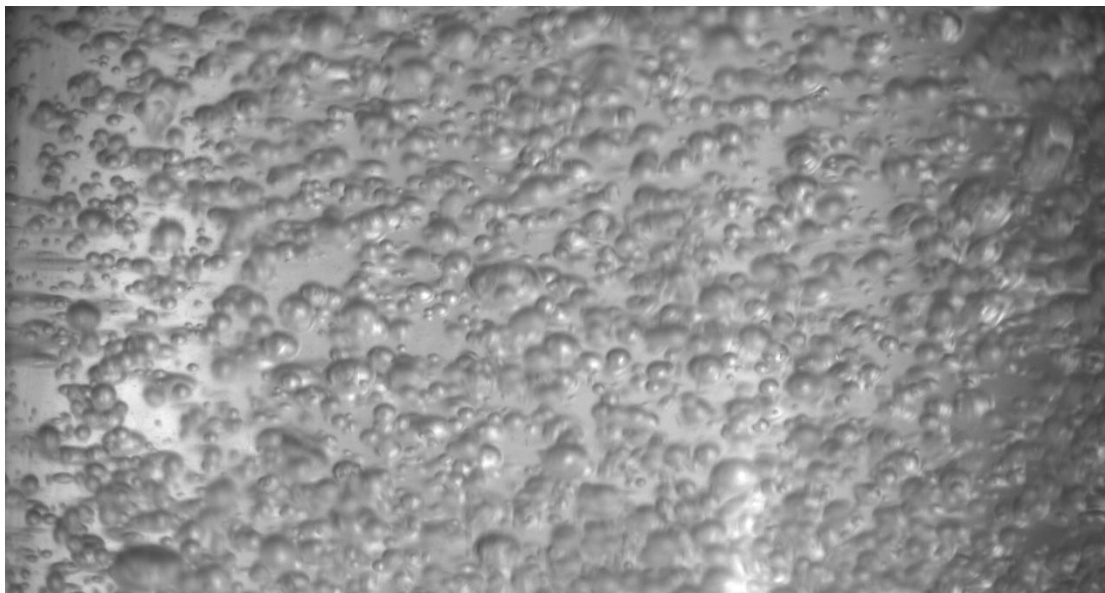
Benzene generated in anionic surfactant 1.0 CMC at flow 1.5 Lmin^{-1}



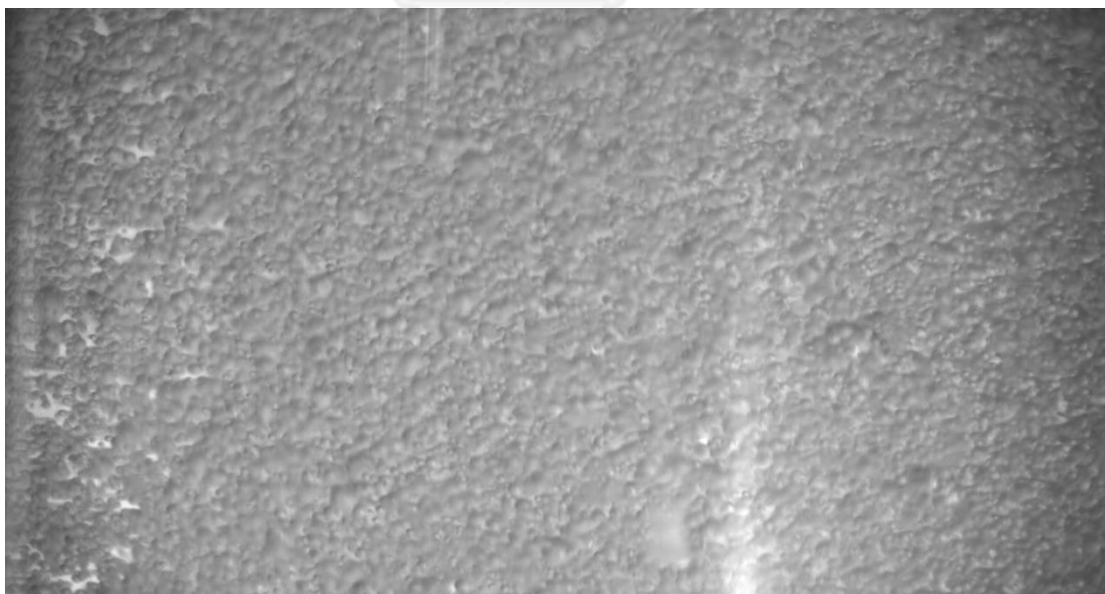
Benzene generated in anionic surfactant 3.0 CMC at flow 1.5 Lmin^{-1}



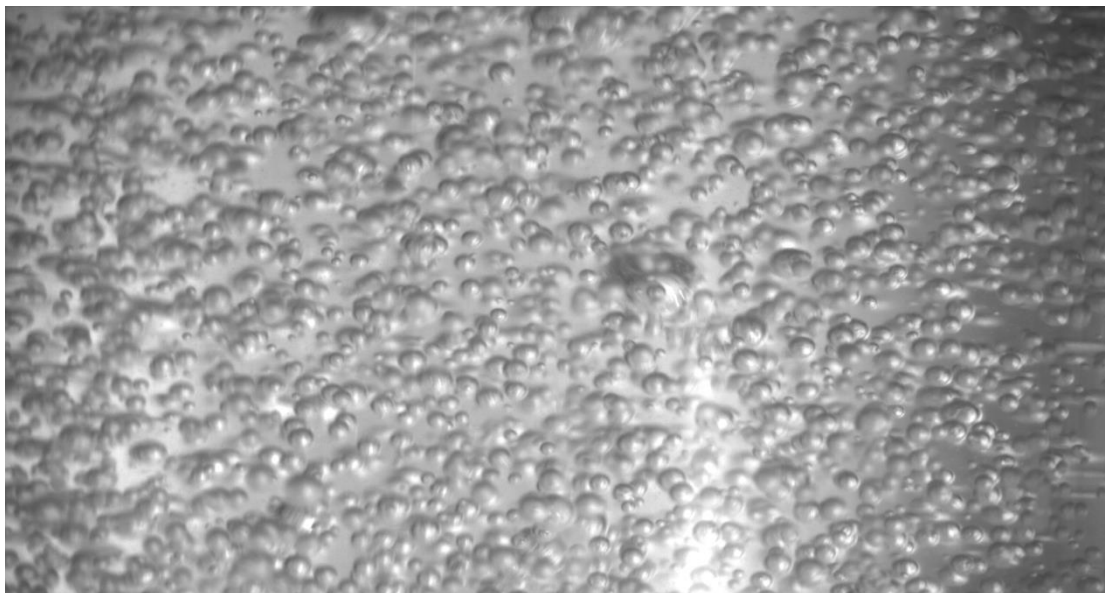
Benzene generated in non-ionic surfactant (Dehydol) 1.0 CMC at flow 1.5 Lmin^{-1}



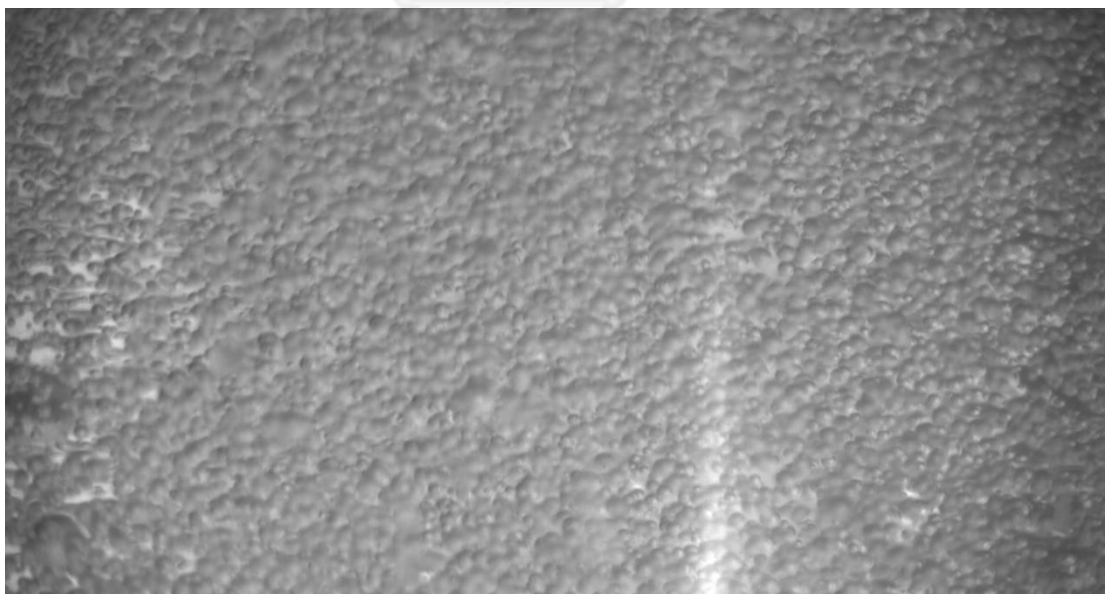
Benzene generated in non-ionic surfactant (Tween80) 0.1 CMC at flow 1.5 Lmin^{-1}



Benzene generated in non-ionic surfactant (Tween80) 1.0 CMC at flow 1.5 Lmin^{-1}



Benzene generated in non-ionic surfactant (Tween80) 3.0 CMC at flow 1.5 Lmin^{-1}



VITA

Name: Miss. Chomthisa Chuenchaem

Date of Birth: November 24, 1989

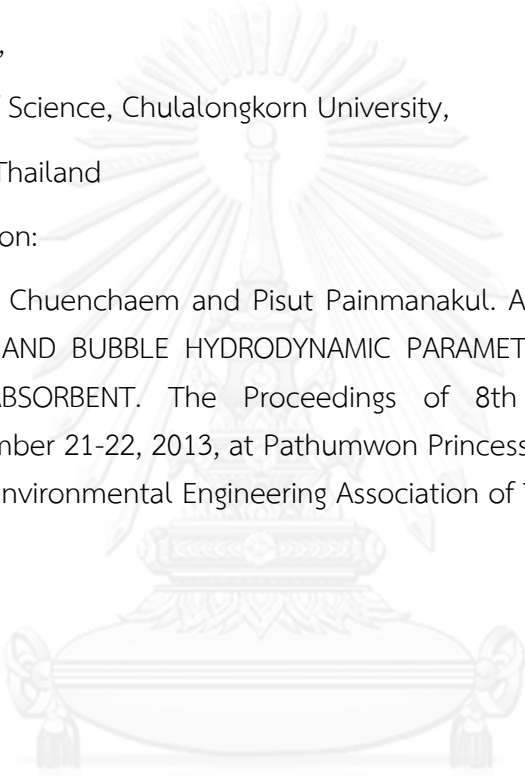
Nationality: Thai

University Education: 2008-2012 Bachelor Degree of Science in
Chemistry,

Faculty of Science, Chulalongkorn University,
Bangkok, Thailand

Presentation:

Chonthisa Chuenchaem and Pisut Painmanakul. A COMPARATIVE STUDY OF
MASS TRANSFER AND BUBBLE HYDRODYNAMIC PARAMETERS IN BUBBLE COLUMN:
DIFFUSER AND ABSORBENT. The Proceedings of 8th National Environmental
Conference, November 21-22, 2013, at Pathumwon Princess Hotel, Bangkok, Thailand,
Organized by the Environmental Engineering Association of Thailand



จุฬาลงกรณ์มหาวิทยาลัย
CHULALONGKORN UNIVERSITY



จุฬาลงกรณ์มหาวิทยาลัย
CHULALONGKORN UNIVERSITY